

University of Alberta

**The effects of hyperlipidemia on the pharmacokinetic and
pharmacodynamic aspects of amiodarone and ketoconazole**

by

Dalia Amr Mostafa Hamdi Hassan El Sayed

A thesis submitted to the Faculty of Graduate Studies and Research
in partial fulfillment of the requirements for the degree of

Doctor of Philosophy

in

Pharmaceutical Sciences
Faculty of Pharmacy and Pharmaceutical Sciences

© Dalia Amr Mostafa Hamdi Hassan El Sayed

Fall 2010

Edmonton, Alberta

Permission is hereby granted to the University of Alberta Libraries to reproduce single copies of this thesis and to lend or sell such copies for private, scholarly or scientific research purposes only. Where the thesis is converted to, or otherwise made available in digital form, the University of Alberta will advise potential users of the thesis of these terms.

The author reserves all other publication and other rights in association with the copyright in the thesis and, except as herein before provided, neither the thesis nor any substantial portion thereof may be printed or otherwise reproduced in any material form whatsoever without the author's prior written permission.

Examining Committee

Dr. Dion R. Brocks, Faculty of Pharmacy and Pharmaceutical Sciences

Dr. Fakhreddin Jamali, Faculty of Pharmacy and Pharmaceutical Sciences

Dr. Ayman El-Kadi, Faculty of Pharmacy and Pharmaceutical Sciences

Dr. Paul Jurasz, Faculty of Pharmacy and Pharmaceutical Sciences

Dr. Glen Baker, Department of Psychiatry

Dr. Sylvie Marleau, Faculty of Pharmacy, University of Montreal

To my great parents Amr and Magda

To my loving husband Ibrahim and my wonderful girls Laila and Farida

Abstract

The influence of hyperlipidemia on the pharmacodynamic and pharmacokinetic aspects of lipophilic drugs was explored. The antiarrhythmic, amiodarone, and the antifungal, (\pm)-ketoconazole, were used as model drugs. Experimental hyperlipidemia was induced in rat using poloxamer 407 and two sensitive novel HPLC assays were developed.

In a multiple dosing study, hyperlipidemia increased amiodarone plasma concentrations, heart concentrations and electrocardiographic changes. The amiodarone heart uptake could not be totally attributed to its unbound fraction, where the cardiac very low density lipoprotein receptors seemed to play a role in the uptake of bound drug.

Amiodarone liver metabolism in presence and absence of hyperlipidemia was studied using isolated primary rat liver hepatocytes. The metabolism of amiodarone was lower in hepatocytes isolated from hyperlipidemic than those from normolipidemic rats. Hyperlipidemic serum resulted in a decrease in amiodarone metabolism and when coincubated, the expected decrease in unbound fraction seemed to result in greater inhibition of metabolism.

(\pm)-Ketoconazole showed stereoselectivity in its pharmacokinetics in rat with (+)-ketoconazole showing higher plasma concentrations than its antipode. This was attributed to its higher protein binding. There was no difference in the total bioavailability of the two enantiomers. Ketoconazole enantiomers exhibited nonlinear pharmacokinetics. In normolipidemic rat plasma ketoconazole

enantiomers were more than 95% bound to lipoprotein deficient fraction. Hyperlipidemia resulted in shifting both enantiomers 20% to very low density and low density lipoprotein fractions.

In a pharmacokinetic assessment, hyperlipidemia was found to increase ketoconazole enantiomer volume of distribution. Moreover, the stereoselectivity ratios of most pharmacokinetic parameters were changed. After oral dosing, the uptake of (-)-ketoconazole was significantly decreased. Since ketoconazole is used as a potent CYP3A inhibitor, alteration in liver concentrations of (-)-ketoconazole, the more potent inhibitory enantiomer, could decrease its CYP inhibitory potential.

Hyperlipidemia potentiated the CYP-mediated interaction between ketoconazole and midazolam with significantly higher midazolam AUC and lower clearance. This was attributed to the inhibitory action of ketoconazole and the effect of hyperlipidemia on the binding of midazolam. Hyperlipidemia was found to unexpectedly decrease midazolam unbound fraction in plasma.

In conclusion, the findings could explain some unexpected dose versus effect outcomes in hyperlipidemic patients receiving amiodarone or ketoconazole.

Acknowledgement

I would like to express my deep gratitude and appreciation for my supervisor Dr. Dion Brocks for his continuous guidance, help, understanding, and support throughout the PhD years.

I would like to thank my supervisory committee Dr. Fakhredin Jamali and Dr. Ayman El Kadi for their generous guidance and support during the PhD program.

I would like to thank Dr. Ayman El Kadi for his help and guidance with the hepatocytes project and for the accessibility of his laboratory facilities.

I would like to extend my thanks to Dr. Kishor Wasan and Jackie Fleitcher from the University of British Columbia for their participation in the lipoprotein fractionation study.

I am thankful to my former colleague Dr. Anoosh Shayeganpour for the preparation of the liver microsomes and for teaching me some of the animal handling techniques.

I would also like to thank my friends Marwa and Jigar for their help and for a friendly work environment in the lab.

I would like to thank the Egyptian Scholarship department, the Dissertation Fellowship, Faculty of Pharmacy and Pharmaceutical Sciences Teaching assistance and Research assistance programs and my supervisor for financial support during my PhD program.

Finally, I would like to deeply thank my father and mother for their time, encouragement, financial and emotional support throughout my program. I would also like to thank my husband for his understanding, support and patience. Laila and Farida, you can start planning for your presents.

Table of contents

List of tables	
List of figures	
List of abbreviations and symbols	
1. Introduction	1
1.1 Hyperlipidemia	2
1.2 Lipids and lipoproteins	5
1.3 Lipoprotein receptors	6
1.4 Experimental models of HL	9
1.5 Effects of HL on PK of drugs	14
1.5.1 Absorption	14
1.5.2 Distribution	19
1.5.3 Metabolism	23
1.5.4 Excretion	28
1.6 The PK and pharmacodynamics of two representative lipophilic drugs: amiodarone and ketoconazole	31
1.6.1 AM	31
1.6.2 KTZ	33
1.7 Rationale	36
1.8 Hypothesis	37
1.9 Objectives	37

2. Experimental	39
2.1 Materials	40
2.2 Effect of HL on the PK and pharmacodynamic aspects of AM	41
2.2.1 Assays	41
2.2.1.1 Determination of AM using an LC-MS	41
2.2.1.2 Lipid measurement	41
2.2.2 Determination of the effect of experimental HL on the electrocardiographic changes associated with AM	42
2.2.2.1 Induction of HL	42
2.2.2.2 Surgical procedures	42
2.2.2.3 Dosing and sample collection	43
2.2.3 Effect of HL on AM metabolism using rat hepatocytes in vitro	45
2.2.3.1 Preparation of perfusion solutions	45
2.2.3.2 Isolation of rat hepatocytes	46
2.2.3.3 Determining the viability of hepatocytes	48
2.2.3.4 Preparation of primary cultures	48
2.2.3.5 Drug solutions	48
a. Stock solutions	48
b. Treatment (working) solutions	49
c. Media preparation	49

d. Collection of NL ad HL serum	49
2.2.3.6 Hepatocytes-AM incubation	50
2.3 Effect of HL on the PK and pharmacodynamic aspects of (±)- KTZ	50
2.3.1 Stereoselective HPLC assay for the determination of KTZ enantiomers in biological specimens	50
2.3.1.1 Instrumentation	51
2.3.1.2 Chromatographic separation	51
2.3.1.3 Preparation of stock solutions	51
2.3.1.4 Extraction procedures	52
a. Rat plasma, blood, buffer and fractions	52
b. Liver microsomes	53
c. Liver homogenates	53
2.3.1.5 Calibration, accuracy and validation	54
2.3.1.6 Assignment of KTZ enantiomer optical rotation and test for racemisation	55
2.3.1.7 Assessment of chromatographic separation	56
2.3.1.8 Application of the assay method for measuring KTZ enantiomers concentrations in rat plasma in vivo	56
2.3.2 Nonlinear stereoselective PK of KTZ in rat after administration of racemate	57
2.3.2.1 Surgical procedures	57

2.3.2.2 Dosing and sample collection	58
2.3.2.3 Microsomal incubations	59
a. Microsomal preparation	59
b. Assay for microsomal protein	59
c. Total CYP 450 measurement	60
d. Microsomal incubation studies	61
2.3.2.4 plasma protein binding	62
2.3.2.5 Determination of blood:plasma KTZ enantiomer ratio	63
2.3.3 Distribution of KTZ enantiomers in rat and human plasma	63
2.3.3.1 Treatment of plasma samples	63
2.3.3.2 Separation of lipoprotein components	64
2.3.4 The effect of increased lipoprotein levels on the PK of KTZ enantiomers in rat	64
2.3.4.1 Induction of HL	65
2.3.4.2 Surgical procedures	65
2.3.4.3 Dosing and sample collection	65
2.3.4.4 Determination of blood:plasma KTZ enantiomer ratio	66

2.3.5 Simultaneous determination of MDZ and KTZ in plasma	67
2.3.5.1 Instrumentation	67
2.3.5.2 Chromatographic separation	67
2.3.5.3 Preparation of stock solutions	67
2.3.5.4 Extraction procedures	68
2.3.5.5 Calibration, accuracy and validation	68
2.3.5.6 Assessment of chromatographic separation	69
2.3.5.7 Application of assay method for measuring KTZ and MDZ concentrations in rat plasma in vivo	69
2.3.6 Effect of HL on KTZ-MDZ drug-drug interaction in rat	70
2.3.6.1 Induction of HL	70
2.3.6.2 Surgical procedures	71
2.3.6.3 Dosing and sample collection	71
2.3.6.4 Determination of plasma protein binding of MDZ	72
2.4 Data analysis	72
2.4.1 PK analysis	72
2.4.2 Calculation of fu	73
2.4.2.1 KTZ enantiomer determination	73
2.4.2.2 MDZ determination	74

2.4.3 Liver concentrations	75
2.4.4 Lipoprotein fractionation	75
2.4.5 Hepatocytes	75
2.5 Statistical analysis	75
2.5.1 PK studies	75
2.5.2 Liver concentrations	76
2.5.3 Lipoprotein fraction distribution studies	76
2.5.4 Microsomal studies	76
2.5.5 Hepatocytes	77
3. Results	78
3.1 Effect of HL on PK and pharmacodynamic aspects of AM	79
3.1.1 Effect of HL on electrocardiographic changes associated with AM	79
3.1.2 Effect of HL on AM metabolism using rat hepatocytes	88
3.1.2.1 Amount remaining vs. time plots	88
a. AM metabolism by hepatocytes from NL and HL rats, in the absence of rat serum.	88
b. AM metabolism in hepatocytes from NL and HL rats, in the presence and absence of rat sera	89
c. AM metabolism in hepatocytes from NL rats when preincubated rather than coincubated with cell media or rat serum (5%).	91

3.1.2.2. Comparisons of the area under the percent AM remaining to be eliminated (ARE) vs. time curves	92
a. Influence of hepatocytes from HL or NL cells on AM metabolism in the absence of rat serum	92
b. Comparison of the effect of sera treatments on the hepatocellular metabolism of AM.	92
3.2 Effect of HL on PK and pharmacodynamics aspects of KTZ	94
3.2.1 Development of an HPLC assay for the determination of KTZ enantiomers in rat plasma	94
a. Chromatography	94
b. Assay validation	96
c. Applicability of the assay	96
3.2.2 Determination of nonlinear stereoselective PK of KTZ in rat after administration of racemate	98
3.2.3 Influence of HL on in vitro distribution of KTZ enantiomers in rat plasma	105
3.2.4 The effect of HL on the PK of KTZ enantiomers in rat.	109
3.2.5 Development of an HPLC assay for the simultaneous determination of MDZ and KTZ in rat plasma	115
a. Chromatography	115
b. Assay validation	116
c. Applicability of the assay	117
3.2.6 Effect of HL on KTZ-MDZ drug-drug interaction in rat	122

3.2.6.1 MDZ kinetics	122
a. Effect of KTZ on the kinetics of MDZ	122
b. Effect of HL on MDZ kinetics	122
3.2.6.2 KTZ kinetics	123
4. Discussion	126
4.1 Effect of HL on PK and pharmacodynamics aspects of AM	127
4.1.1 Effect of HL on electrocardiographic changes associated with AM	127
4.1.2 Effect of HL on AM metabolism using rat hepatocytes	132
4.2 Effect of HL on PK and pharmacodynamic aspects of KTZ	134
4.2.1 Development of an HPLC assay for the determination of KTZ enantiomers in rat plasma	134
4.2.2 Determination of nonlinear stereoselective PK of KTZ in rat after administration of racemate	138
4.2.3 Influence of HL on in vitro distribution of KTZ enantiomers in rat and human plasma	142
4.2.4 The effect of HL on the PK of KTZ enantiomers in rat	143
4.2.5 Development of an HPLC assay for the simultaneous determination of MDZ and KTZ in plasma	146
4.2.6 Effect of HL on KTZ-MDZ drug-drug interaction in rat	149

5.	Conclusion	154
6.	Future Directions	158
7.	Bibliography	159

List of tables

Table 1: Classification of familial hyperlipoproteinemia based on Fredrickson classification	3
Table 2: Characteristics and functions of plasma lipoproteins	8
Table 3: Effect of different chemicals on the cholesterol and triglyceride levels of rat	12
Table 4: Comparison of different hyperlipidemic animal models	13
Table 5: The ECG parameters, AM and DEA concentrations in plasma and heart, and CHOL and TG content of NL and HL saline control and AM-treated rats 12 h after the last dose	82
Table 6: Summary of the percent amount of drug remaining to be eliminated (ARE, %·h) from 0-72 h after exposure of cells to AM.	93
Table 7: Validation data of ketoconazole enantiomers assay in 100 µL rat plasma	97
Table 8: Pharmacokinetic parameters (mean±SD) of ketoconazole enantiomers (KTZ) after <i>iv</i> and oral doses of racemate.	101
Table 9: The mean ±SD cholesterol and triglyceride present in rat plasma	106
Table 10: Association of (+)- and (-)-KTZ in each fraction of normolipidemic (NL) and hyperlipidemic (HL) rat plasma samples	107
Table 11: The pharmacokinetic parameters (mean ±S.D.) of ketoconazole enantiomers (KTZ) in normal and hyperlipidemic rats after <i>iv</i> administration of 10 mg/kg of racemate.....	111

Table 12: The area under the concentration time curve (mean±S.D.) of ketoconazole enantiomers in normal and hyperlipidemic rats after oral administration of 40 mg/kg of racemate	113
Table 13: Validation data for midazolam in 100 µL rat plasma and 500 µL human plasma	118
Table 14: Validation data for ketoconazole in 100 µL rat plasma and 500 µL human plasma	119
Table 15: Plasma pharmacokinetic parameters of midazolam and ketoconazole after co-administration in individual rats.....	120
Table 16: Effect of racemic ketoconazole (40mg/kg, po) on midazolam pharmacokinetics in NL and HL rats	124
Table 17: Ketoconazole pharmacokinetic parameters in NL and HL rats.....	124

List of figures

Figure 1: overview of lipoprotein metabolism. (ACAT= acyl CoA:cholesterol acyltransferase; CETP= cholesteryl ester transfer protein; FA= fatty acid; FFA= free fatty acid; HMGR= HMG CoA reductase; LCAT= lecithin:cholesterol acyltransferase; PAP= phosphatidic acid phosphatase). From ref. [7].....	6
Figure 2: PK and pharmacodynamics from ref [67]	14
Figure 3: drug transporters in renal proximal tubules.....	29
Figure 4: major solute carriers and ABC transporters in liver hepatocytes	29
Figure 5: Chemical structure of amiodarone. Shaded area (butyl side chain) is one of the parts responsible for the unique pharmacokinetics properties of AM.	32
Figure 6: Chemical structures of ketoconazole enantiomers	34
Figure 7: Percent change in QTc interval (mean \pm SD) in normolipidemic (NL) and hyperlipidemic (HL) rats after <i>iv</i> doses of 0, 25, 50 and 100 mg/kg/d amiodarone HCl on Days 1, 3 and 6 of the study. *Significant difference between HL and NL rats ($p < 0.05$).	81
Figure 8: Amiodarone plasma and heart concentrations ($\mu\text{g/mL}$) in normolipidemic (NL) and hyperlipidemic (HL) rats 12 h after the last amiodarone HCl doses of 25, 50 or 100 mg/kg/d. * Significant difference between NL and HL rats, $p < 0.05$	83
Figure 9: The correlation between % increase in QTc interval in normolipidemic (NL) and hyperlipidemic (HL) rats and amiodarone (AM) plasma or heart concentrations of all drug-treated rats at the time of heart collection. Open circles, closed triangles and open squares represent 100, 50 and 25 mg/kg/d AM dose groups, respectively.	85

Figure 10: The correlation between heart and total or unbound plasma amiodarone concentrations in all drug-treated normolipidemic (NL) and hyperlipidemic (HL) rats..... 86

Figure 11: The correlation between plasma total cholesterol (CHOL) to triglyceride (TG) ratio with plasma amiodarone concentration, heart amiodarone concentration, and QT interval in normolipidemic (NL) and hyperlipidemic (HL) rats. Open circles, closed triangles and open squares represent 100, 50 and 25 mg/kg/d AM dose groups, respectively. 87

Figure 12: Amiodarone metabolism represented as % AM remaining vs. time curve. 500 mg/mL AM was exposed in regular cell media in the presence of hepatocytes from NL (open squares) and HL rats (closed circle) in the absence of serum. *Significant difference between NL and HL ($p < 0.05$) 88

Figure 13: Amiodarone metabolism by NL hepatocytes (NLH) treated with media alone (open square) or co-incubated with 500 mg/mL AM within NL (closed circle) or HL (open triangle) serum (5%). 90

Figure 14: Amiodarone metabolism by HL hepatocytes (HLH) treated with media alone (open square) or co-incubated with 500 mg/mL AM within NL (closed circle) or HL (open triangle) serum (5%). 90

Figure 15: Amiodarone (500 mg/mL) metabolism by NL hepatocytes treated with media alone (open square), or preincubated with 5% NL (closed circle) or HL (open triangle) serum. 91

Figure 16: Chromatograms of A. blank rat plasma sample, B. rat plasma spiked with 2500 ng/mL of (\pm)-KTZ, C. rat plasma obtained after 2h of 10mg/kg KTZ racemate dose. Abbreviation: IS internal standard. 95

Figure 17: A representative standard curve of KTZ enantiomers in rat plasma (From 62.5-5000 ng/mL) 95

Figure 18: Plasma KTZ enantiomer concentrations versus time curves from 2 rats given an oral dose of 10mg/kg KTZ racemate. (+) KTZ enantiomer represented by closed diamonds and (-) KTZ enantiomer represented by open circles..... 98

Figure 19: Plasma concentration vs. time plots of KTZ enantiomers after administration of 10 mg/kg of the racemate as *iv* doses. a.) mean±SD of all 7 rats, b.) an individual rat displaying monoexponential decline, c.) an individual rat displaying apparent nonlinearity in decline. 100

Figure 20: Mean (± S.D.) plasma concentration vs. time curves of ketoconazole enantiomers after oral racemic doses of 10, 20, 40, 50, or 80 mg/kg (n=3-4 rats per dose group). 102

Figure 21: Relationship between the racemic ketoconazole oral doses and enantiomer a.) C_{max}, and b.) AUC. 103

Figure 22: Mean rates of disappearance of ketoconazole enantiomers vs. enantiomer concentration in the presence of rat liver microsomes. Incubations were run over 15 min after being spiked with the racemate (n=2 to 4 per concentration). 104

Figure 23: Association of (±)-KTZ (sum of the enantiomers) with lipoprotein fractions incubated with NL and HL rat plasma, expressed as percentage of total recovered drug.* denotes p<0.05 between HL and NL 108

Figure 24: Association of (+)- and (-)KTZ with lipoprotein fractions incubated with NL and HL rat plasma, expressed as percentage of total recovered drug. * denotes p<0.05 between HL and NL. 108

Figure 25: Mean (± S.D.) plasma concentrations vs. time plots of KTZ enantiomers in normal and hyperlipidemic rats after *iv* administration of 10 mg/kg of racemate..... 110

Figure 26: Mean (± S.D.) plasma and liver concentrations vs. time curves of KTZ enantiomers in normal and hyperlipidemic rats after oral administration of 40 mg/kg of racemate. * Significant difference between NL and HL (p<0.05) 112

Figure 27: The mean (\pm S.D.) liver to plasma concentrations (K_p) of ketoconazole enantiomers vs. time plots and the (-):(+) -KTZ K_p ratio vs. time plots in normal and hyperlipidemic rats after oral administration of 40 mg/kg of racemate..... 114

Figure 28: Chromatograms of A. blank rat plasma sample, B. rat plasma spiked with 1000 ng/mL of KTZ and MDZ, and C. rat plasma obtained after 1h of i.v. MDZ administration (1.5h of KTZ administration)..... 115

Figure 29: Chromatograms of A. blank human plasma sample, B. human plasma spiked with 100 ng/mL of KTZ and MDZ..... 116

Figure 30: A representative standard curve of midazolam and ketoconazole assay in rat plasma (From 25-10000 ng/mL)..... 117

Figure 31: Plasma KTZ and MDZ concentration vs. time curve taken from 2 rats given 40 mg/kg KTZ orally followed 1.5 h later by 5 mg/kg MDZ i.v..... 121

Figure 32: Plasma MDZ concentration-time profile in control normo (closed diamond) and hyperlipidemic (opened circle) rats and after 40 mg/kg (\pm)-KTZ oral pre-treatment in normo (open square) and hyperlipidemic (closed triangle) rats..... 123

Figure 33: Comparative plasma concentration vs. time curves of oral (\pm)-ketoconazole (KTZ) and *iv* midazolam in the presence of ketoconazole (MDZ+KTZ). Left panel, profiles of the drugs in normolipidemic rats. Right panel, profiles of the drugs in hyperlipidemic rats. 125

List of abbreviations and symbols

~	Approximately
ABC	ATP-Binding cassette
AM	Amiodarone
Apo	Apolipoprotein
ARE	Area under % AM remaining to be eliminated
AUC	Area under the concentration versus time curve
AUMC	the area under the first moment concentration vs. time curve
CETP	Cholesteryl-ester-transfer-protein
CHOL	cholesterol
CL	Clearance
CL/F	Oral Clearance
CM	Chylomicrons
C _{max}	Peak plasma drug concentration
CV	Coefficient of variation
CYA	Cyclosporine A
CYP450	Cytochrome P450
DEA	Desethylamiodarone
DHA	Docosahexanoic acid
DME	Dulbecco's modified eagle's
E	Hepatic extraction ratio
F	Oral bioavailability
fa/fa	Fatty/fatty

fu	Unbound fraction
fg	Gastrointestinal availability
GST	Glutathione S-transferase
HCl	Hydrochloride salt
HDL	High density lipoprotein
HF	Halofantrine
HL	Hyperlipidemia (Hyperlipidemic)
HPLC	High performance liquid Chromatography
h	Hour
ip	Intraperitonealy
iv	Intravenously
IDL	Intermediate density lipoprotein
IS	Internal standard
KCl	Potassium chloride
KH ₂ PO ₄	Potassium dihydrogen phosphate
K _m	Affinity constant
K _p	Tissue to plasma concentration
K _{pu}	Tissue to unbound plasma concentration
KTZ	Ketoconazole
Kg	Kilogram
LC-MS	Liquid chromatography-mass spectrometry
LDH	Lactate dehydrogenase
LDL	Low density lipoprotein
LDL-R	Low density lipoprotein receptor

LLQ	Lower limit of quantification
Log P	Logarithm octanol/water partition coefficient
LPDP	Lipoprotein deficient plasma fraction
LPL	Lipoprotein lipase
LRP	LDL-R related proteins
L	Liter
μL	Micro liter
mL	Milli liter
μM	Micro Mole
mg	milligram
μg	micogram
min	minutes
MgSO ₄	Magnesium sulfate
mRNA	Messenger RNA
MS	Mass spectrometer
NADPH	P-Nicotinamide adenine dinucleotide phosphate terra sodium
ng	nanogram
OATs	Organic anion transporters
OATP	Organic anion transport protein
OCTs	Organic cationic transporters
°C	Degree Celsius
PK	Pharmacokinetics
PL	Phospholipids
P407	Poloxamer 407

Pgp	P-glycoprotein
r^2	Correlation coefficient
rpm	Rotations per minute
SFC	Supercritical Fluid Chromatography
SD	Standard deviation
$t_{1/2}$	Terminal elimination phase half-life
TBME	Tertiary Butyl Methyl Ether
TG	Triglyceride
Tmax	Time to reach Cmax
TRL	Triglyceride-rich lipoproteins
UV	Ultraviolet
v/v	Volume/Volume
Vd	Volume of distribution
Vdss	Volume of distribution at steady state
VLDL	Very low density lipoprotein
VLDL-R	Very low density lipoprotein receptor
Vmax	Maximum rate of formation
Vs.	Versus
W/V	Weight/Volume
W/W	Weight/Weight
α	Level of significance
λ_z	Elimination rate constant

1. Introduction

1.1 Hyperlipidemia

Hyperlipidemia (HL) is a medical condition characterized by abnormally high concentrations of plasma lipoproteins. Based on the National Health and Nutrition Examination Survey (NHANES 2005-2006), 16% of American adults over 20 years of age have total CHOL levels of 240 mg/dL or higher of which 50% are not aware of its possession[1]. HL can be caused primarily by genetic makeup, as in familial HL, or secondarily to other factors including diet, sedentary lifestyle, obesity, diseases or drugs [2-4]. Familial HL is further classified according to the Fredrickson classification based on the pattern of lipoproteins on electrophoresis or ultracentrifugation (Table 1) [5, 6]. Conditions that have been correlated with the induction of HL include diabetes mellitus, hypothyroidism, pregnancy, HIV/AIDS, malaria, nephrotic syndrome and obesity [4, 7]. Drugs associated with development of HL include birth control pills, estrogens, corticosteroids, isotretinoin, beta blockers, some diuretics, immunosuppressives such as cyclosporine A (CYA) and anti-HIV medications [4, 7].

HL is identified as a major risk factor of cardiovascular diseases specifically atherosclerosis and ischemic heart diseases [8-11]. The mechanism involved in atherosclerotic lesion formation is thought to be through a sequence starting with a chemical alteration of low density lipoproteins (LDL) in arterial walls through oxidation and nonenzymatic glycation. Mildly oxidized LDL (OxLDL) then recruits monocytes in the arterial endothelium, which become transformed into

Table 1: Classification of familial hyperlipoproteinemia based on Fredrickson classification

Lipoprotein phenotype	Familial hyperlipidemia subtype	Defect	Lipoprotein Elevation	Drug of choice
I (rare)	Familial LPL deficiency	Low activity of lipoprotein lipase	Chylomicrons	No treatment
IIa	Familial hypercholesterolemia, polygenic hypercholesterolemia, familial defective apo B100	Defective or decreased LDL receptors	LDL	Statins, bile acid sequestrants, niacin
IIb	Combined hyperlipidemia	Increased apolipoprotein B	LDL+VLDL	Statins, fibrates, niacin
III	Dysbetalipoproteinemia	Defective structure of apolipoprotein E	IDL (IDL ₁)	Fibrates, niacin
IV	Familial hypertriglyceridemia	Increased VLDL production and decreased elimination	VLDL	Fibrates, niacin
V	Endogenous hypertriglyceridemia	Increased VLDL production and decreased LPL	VLDL+Chylomicrons	Fibrates, niacin

Taken from references [6, 7]

macrophages. Macrophages then accelerate LDL oxidation, apolipoprotein B accumulation and alter the regulation of LDL receptors, making them insensitive to the increase in cell content of cholesterol (CHOL). OxLDL then increases plasminogen inhibitor levels promoting coagulation, induces expression of the vasoconstrictor endothelin, and inhibits the expression of nitric oxide (a vasodilator and platelet inhibitor). A damaging cycle then becomes entrenched, because as macrophages oxidize LDL, OxLDL in turn, both directly and indirectly, helps recruit more monocytes into the region. These events lead to massive accumulations of CHOL and formation of CHOL-laden cells called foam cells that form the first signs of fatty streaks. As the fatty streaks grow larger, the surrounding fibrous and smooth muscle tissues proliferate and form larger plaques, a process exacerbated by release of inflammatory substances from macrophages [7, 12, 13].

The contribution of HL to cardiovascular risks was shown in the Heart Protection Study (HPS) trial which included randomized patients with a nonfasting total CHOL ≥ 3.5 mmol/L. Where, administration of simvastatin 40 mg/day, an antiHL medication, decreased the relative risk of death by 13%, nonfatal myocardial infarction by 37% and nonfatal stroke by 26% compared to placebo [14]. In addition to the cardiovascular risks, HL can also be involved in other physiological effects such as increased renal failure progression and acute pancreatitis [15, 16].

1.2 Lipids and Lipoproteins

According to the current guidelines of Canada's Food Guide Facts for healthy eating, lipids should compose no more than 30% of total daily caloric intake. There are several nutritional components that are classified as lipids. Those include triglycerides (TG); phospholipids (PL); and CHOL. The basic lipid moiety of the TG and PL is fatty acid whereas the sterol nucleus of CHOL is synthesized from degradation products of fatty acid molecules [13]. TG are mainly used in the body for energy production while PL and CHOL and their derivatives are utilized to perform intracellular functions [13]. Lipid digestion and absorption involve bile salts, phospholipids, salivary, gastric and pancreatic lipases and colipase [17, 18]. Almost all fats in the diet are absorbed from the intestines and shunted into the intestinal lymph from enterocytes in the form of chylomicrons (CM) [18]. CM are then transported in the thoracic duct and enter into venous blood where they are taken up by adipose and liver tissues (Figure 1).

Lipoproteins can be classified based on their density and content of lipid, protein, and apoprotein into CM, very low density lipoproteins (VLDL), intermediate-density lipoproteins (IDL), LDL, and high-density lipoproteins (HDL) (Table 2) [4, 7, 19]. CM are primarily synthesized by the enterocytes and the remainder of the lipoproteins are almost entirely produced by liver [4, 13, 17]. The lipoprotein metabolic pathway is described in Figure 1. The presence of apolipoproteins confers some important structural and functional roles one of which is their action as ligands for lipoprotein receptors [20].

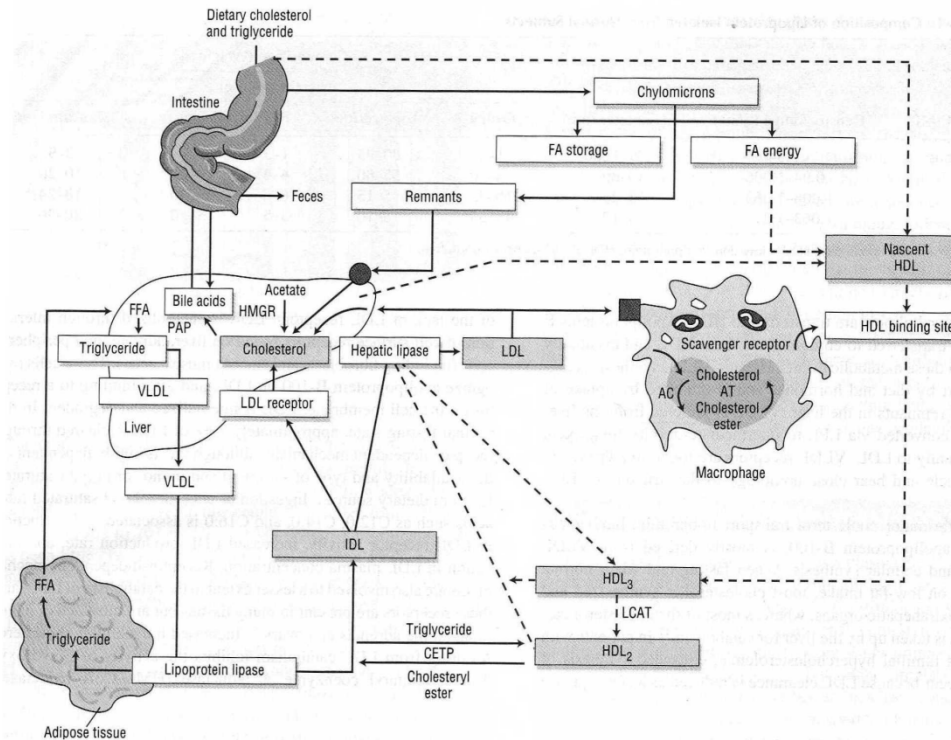


Figure 1: overview of lipoprotein metabolism. (ACAT= acyl CoA:cholesterol acyltransferase; CETP= cholesteryl ester transfer protein; FA= fatty acid; FFA= free fatty acid; HMGR= HMG CoA reductase; LCAT= lecithin:cholesterol acyltransferase; PAP= phosphatidic acid phosphatase). From ref. [7].

1.3 Lipoprotein receptors

The LDL receptor (LDL-R) family is composed of more than ten receptors [21]. Only five of the LDL-R family members have been identified to bind to lipoproteins; those include LDL-R, very low density lipoprotein receptor (VLDL-R), megalin, LDL-R related proteins (LRP), and apoER2 [20, 22, 23]. They are located in coated pits in cells and have seven characteristic features: cell surface expression, extracellular ligand binding domain consisting of complement type repeats, requirement of Ca^{2+} for ligand binding, recognition of receptor protein

and apolipoprotein (apo) E, epidermal growth factor (EGF) precursor homology domain containing YWTD repeats; single membrane spanning region, and receptor mediated endocytosis of different ligands [22].

They are synthesized by the Golgi bodies then transported in vesicles to the cell membranes. Upon recognition of their substrates, they bind, internalize and transport them intracellularly through a vesicle [20, 24]. The vesicle then degrades upon binding to lysosomes, releasing the lipids into the cytoplasm; meanwhile the receptor recycles back to the cell membrane to bind more substrates [19, 20]. The five receptors differ in their distribution in the body and the nature of their substrates. In fact, LDL-R is found in almost all tissues except for the adipose, thyroid and salivary gland. LDL-R, which are extensively expressed by the liver and adrenals [20, 25], mainly transport apo-B and apo-E containing lipoproteins including VLDL, IDL and LDL [21, 26]. The major role of the LDL-R is to regulate plasma CHOL by mediating uptake and catabolism of plasma LDL, the major carrier of plasma CHOL [22]. VLDL-R are abundant in fatty acid-active tissues (heart, muscle, adipose), macrophages and brain but not expressed in liver [21, 27]. They sequester apo-E-containing lipoproteins including VLDL and IDL but not LDL [21]. It has been also suggested that it is the VLDL-remnants, IDL, rather than VLDL, which are taken up through the action of VLDL-R mediated endocytosis [28]. Thus VLDL-R is responsible for uptake of the TG rich, apo-E-containing lipoproteins by tissues active in fatty acid metabolism [22]. Unlike LDL-R, VLDL-R expression is not down regulated by intracellular lipoproteins [21, 27]. Megalin, also known as LRP 2, is expressed in

Table 2: Characteristics and functions of plasma lipoproteins

Lipoprotein	Diameter (nm)	Density (g/mL)	Protein %	Lipid%			Apolipoprotein	Lipid transport role
				TG	CHOL	PL		
CM	75-1200	<0.94	1	88	4	7	A(1,2,4), B48, E, C(1,2,3)	Dietary TG from intestine to blood, skeletal muscle and adipose tissues
VLDL	30-80	0.94-1.006	8	54	22	16	B100, C(1, 2, 3), E	Endogenous TG from liver to extrahepatic tissues
LDL	18-25	1.019-1.063	21	11	46	22	B100, C3	CHOL from liver to peripheral tissues
HDL	5-12	1.063-1.21	50	4	20	26	A1, A2, C(1,2,3), D, E	CHOL from peripheral tissues to liver (reverse CHOL transport)

Adapted from references [4, 7, 19, 20]

absorptive epithelial cells such as those of the kidney (mainly in the glomerulus and proximal tubule cells) and lung and to a lesser extent in placenta and ovary [22, 29]. Megalin ligands include apo E, apo B, clusterin, proteases and protease inhibitors, carrier proteins for lipophilic vitamins, parathyroid hormones and polybasic drugs as aminoglycosides [20]. Therefore, megalin is involved in LDL catabolism, vitamins reabsorption by kidney [30] and can bind and help cells to take up several antibiotics [31]; thus it may be responsible, along with other members of the LDL-R family, for some of the toxic side effects observed in various tissues after the use of antibiotics [32, 33]. LRP are abundant in liver, brain, adrenal and lung [20, 34], specifically in hepatocytes, macrophages, trophoblasts, neurons, fibroblasts, pneumocytes, and smooth muscle cells [20, 34]. They are involved in the uptake of lipoprotein particles containing apo E and lipoprotein lipase and cooperate with LDL-R in removal of CHOL from the circulation [35, 36]. ApoER2 is closer to VLDL-R rather than LDL-R, with a similar broader ligand binding ability [22]. They are mostly expressed in brain and together with VLDL-R play an important role in Reelin, a cytosolic protein which help regulate neuronal migration and positioning in developing brains, signalling pathway and may act as Reelin receptors in the extracellular domains [37, 38].

1.4 Experimental models of HL

HL animal models have been developed and utilized to study the pathophysiological effects of HL on vital organs, the mechanisms involved in HL

and cardiovascular diseases and to develop new drugs, devices or techniques for HL and/or atherosclerosis therapeutics [39-44]. The choice of the animal model is usually critical and dependent on the cost, time and experimental theme to be addressed [40, 45]. Several species including monkeys, dogs, mini pigs, rabbits, golden hamsters, rats and mice have been recruited in such models. The use of non-human primates and swine is normally not practical due to cost, longevity, and ethics [40]. On the other hand small animal models are comparably cheaper and amenable to genetic manipulation [40].

The induction of HL has been initiated using several approaches in the literature, the simplest of which is through the administration of a high CHOL, Western style, diet for several weeks [40, 46, 47]. However, such methods are time consuming and present highly abnormal conditions where primarily herbivorous species are fed lipid-rich meals [40]. Such an abnormal situation may lead to unexpected outcomes such as promotion of colon cancer in some mice species [48]. HL induction has been also suggested post administration of thyrotoxic compounds leading to hypothyroidism [40, 43], treatment with estrogen, ethanol or isotretinoin [49, 50]. The mechanisms behind HL induction differ among agents. For example, the role of thyroid hormone on VLDL TG metabolism and TG homeostasis was latter attributed partially to its effect on ApoA5 levels [51].

Non-ionic surface active agents as Triton WR1339 and poloxamer 407 (P407) have been also used to induce HL [16, 44, 52, 53]. Triton WR 1339 induces HL through altering the VLDL physically rendering it resistant to lipolytic enzymes

in blood and tissues. It also increases hepatic cholesterogenesis and HMG-CoA reductase activity through the depletion of liver CHOL [53, 54]. Unfortunately, triton was found to cause hemolysis and thus its chronic administration to rodents is not feasible [55]. The increase in plasma TG and CHOL after P407 injection *ip* is due to the direct inhibition of LPL and CHOL 7- α hydroxylase enzymes and an indirect increase in CETP and lecithin CHOL acyltransferase (LCAT) enzymes to compensate for the increased CHOL burden [52, 55]. Table 3 compares the TG and CHOL levels among different HL-induced models.

In addition to rendering regular animal models HL, some genetically modified HL models have been developed. These include the Watanabe heritable hyperlipidemic (WHHL) rabbit, Zucker diabetic fatty (ZDF) *fa/fa* rat, stroke-prone spontaneously hypertensive rat (SHRSP), JCR:LA-cp rat, apoE and LDL-R knockout mice [39, 41, 42, 56-58]. Table 4 compares the different HL models.

In practice there is no perfect HL animal model, as each has its own positive and negative aspects. P407, also known as pluronic F127, is a thermoreversible, nonimmunogenic block copolymer of polyethylene and polypropylene repeating units. It is used as vehicle in controlled drug delivery applications and as a barrier for prevention of postsurgical adhesions in experimental animals [55, 59]. After P407 *ip* dosing, its half life was 21 h with only less than 3% of drug found in rat circulation at ~ 120 h [59]. Its pharmacodynamic response, increase in TG and CHOL levels, was found to

Table 3: Effect of different chemicals on the cholesterol and triglyceride levels of rat

Chemical treatment	Dose	Duration	Plasma/serum total cholesterol (mmol/L)	Plasma/serum triglyceride (mmol/L)
Control rat	-	-	1.48±0.02	1.23±0.25
HFHC diet	Added 2% CHOL	21days	2.90±0.75	0.70±0.19
Triton WR1339	250mg/kg	Single <i>iv</i> (24 h post dose)	10.05±0.39	18.23±0.41
Poloxamer P407	1g/kg	Single <i>ip</i> (36h post dose)	62.58±13.45	40.31±4.85
Isotretinoin +peanut oil	10mg/day	intragastrically for 11days	2.14±0.25	1.88±0.1
Experimental Hypothyroidism (polythiourasil)	0.1% (w/v)	In drinking water for 25 days	2.46±0.10	0.33±0.04

Adapted from ref [50, 60-63]

correlate with its pharmacokinetics (PK) data, i.e. no residual HL effect 120 h after P407 *ip* injection [55]. In addition to its use as HL animal model, chronic injection (> 4 months) of P407 to mice resulted in aortic atherosclerotic lesions [64]. Despite the dramatic increase in CHOL and TG levels post P407 injection, it is considered an acceptable model with little toxicity [64], non inflammatory action [65], absence of other metabolic diseases such as diabetes, acceptable time and cost [55].

Table 4: Comparison of different hyperlipidemic animal models

Species/Name	Mutation	Metabolic effects	Vascular pathology	Predominant plasma lipoprotein fraction
Rabbit				
WHHL	LDL-R deficient	hyperlipidemia	Atherosclerosis, spontaneous MI, valvular diseases	LDL
Mouse				
ApoE-KO	ApoE deficient	hyperlipidemia	No CVD	VLDL
LDL-R-KO	LDL-R deficient	hyperlipidemia	No CVD	LDL, HDL
Rat				
Zucker-fa	Defective ObR	Obesity/insulin resistance and hyperlipidemia	No CVD	Chylomicrons, VLDL
JCR:LA-cp	ObR truncated in the extracellular domain	Obesity/severe insulin resistance and hyperlipidemia	Vasculopathy, atherosclerosis, thrombosis	VLDL
SHRSP	Lower ApoE levels	Hyperlipidemia post HFHC diet	Atherosclerosis, hypertension	VLDL, LDL

From references [39, 41, 56, 66]

ObR: leptin receptor, CVD: cardiovascular disease, JCR:LA-cp: James C. Russel corpulent rat, HFHC: high fat-high cholesterol diet

1.5 Effect of HL on PK of drugs

The effect of systemic and postprandial HL on drug disposition will be addressed on each of the ADME elements of PK, where ADME stands for Absorption, Distribution, Metabolism, and Excretion.

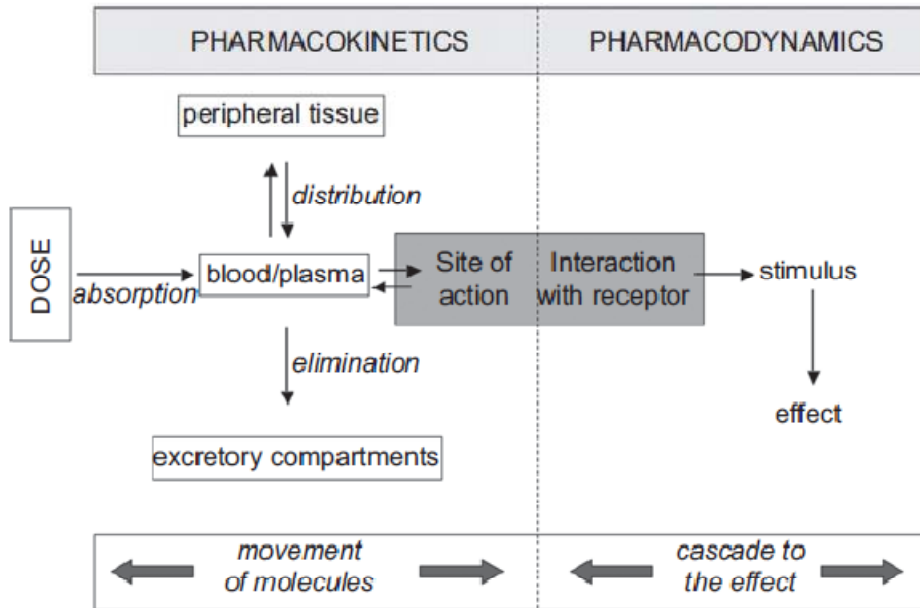


Figure 2: PK and pharmacodynamics from ref [67]

1.5.1 Absorption

The effect of lipids on oral absorption and bioavailability of drugs have been studied extensively in the literature. In fact, high fat meal studies are recommended by the FDA as they are expected to affect gastrointestinal physiology and thus the systemic availability of the medication [68]. High fat food can affect drug bioavailability through alteration of drug solubility, delaying of gastric emptying rate, stimulation of bile acid and stomach acid secretion,

changing gastrointestinal tract pH, increasing splanchnic blood flow, altering luminal metabolism and enterocyte enzyme expression and finally physically or chemically interacting with dosage forms or drug substances as in competition for active transporters [68, 69]. Such alterations in rate and extent of absorption are usually measured using C_{max} (peak plasma drug concentration), T_{max} (time to reach C_{max}) and AUC (area under concentration versus time curve).

The absorption of drugs is highly dependent on their aqueous solubility. Thus oral administration of poorly soluble drugs with lipids can increase their absorption due to their prolonged gastric residence time [70, 71]. The prolonged residence in the stomach acidic environment is likely to enhance the dissolution of basic drugs [69]. In addition to the prolongation of the gastric residence time, lipids enhance the secretion of gastrointestinal tract and pancreatic fluids, resulting in an increase in the total gastrointestinal tract fluid volume and further enhancement of drug dissolution and absorption [69, 70]. In fact fatty meals increased the AUC of albendazole and phenytoin in man by 4.5 and 2 fold, respectively [72, 73], elongated T_{max} and increased AUC of sodium salicylate in rabbit [74], and increased C_{max}, T_{max} and absolute bioavailability of the poorly soluble drug danazole in normal subjects by 2.4, 1.3 and 4 fold respectively [75]. Other drugs that were reported to have better availability due to delayed gastric emptying include chlorothiazide, rufinamide, propoxyphene, spironolactone, hydrochlorothiazide, nitrofurantoin and riboflavin [72, 76, 77]. On the other hand, increasing gastric residence time may decrease the absorption of drugs that are

acid labile, ionisable or sensitive to the action of gastric enzymes [69]. Food ingestion results in an increase in gastric hydrochloric acid and enzyme secretion and renders the blood and urine alkaline in a phenomenon known as postprandial alkaline tide [69]. Such affected medications include a variety of antibiotics such as penicillin V, erythromycin stearate, ampicillin, amoxicillin and penicillin G [69, 72, 77], as well as diclophenac sodium and chlorpromazine [72]. Marathe et al have reported that the bioavailability of avitriptan was decreased by fatty food due to the changes in gastric emptying and motility [78]. Similarly, high fat meals resulted in lower C_{max} and AUC and prolonged T_{max} for tacrolimus following 5mg doses to human subjects, indicating slower absorption and lower bioavailability [79].

High fat meals have also been shown to increase the rate of estimated splanchnic blood flow resulting in an increase in passive drug absorption due to an altered transmucosal concentration gradient [69]. In addition they increase bile secretions to the duodenum [80]. Approximately 40% of bile salts are conjugates of cholic acid, 40% are conjugates of chenodeoxycholic acid and 20% are conjugates of deoxycholic acids [81]. Bile components including bile salts, acids, PL, TG and CHOL are known modulators of drug bioavailability [82]. Bile salts above critical micellar concentrations help dissolve the lipophilic drugs, having high log octanol/water (log P) partition coefficient, through micellar solubilisation [81]. Micelles can be simple micelles consisting of merely bile salts and drug or mixed micelles containing bile salts, lecithin, lysolecithin and components of bile

digestion [81]. Among the drugs that have increased bioavailability due to bile salt solubilisation are phenytoin, griseofulvin, tocopherol, carbamazepine, diazepam, dicumarol, ketoconazole (KTZ), mefloquin, mebendazole, hydrocortisone, and dexamethasone [72, 73, 76, 77, 83, 84]. In fact postprandial HL increased the bioavailability of amiodarone (AM) in humans with an increase in AUC and Cmax of 3.8 and 2.4 fold, respectively [85]. Similarly, after administration of oral lipids to rats, AM Cmax and AUC were increased after oral dosing by 2.7 and 2.1 fold, respectively whereas there was no increase in AUC after iv dosing. The increased bioavailability after oral dosing was accompanied by no change in Tmax nor half life indicating an increase in the extent rather than the rate of absorption [86]. Similarly, oral lipids increased the bioavailability of halofantrine in man, dog and rat [87, 88]. This was attributed partly to increase in absorption possibly due to an increase in solubility and also to a decrease in clearance (CL) of the drug. It is worth mentioning that halofantrine (HF) is a chiral drug that displays stereoselectivity in its PK with the (+) enantiomer showing higher blood concentrations and AUC and lower CL and volume of distribution (Vd) in rat [89]. On the other hand bile salts can result in a decrease in absorption of some drugs that form complexes with them. Such drugs are neomycin, kanamycin, pafenolol [81].

Administration of a lipid source with lipophilic drugs ($\log P > 5$) can enhance their lymphatic transport [81]. The intestinal lymphatics are responsible for the transport of highly lipophilic drugs, lipids and lipidic derivatives through the

thoracic lymph duct and into the systemic circulation by passing the hepatic first pass metabolism thereby increasing their bioavailability [81]. Examples of compounds that are transported through the lymphatic system are HF [90], CYA [91], and many other lipophilic drugs [81].

High fat meals can interact physically or chemically to inhibit or decrease drug absorption [69]. For instance, food can act as a physical barrier preventing the drug from reaching mucosal surfaces of the gastrointestinal tract, thus affecting both passive and active transport [69]. It can also compete with drugs on the active transporters or metabolic enzymes or it may even exhibit an inhibitory effect on them [72, 81]. Increased CHOL levels resulted in a higher HF intestinal availability in rat everted intestinal sacs due to their competitive inhibition on efflux transporters of the ATP-Binding cassette (ABC) family [92]. Pre-treatment of rats with 1% CHOL in peanut oil resulted in a reduced metabolite:drug ratio of AM in rat everted intestinal sacs indicating a reduction of intestinal metabolism of AM [93].

In other cases, despite the above mentioned effects of high fat meals, some drugs' absorption were reported as not being affected. In fact, thalidomide and CYA C_{max} and AUC were not changed before and after administration of high fat meals to humans and rats, respectively [94, 95].

1.5.2 Distribution

The drug distribution in the body dictates its pharmacological and toxicological activities. In the study of drug PK, we look into rate and extent of distribution. Distribution rate is governed by tissue perfusion and drug permeability, whereas its extent is measured using a PK parameter called Vd.

The extent of drug distribution is dependent on many factors including molecular size of the drug, plasma and tissue protein binding, receptor mediated drug uptake and efflux transporters. One of the most important effects of HL on distribution extent is through the increase of the lipid fraction in plasma. Lipophilic drugs then tend to bind to plasma lipoproteins, resulting in a decrease of the unbound fraction (f_u) of the drug in plasma and in its Vd [86, 96, 97]. CYA, nelfinavir and AM showed 3.4-, 10.4- and 23-fold lower Vd, respectively, in poloxamer induced HL rat model [86, 94, 98]. Similarly, racemic HF was shown to exhibit stereoselective decreases of 26- and 36-fold in Vd of its (+) and (-) enantiomer respectively, in the same animal model [87]. HF was also observed to have 21% decrease in its Vd in HL beagle dogs [99]. In hypertriglyceridemic patients, propranolol PK parameters were changed, including a 48% decrease in Vd. This was not the case in hypercholesterolemic and mixed HL patients where no change in PK parameters was noted [100]. In HL phenytoin treated patients the extent of distribution, the Vd of phenytoin was not altered although other PK parameters such as AUC and CL were significantly increased and decreased, respectively in

hypercholesterolemic and mixed HL patients but not in hypertriglyceridemic ones where AUC tended to decrease [101].

The distribution pattern of drugs among plasma proteins differs between the NL and HL state. Albumin and α_1 -acid glycoprotein are considered the most significant plasma proteins, having preferential affinities for acidic and basic drugs, respectively. The increase in plasma lipoproteins in the HL state increases the drug binding to the lipoprotein fraction as well as decreases the drug binding to the previously mentioned lipoprotein deficient plasma fraction (LPDP) [61, 102, 103]. In HL human and rat plasma, AM was found to shift from the LPDP fraction to the VLDL, LDL and HDL fractions, with LPDP AM concentrations decreased by 3.5- and 55- fold in human and rat plasma, respectively [61]. In fact in HL, most of the drug was bound to the VLDL followed by the LDL then the HDL fraction [61]. The desethylamiodarone (DEA), AM major and active metabolite, behaved similar to the parent drug [61]. CYA was mostly found in the HDL fraction in NL patients but in the VLDL/LDL fraction in HL patients; its percentage in the VLDL/LDL fraction moved from 32% in NL patients to 46, 54 and 55% in hypercholesterolemic, hypertriglyceridemic and mixed HL patients, respectively [103]. The LPDP concentrations did not differ much among the different NL and HL groups [103]. In rat plasma CYA was mostly found in the LPDP fraction in NL rats but shifted to be mostly found in the VLDL fraction in P407 HL rats [104]. Thus in the HL state CYA concentrations increased by 5.3-, 19- and 2.2- fold in the VLDL, LDL and HDL fractions, respectively [104].

HF (+)-enantiomer was found mostly in the LPDP and HDL fractions in NL rat plasma while the (-)-enantiomer was mostly found in the LPDP fraction [102]. In P407 HL rat plasma, both (+) and (-)-enantiomers were mostly found in the VLDL fraction, not detected in the HDL fraction and their concentration in the LPDP fraction decreased by 2.5- and 3.4- fold, respectively [102]. For desbutylhalofantrine, HF's major and active metabolite, the (+) and (-) enantiomers shifted from the LPDP fraction to the VLDL fraction in HL rat plasma [102]. Amphotericin B shifted from the LPDP fraction in fasted rabbits serum to the LDL/VLDL fraction in CHOL fed ones [105]. It is worth mentioning that upon changing the formulation of amphotericin B to a lipid complex it shifted to HDL fraction in both fed and fasted rabbits [105].

The alteration in the plasma protein binding and the consequent decrease in V_d would be expected to result in a decrease in tissue concentrations of moderate and high extraction ratio (E) drugs. However, the tissue distribution of lipophilic drugs behaves in quite a complex manner [97, 102, 106]. Despite the lower f_u and V_d , AM, a moderately hepatically extracted drug, showed significantly higher plasma, heart, spleen, and liver concentrations and lower lung, kidney, and brain concentrations in rat post *iv* AM dosing [97]. Increasing the heart uptake of AM 2-fold may lead to a significant increase in pharmacological activity as heart is the site of action of this medication. It is also important to note that although the HL apparently decreased the lung concentrations of AM, DEA concentrations were increased [97]. It is known that one of the dangerous side effects of this drug is

pulmonary fibrosis and that the toxicity potency of DEA even exceeds that of the parent drug [107]. HL obese Zucker rats showed higher kidney levels of amphotericin B than control lean ones [108]. CYA concentrations in heart and spleen decreased whereas, kidney, plasma, blood and liver showed higher levels in HL rats after single *iv* dose [106]. The increase in the kidney concentrations in HL could increase the nephrotoxicity of the medication [106]. This was shown in patients with hypercholesterolemia where an increase in drug binding to LDL resulted in an increase in nephrotoxicity of CYA [109]. On the other hand, the increase of VLDL and HDL levels was found to reduce cellular uptake of CYA within LLC-PK1 pig kidney cells [110]. The (+)-HF enantiomer increased in plasma, liver, lung and spleen and decreased in heart of HL rat after single *iv* dose of HF racemate [102]; however, the (-)-enantiomer concentration increased in plasma, lung, and spleen and decreased in brain and kidney in the same animal model [102]. Despite the increase in plasma concentration in HL, it was reported that the IC_{50} of HF against *Plasmodium falciparum* significantly increased indicating a decrease in its pharmacological effect [99]. HF cardiotoxicity was enhanced in HL rats, with longer QT interval than in NL ones despite the equivalent heart concentrations between the two groups [111].

A decrease in drug concentration in some tissues in HL is expected for high and moderate E drugs, on the basis of a decrease in the f_u . However, in HL the increase of the drug concentrations and uptake in tissues is not expected based on the theory that only the unbound concentrations are capable of traversing cell

membranes. Based on such data a new concept has evolved pointing at the contribution of the LDL-R family in the transport of drugs bound to lipoproteins. The binding affinity of the drug to the lipoprotein fraction, the type of lipoprotein fraction the drug is bound to and the expression, regulation and type of LDL-R in tissues are all factors affecting such transport.

1.5.3 Metabolism

Ideally once in the circulation, drugs should reach their target organ, exert their effect and then be eliminated once the effect is no longer required. Some medications are excreted unchanged; however, most drugs are first rendered more water soluble followed by their excretion into urine or bile [67]. This occurs through several metabolic reactions involving Phase I and II enzymes. First a polar group is introduced or unmasked (Phase I), then such a group is conjugated to a hydrophilic endogenous species using conjugating enzymes (Phase II) and finally the conjugate, more water soluble and higher molecular weight, is excreted through liver or kidney through carrier mediated transport [67, 112]. Phase I enzymes include cytochrome P450 (CYP450), epoxide hydrolase and monoamine oxidase, aldehyde and alcohol dehydrogenases, and flavin containing monooxygenases and are located in the membrane of the endoplasmic reticulum. Phase II enzymes include glucuronyl transferase and glutathione S-transferase. Phase II enzymes are generally cytosolic except for glucuronyl transferase, which is microsomal [113].

The liver is the major organ involved in the metabolism of endogenous compounds and xenobiotics. The small intestine plays also an important role in oral drug metabolism prior to transport of the drug via portal circulation to the liver [67]. Other organs and tissues, including nasal mucosa, lung, kidney and blood, can also perform metabolizing activities [67, 114, 115]. If drugs are not eliminated by other means, drugs that are poorly metabolized remain longer in the body and have lower clearance and longer half life.

The rate of drug biotransformation is dependent on several factors including the drug concentration and availability at site of metabolism, the levels of enzymes, availability of cofactors and drug protein binding. It is known that only free drug is available for metabolism. Since HL usually decreases the f_u of drugs through increasing its lipoprotein binding, it is expected to decrease the metabolism and hepatic CL of drugs with moderate and low hepatic extraction ratios (E) [17, 86, 87]. In addition, liver is considered the terminal site of catabolism for lipoproteins containing apoB (Table 2) [17, 22]. Fatty acid liberation due to lipoprotein catabolism in hepatocytes was reported to directly reduce the metabolism of the drugs bound to lipoprotein [17, 116]. This happens either through direct competition with drug molecules or indirectly through modulation of drug metabolising enzymes [17]. For instance, unsaturated fatty acids have higher CYP3A inhibitory action than saturated ones [117, 118]. The mechanism by which arachidonic, linoleic and docosahexaenoic (DHA) acids down regulate phenobarbital induction of the CYP2B1 gene in rat hepatocytes is reported to be

through inhibition of constitutive androstane receptor (CAR) translocation from cytosol to nucleus [119].

HL as a disease also can alter the expression of CYP450 enzymes in liver and other tissues [17]. The P407-induced HL model showed 1.94-fold lower total CYP content compared to NL Sprague-Dawley rats, but not Wistar rats [97, 98]. CYP2C11 and CYP3A1/2 isoenzymes were the isoenzymes downregulated in the P407 model [97]. Such downregulation is not restricted to the P407 rat model but was also documented in the obese Zucker rat model; CYP1A1, 1A6, 2B1, glutathione-S transferase, and quinone reductase were also inhibited in the obese Zucker rat model [17, 120]. The downregulation of CYP3A in obese Zucker rat is thought to be due to the lower CAR levels [121], while that of CYP 3A1/2 and CYP2C11 in P407 Sprague-Dawley rat is suggested to be due to decreased expression of CAR and pregnane X transcription factors [17]. Thus HL can reduce metabolism through f_u reduction and inhibition of CYP enzymes. Although LDL-R mediated transport for the bound drug fraction counteracts such inhibition by making more drug available to the liver and other tissues metabolizing enzymes [97, 102], usually the result is a net reduction of metabolism associated with lipoproteins [86, 87].

Despite the decrease in f_u and V_d in HL rats, AM showed higher liver concentrations, possibly due to LDL-R mediated uptake [17]. There was no significant difference between the affinity constant (K_m) and the maximum rate of formation (V_{max}) of AM between NL and HL rat microsomes [97]. However, for the AM major metabolite, DEA, its formation rate was found to be higher in NL

than HL; CL through DEA formation was similarly lower in HL livers [97]. These *in vitro* results were also confirmed *in vivo* where the DEA:AM level in rats was lower in HL than NL after single *iv* AM dose, with a lower liver tissue to total plasma concentration (K_p) also being observed in HL [97]. If the f_u was solely responsible for the AM liver uptake then the liver tissue to unbound plasma concentration ratio (K_{p_u}) should match between NL and HL, However, HL liver K_{p_u} was higher indicating the possible contribution of lipoprotein receptor uptake [97]. As mentioned earlier, AM shifts mostly towards VLDL binding in HL and LDL receptors are downregulated in HL, and liver does not express VLDL receptors. This diminishes the possible role of LDL-R mediated uptake in increasing liver uptake of AM, leaving a decrease in f_u and the downregulation of CYP enzymes to decrease AM metabolism.

HF showed enantioselective PK in NL and HL conditions. It has been demonstrated that HF enantiomers showed a 10-fold decrease in the f_u , and a decrease in V_d and CL in the P407 rat HL model [87]. Despite such a decrease in the f_u , liver concentrations of (+)-HF were higher and (-)-HF concentrations were unchanged from those of the NL rats after an *iv* dose of HF [102]. This may indicate the involvement of LDL-R mediated uptake of HF. Despite the downregulation of CYP3A1/2 and 2C11 in this model, isolated liver microsomes from NL and HL rats showed no difference in V_{max} and intrinsic CL of HF enantiomers [102]. This was attributed to the involvement of other CYP enzymes in the metabolism of HF that were not affected by HL. Finally the net result, as for AM, favoured a total decrease in CL of the drug.

CYA behaved somewhat differently than AM and HF [94]. Despite the decrease in the fu in HL, human subjects and rats given P407 showed a tendency towards enhanced CL [94, 122]. This was accompanied by an increase in liver concentrations and unchanged liver to blood uptake ratio in the P407 rat model [106]. This may indicate that the effect of LDL-R mediated transport for this drug outweighs the decrease in fu and the downregulation of the enzymes, leading to a net increase in metabolism and CL.

Postprandial HL also affects metabolism. In fact, ingestion of a high fat meal was reported to decrease hepatic blood flow [69, 123]. The decrease in hepatic blood flow would be also expected to increase the bioavailability (F) of high E drugs that undergo first pass through the hepatoportal circulation [69, 123]. Such drugs include propranolol, labetolol and metoprolol [123-125]. In fact labetolol showed higher AUC, longer Tmax with no significant change on half life with food in humans [125]. In addition, a high fat meal can produce an inhibitory activity on intestinal metabolism. In fact, DHA incubation with rat liver microsomes decreased the metabolism of squinavir in a dose-dependent manner *in vitro* [126]. Similarly, coadministration of DHA with squinavir *in vivo* increased its bioavailability when given orally but not *iv*. This suggests that DHA increases the bioavailability of squinavir through inhibition of its intestinal CYP3A metabolism [127]. DHA was also reported to decrease intestinal metabolism of MDZ and CYA after oral dosing through competitive inhibition of gut CYP3A [118, 128]. An increase in AUC and a decrease of 80% in CL of diosgenin after prolonged

administration of high fat meal in rat was attributed to a reduction of its intestinal first pass metabolism due to fat ingestion [129].

1.5.4 Excretion

The pathways of drug elimination from the body involve either biotransformation to active or inactive metabolites or direct organ excretion [67]. Since we have covered drug metabolism above, in this section we will be focusing on the organ excretion of the drugs. Kidney and liver are the major excretory organs in the body.

In PK, excretion is measured through the CL parameter which is defined as the volume of blood or plasma that is irreversibly cleared from xenobiotics per unit time. Another parameter that relates to excretion is the half life which is the time for half the amount of drug in the body to be excreted.

Active transport through anionic and cationic transporters is important in renal active secretion and reabsorption as well as in biliary excretion. The transporters involved in such processes include organic anionic transporters (OATs), organic cationic transporters (OCTs), organic anion-transporting polypeptide family (OATP), type I sodium-phosphate transporter (NTP), ATP-dependent organic ion transporters including multi-drug resistance 1/p-glycoprotein (MDR1/Pgp) and multidrug resistant associated proteins (MRP). The distribution of such transporters in kidney and liver is described in Figure 3 and Figure 4.

HL could potentially affect the renal and biliary excretion of medications, thus contributing to the net CL of the lipophilic drugs. Unfortunately, the exact

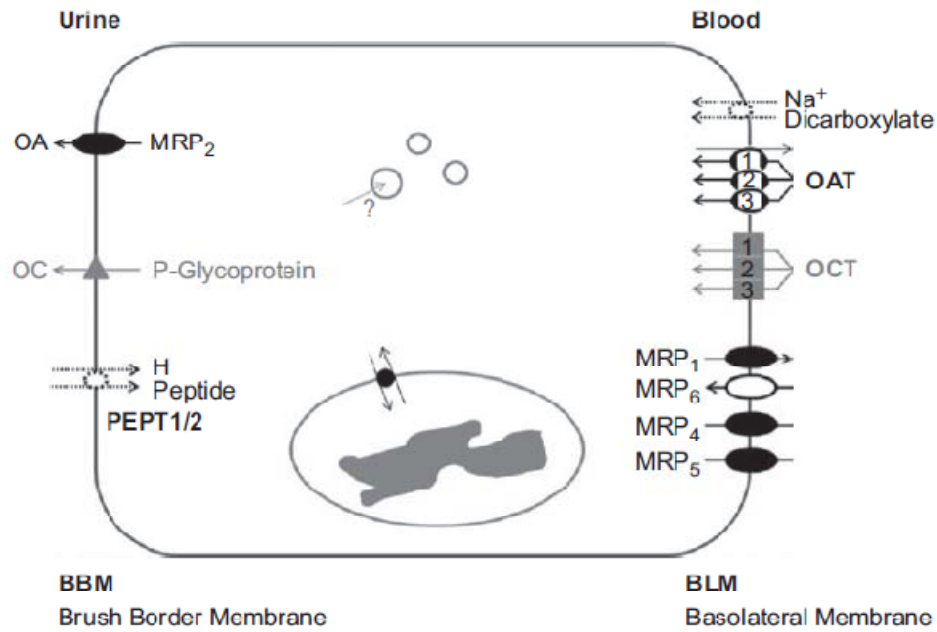


Figure 3: drug transporters in renal proximal tubules
From ref[67]

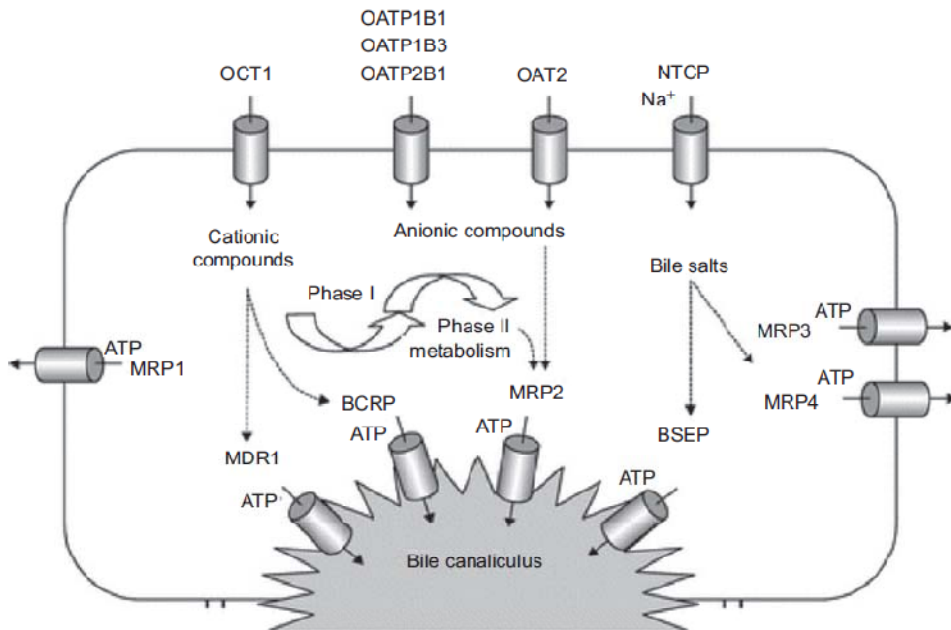


Figure 4: major solute carriers and ABC transporters in liver hepatocytes
From ref[130]

clinical contribution of such an effect is not clearly reported in the literature.

HL has been shown to affect the glomerular filtration rate [15]. It results also in an increase of bound drug, both actions would potentially decrease the drug filtered passively by glomerulus. HL has also shown an inhibitory effect on kidney P-gp activity. Where renal epithelial cell line models of rifampin induced porcine (LLC-PK1) and rat (NRK-52E) treated with 20% rat HL serum have demonstrated a 25% increase in the rhodamine (Rh 123) uptake over equivalent cells treated with 20% rat NL serum [131]. This could possibly result in a decrease of CL of drugs transported via kidney Pgp.

CYA is cleared through a combination of metabolism, biliary excretion and kidney excretion [132]. Renal CL of CYA does not represent a high portion of its total CL, reported as 2.97 mL/min for nontransplant subjects which is close to the predicted filtration rate of 2.6 mL/min. In bone marrow transplant patients the values of renal CL increased 10-fold, indicating a higher contribution of about 5% in CYA total CL [132]. Kidney AUC 24 h of CYA was 1.48 fold elevated in the P407 HL rat model [106]. Rifampin induced porcine (LLC-PK1) and rat (NRK-52E) treated with 20% rat HL serum resulted in an inhibition of Pgp and an increase of CYA concentration in cells [104]. CL

Similarly, CYA was shown to be excreted in bile with the involvement of Pgp using isolated perfused rat liver system and verapamil as a Pgp modulator. A tracer dose of CYA was excreted in bile and this amount was decreased by verapamil and that was accompanied by an increase in cholestasis [133]. Thus HL

would be expected to affect biliary excretion of CYA and other lipophilic Pgp substrates through Pgp modulation.

1.6 The PK and pharmacodynamics of two representative lipophilic drugs: AM and KTZ

1.6.1 AM

AM is classified as a Vaughan-Williams class III antiarrhythmic agent. It is chemically defined as 2-butylbenzofuran-3-yl)-[4-(2-diethylaminoethoxy)-3,5-diiodophenyl]-methanone (Figure 5). In addition to being a blocker of potassium channels, as are all class III antiarrhythmic agents, AM also possesses weak sodium channel-blocking activity, noncompetitive inhibition of α - and β -adrenergic receptors, and vagolytic and calcium channel-blocking effects [134, 135]. Such activity results in an increase in atrial and ventricular refractoriness. It also depresses automaticity of the sinoatrial node, resulting in slowing of the heart rate. The drug also slows conduction and increases refractoriness of the atrioventricular node [134]. These parameters are measurable on the electrocardiogram (ECG) as prolongation of the QRS complex and RR, PR, and QTc intervals. Owing to its proven record of efficacy and ability to reduce mortality, AM is commonly used as first-line therapy for the treatment of patients with arrhythmia [134, 136, 137].

AM is a highly lipophilic drug, with log P of 9, which contributes to its complex PK properties [134, 138]. It is extensively bound to plasma proteins

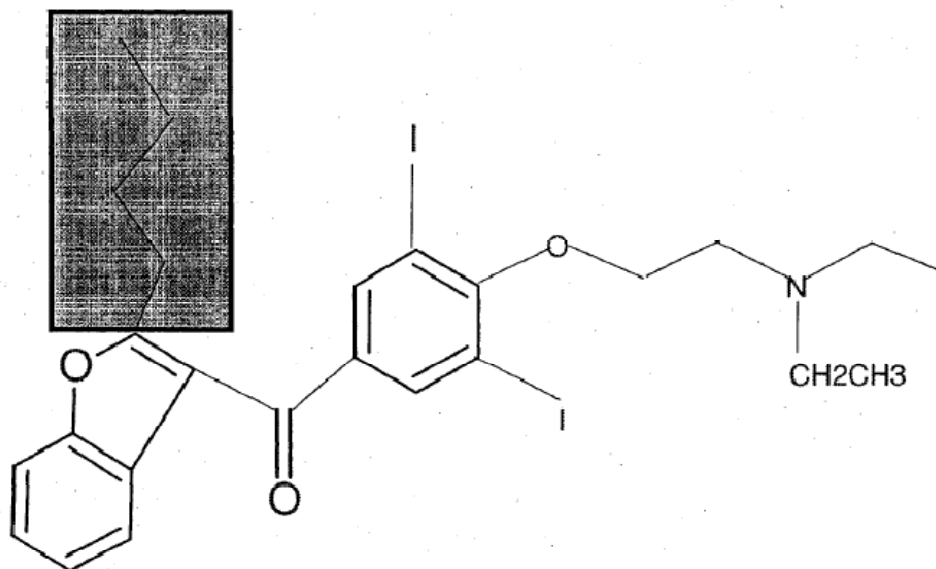


Figure 5: Chemical structure of amiodarone. Shaded area (butyl side chain) is one of the parts responsible for the unique pharmacokinetics properties of AM.
From ref [139]

of humans and rats, with a significant amount of this binding to lipoproteins [140]. AM possesses erratic absorption (35%–65%) with low and unpredictable oral bioavailability (F) [141]. Its extensive tissue uptake results in a large Vd and long terminal phase half-life ($t_{1/2}$) [86, 142, 143]. The drug also possesses a low and a low to moderate E in human and rat, respectively [86]. AM is well taken up by heart tissues, and a positive cardiac concentration versus effect relationship accounts for its changes in the ECG [97, 144, 145]. AM has a narrow therapeutic range of 0.5-2 mg/L thus have high chances of toxicity.

Replacement of the shaded butyl side chain in Figure 5 with methyl and ethyl acetate ester moieties appears to reduce the stability of the agents when incubated in plasma (possibly due to the actions of esterases), and also decreases the duration of their electrophysiological activity when in vitro or ex vivo techniques

were applied [139]. To our knowledge, actual pharmacokinetic data on these agents are not available.

AM is extensively metabolized via five pathways namely N-deethylation, hydroxylation, O-dealkylation, deiodination, and glucuronidation. N-dealkylation is probably the most important pathway in human and rat, yielding DEA, which shares many of the PK and pharmacodynamic properties of the parent drug [146]. In fact DEA has demonstrated higher potency and toxicity than its parent drug [147]. Several enzymes have been shown to be responsible for DEA formation in liver and intestine. CYP3A4 and CYP2C8 are the main isoenzymes involved in such metabolism in humans [148, 149], while CYP3A1, 3A2 and 1A1 are the major enzymes involved in rat [150]. AM was found to inhibit CYP1A1, CYP1A2, CYP2B6, CYP2C9 and CYP2D6 as well as Pgp; therefore it is expected to have drug interactions with their substrates [151].

1.6.2 KTZ

KTZ, cis-1-acetyl-4-[4-[[2-(2,4-dichlorophenyl)2-(1H imidazol-1-ylmethyl)-1,3-dioxolan-4-yl]methoxy] phenyl]-piperazine, is a broad spectrum antifungal agent used for systemic and local infections. It is a chiral drug that is administered clinically as a racemic (1:1) mixture of the enantiomers of the cis configuration (Figure 6). The cis configuration indicates that the hydrogen and the 2,4-dichlorophenyl group at the two chiral centers are on the same side of the five membered (dioxolane) ring. Their absolute configuration has been reported via

properties, KTZ is extensively used as a CYP and Pgp modulator for *in vitro* and *in vivo* drug interaction studies [127, 159-162].

Surprisingly, the PK information pertaining to KTZ is relatively limited. Human studies have shown that disproportionate changes in AUC can occur with changing dose levels, in conjunction with alterations in terminal elimination $t_{1/2}$, thereby suggesting nonlinear kinetics [163, 164]. Human studies have been limited primarily to oral administration due to the lack of intravenous (*iv*) formulations. The primary PK parameters of CL and Vd (Vd), have been determined in rats and dogs [165-168]. It is reported that a one compartment open model conforms well to KTZ plasma concentration vs. time data, with oral absolute bioavailability (F) ranging from 32% to 37% in rats and 12% to 88% in dogs [165-167]. After KTZ *iv* bolus and infusion over a range of doses, rats exhibited dose-dependent changes in the Vd, and a disproportionate increase in AUC with escalating dose [167, 168]. Over the concentration range of 0.1 to 10 mg/L, KTZ showed strong linear plasma protein binding with an average f_u of 0.037 [167]. KTZ undergoes several metabolic biotransformations, including oxidation, scission, and degradation of the imidazole ring, scission and degradation of the piperazine and dioxolane rings and oxidative O-dealkylation [169, 170].

Although some information is available regarding KTZ PK, it should be recognized that it is chiral. All previous PK data were generated using

nonstereospecific assay methodologies and as such reflected the combined kinetic properties of both KTZ enantiomers. It has been shown for many enantiomeric pairs of drugs that the pharmacological activity of one enantiomer may differ from that of its antipode [171, 172]. In fact *in vitro* studies applying KTZ enantiomers to human CYP3A4 supersomes using testosterone and methadone as substrates suggested stereoselective inhibition, with the (-)-KTZ enantiomer displaying approximately two-fold more inhibitory potency [173]. In many cases as well, the PK behaviour of one enantiomer may differ from its antipode [174, 175].

1.7 Rationale

HL is a pathological state characterized by an elevation of lipoproteins in plasma [2, 176]. Patients with HL pose clinical concerns because sustained increases in low density lipoprotein are a direct contributor to an increased risk of atherosclerosis, often resulting in hypertension and coronary heart diseases [8, 9, 177]. Elevated plasma lipoprotein levels also can influence the behaviour of lipophilic drugs *in vivo* through reducing f_u , reducing metabolism or by facilitating lipoprotein receptor-mediated drug tissue uptake [3, 106, 178-180]. AM is a lipophilic drug of $\log P=9$ with a moderate to low E. It is strongly bound to plasma proteins and was shown to be strongly bound to plasma lipoprotein in HL state, mainly to the VLDL fraction [61]. HL was shown to affect its PK and tissue distribution after single dosing [86, 97]. In fact, HL resulted in higher heart and liver concentrations and lower clearance. Whether the increase in heart uptake

is accompanied by an increase in AM pharmacodynamics on the heart and the reason behind the decrease in CL despite the higher liver concentrations needs to be explored.

Despite the fact that KTZ is a chiral drug, there are no data on its enantiomeric PK in the literature. This is due to the lack of an analytical method for their quantitation in biological specimens. KTZ is also extensively (~97-99%) bound to plasma proteins. Its Log P of 4.4 [167] suggests it to be a possible candidate for binding by serum lipoproteins and hence present altered PK in the face of HL.

1.8 Hypotheses:

1. Experimental HL increases the heart uptake and electrocardiographic changes associated with repeated-dose AM.
2. HL decreases AM metabolism.
3. The lipophilic chiral antifungal drug, KTZ, possesses stereospecific PK in rat plasma.
4. KTZ binds to lipoproteins.
5. HL affects the stereospecific PK of KTZ.
6. HL can modify the strength of drug-drug interactions involving KTZ.

1.9 Objectives:

This project has the following specific aims:

1. Examine the effect of experimental HL on the heart uptake and electrocardiographic changes associated with repeated-dose AM;
2. Examine the effect of HL on AM metabolism using rat hepatocytes;

3. Develop an HPLC assay for the determination of KTZ enantiomers in rat plasma;
4. Determine the nonlinear stereoselective PK of KTZ in rat after administration of racemate;
5. Examine the influence of HL on in vitro distribution of KTZ enantiomers in rat plasma;
6. Examine the effect of HL on the PK of KTZ enantiomers in rat;
7. Develop an HPLC assay for the simultaneous determination of MDZ and KTZ in rat plasma;
8. Explore the effect of HL on KTZ-MDZ drug-drug interaction in rat.

2. Experimental

2.1 Materials

AM HCl, ethopropazine HCl, KTZ, β -nicotinamide adenine dinucleotide phosphate tetrasodium (NDPH), sodium chloride, sodium bromide, P407, NaOH, fetal calf serum, collagenase, sodium dithionate, thiobarbituric acid, diethyldithiocarbamic acid, butylated hydroxytoluene, ethylene diamine tetraacetic acid (EDTA), trypsin inhibitor, Percoll, collagen, HEPES sodium salt, and bovine serum albumin were purchased from Sigma-Aldrich (St. Louis, MO). DEA was obtained as a gift from Wyeth Research (Monmouth Junction, NY). Methanol, acetonitrile, isopropyl alcohol, absolute ethanol, tert-butyl methyl ether (TBME), diethyl ether and hexane [all high performance liquid chromatography (HPLC) grade], diethylamine, propylene glycol, and polyethylene glycol (PEG) 400 (analytical grade) were purchased from Fisher Scientific (Fair Lawn, NJ, USA). Potassium dihydrogen orthophosphate (KH_2PO_4), dipotassium hydrogen orthophosphate, KCl, $\text{MgCl}_2 \cdot 6\text{H}_2\text{O}$, sucrose, and $\text{CaCl}_2 \cdot 2\text{H}_2\text{O}$ (all analytical grades) were obtained from BDH (Toronto, ON, Canada). Isoflurane USP was purchased from Halocarbon Products Corporation (River Edge, NJ, USA). Penicillin-streptomycin, insulin, dexamethasone phosphate, DME media, and trypsin were obtained from GIBCO, Invitrogen Corporation (Carlsbad, CA, USA). Heparin sodium injection, 1000 U/mL and 10000 U/mL, were obtained from Leo Pharma Inc. (Thornhill, ON, Canada). AM HCl (50 mg/mL), midazolam (MDZ) (5 mg/mL) and diazepam (5 mg/mL) as sterile injectable solutions were manufactured by Sandoz (Boucherville, QC, Canada). KTZ oral tablets (Nizoral[®], McNeil Consumer Healthcare, Guelph, Ontario, Canada) were

purchased from the hospital pharmacy department at the University of Alberta Hospitals.

Enzymatic assay kits for determination of total CHOL and TG in human and rat plasma samples were purchased from Diagnostic Chemicals Limited (Charlottetown, Prince Edward Island, Canada).

2.2 Effect of HL on the PK and pharmacodynamic aspects of AM

2.2.1 Assays

2.2.1.1 Determination of AM using an LC-MS method

A previously reported validated LC-MS method was used for the analysis of AM and DEA in plasma, heart tissues and hepatocytes [180]. For the assay of drug and metabolite, corresponding blank drug-free plasma, homogenized heart tissues and hepatocyte cells from HL and NL rats spiked with known amounts of AM and DEA were used for the construction of standard curves.

2.2.1.2 Lipid measurement

Total CHOL and TG concentrations were determined using peroxidase enzymatic CHOL and TG assay kits. Two mL of CHOL or TG reagents was added to human or rat NL or HL plasma samples or fractions. Normolipidemic (NL) plasma was defined as having CHOL and TG concentrations of <200 mg/dL. Tubes were incubated at 37°C for 5 or 10 min and scanned at 505 or 515 nm, respectively, using an colorimetric spectrophotometer [105].

2.2.2 Determination of the effect of experimental HL on the electrocardiographic changes associated with AM

All study protocols were approved by the University of Alberta Health Sciences Animal Policy and Welfare Committee. Male Sprague–Dawley rats (Charles River, Quebec, Canada) with body wt ranging from 250 to 350 g were used for PK, pharmacodynamic, and tissue distribution studies. All rats were housed in temperature controlled rooms with 12 h light per day. The animals were fed a standard rodent chow containing 4.5% fat (Lab Diet® 5001, PMI nutrition LLC, Brentwood, USA). Free access to food and water was permitted prior to the experiments.

2.2.2.1 Induction of HL:

The HL rats were injected 1 g/kg intraperitoneal (*ip*) doses of P407 (0.13 g/mL solution in normal saline). To ensure the proper injection of P407, the animals were lightly anesthetised using isoflurane, and then allowed to recover. The NL control groups were injected normal saline in equivalent amounts. Dosing is usually performed at 36 h after *ip* injection.

2.2.2.2 Surgical procedures:

The day before the experiment, the jugular veins of the rats were catheterized with a cannula under isoflurane anesthesia (Surgivet, Waukesha, WI, USA). Each cannula was made by inserting 2-3 cm of silastic tubing (Laboratory tubing, 508-003, Dow Corning Corporation, Midland, MI, USA) over the tip of approximately 5 cm length of polyethylene tubing (Intramedic[®], Clay Adams, Sparks, MD, USA)

with about 0.5 cm of overlap. The silastic tubing end was inserted into the right jugular vein and the polyethylene end was pulled out through the dorsal side of the neck. The exposed areas were closed using a surgical suture. The cannula was flushed with 20 u/mL heparin in 0.9% saline and the end of the cannula was capped with a 23 G stainless steel needle, which was crimped using pliers. After recovery, each rat was allowed to have free access to water but not food. The morning after, each rat was transferred to a metabolic cage and after adaptation for approximately 30 minutes with free allowance to water, they were dosed intravenously or orally (feeding gavage) with the desired drug based on the protocol of the study. After obtaining the two hour samples they were given food. However, for the AM multiple dosing PK-pharmacodynamic study access to food was allowed throughout the whole study.

2.2.2.3 Dosing and sample collection

This study was performed using a total of 56 male Sprague–Dawley rats. The rats were allocated into several groups, stratified by lipoprotein status and AM dosage. The protocol included saline-treated control rats, and rats given discreet AM dose levels of 25, 50 and 100 mg/kg/d. For each of these groups there was a matching NL and HL group. Each drug-free control group included 4 rats, whereas each of the AM dosed groups for NL and HL status contained 8 rats.

At the dose levels described above, AM or equivalent volume of saline vehicle was injected every 12 h for 5 d, for a total of 10 doses starting ~36 h after the first *ip* doses of P407 or saline. The AM injectable solution was diluted using saline for injection to provide a final concentration of 12.5 mg/mL. Each *iv* dose was

injected over 60 s via the jugular vein cannula, followed immediately by injection of 0.5 mL of 0.9% NaCl for injection and 0.15 mL of cannula lock solution consisting of 25% heparin 1000 U/mL, 55% polyethylene glycol 400, and 20% cefazolin 100 mg/mL. Because of the known PK and duration of effect of P407 [59], the HL state was maintained over the course of the study by injecting the animals with a second dose of P407 just after the 5th dose of AM was administered. The NL rats were injected equivalent volumes of saline i.p. at the same times.

Under light isoflurane anaesthesia, 12 s ECG strips were recorded using stainless steel subdermal needle electrodes, P55 general purpose AC preamplifier and PolyVIEW[®] data acquisition and analysis system (Grass Instrument Division, Astro-Med, Inc, West Warwick, RI). The ECG recordings were collected at baseline conditions (at the time of the first pre-study dose of P407) and 12 h after doses 1, 5 and 10 during the AM post-distributive phase [86]. The PR, RR and QT intervals, the latter of which was measured from the Q wave deflection to the time where the isoelectric point was reached following the T-wave, were recorded. The QT interval was normalized to the heart rate (QTc) using Fridericia's ($QTc=QT/(RR)^{1/3}$) and Bazett's ($QTc=QT/RR^{1/2}$) formulas [181, 182]. After collection of all the ECG strips, a random code value was assigned to each strip prior to measurement of ECG parameters. This ensured that the ECGs were evaluated in a blinded fashion by the assessor, who did not know which treatment was given or time of ECG obtainment of each measurement.

In conjunction with the ECG data collection, blood samples (0.15-0.2 mL) were withdrawn from the tail vein immediately after measurement of the ECG at baseline, and after doses 1 and 5. Cardiac puncture was used to withdraw blood at the end of the study. The plasma was separated from blood by centrifugation for 5 minutes at 2500 g and used for measurement of AM and DEA plasma concentrations. The blood withdrawn at the end of the study was also used to measure plasma lipid concentrations. After blood withdrawal by cardiac puncture, hearts were also harvested followed by blotting with tissue paper to remove excess blood. All plasma and tissue specimens were stored at -30°C until assayed.

2.2.3 Effect of HL on AM metabolism using rat hepatocytes *in vitro*

The isolation of hepatocytes followed a two step liver perfusion procedure [183] with minor modifications.

2.2.3.1 Preparation of perfusion solutions

Three different perfusion solutions were used for the isolation of hepatocytes. Among those, solution A was prepared by dissolving 115 mM sodium chloride, 5 mM potassium chloride, 1 mM of potassium dihydrogen phosphate, 25 mM HEPES sodium salt, 0.5 mM ethylene glycol tetraacetic acid, 0.8 g of glucose and 0.8 mL of heparin in a final volume made up with 500 mL of deionized water. Solution B was prepared by dissolving 115 mM sodium chloride, 5 mM potassium chloride, 1 mM potassium dihydrogen phosphate, 25 mM HEPES sodium salt, 0.8 g of glucose, 0.8 mL of heparin, 1 mM calcium chloride, trypsin

inhibitor and collagenase (collagenase was added just before perfusion) in 500 mL of deionized water. Solution C consisted of 100 mL of solution B supplemented with 1.2 mM magnesium sulphate and 1 mL of DME media. All the solutions were brought to pH 7.4 (by using 1M HCl or 1M NaOH) and filtered through a 22µm membrane prior to use. One day before the experiment, preliminary perfusion solution A₁ (500 mL of 115 mM sodium chloride, 5 mM potassium chloride and 1 mM potassium dihydrogen phosphate in water), A₂ (100 mL of 25 mM Hepes sodium salt in water), A₃ (0.5 methyleneglycol tetra acetic acid dissolved in 50 mL of deionized water), 1 mM calcium chloride solution and 1.2 mM magnesium sulphate solution, were prepared. On the day of experiment solution A, B and C were prepared with appropriate proportions of preliminary perfusion solutions.

2.2.3.2 Isolation of rat hepatocytes

This study was approved by the University of Alberta Health Sciences Animal Policy and Welfare Committee. Sprague-Dawley rats (350-450 g) were used for isolation of hepatocytes. These rats were housed in cages and fed with water and food. At 36 h before the experiment, rats were rendered NL or HL by intraperitoneal injection of saline or poloxamer 407 (1g/kg) under light isoflurane anaesthesia. On the day of experiment the rats were anaesthetised with isoflurane. A midline laparotomy was performed and the portal vein and the suprahepatic inferior venacava were cannulated. All tubing and solutions were maintained at 37°C and saturated with 100% O₂. The liver was perfused through the portal vein

with solution A with a flow rate of 35mL/min for 8-10 min using a peristaltic pump until all the blood was out. Then the liver was perfused with solution B with a flow rate of 30 mL/min for 10-15 min until the liver appeared completely blanched and softened. Externally the liver was washed with normal saline (0.9% sodium chloride solution) during the entire period of isolation. After perfusion with solution B, the liver was removed and placed in a Petri dish containing 100 mL of solution C and the capsule was stripped away from one side of the liver and cells dissociated by brushing the liver with a plastic comb. The cells were then filtered through a cloth filter into a funnel and kept in a shaking water bath for 5 min at 37°C and supplemented with 100% O₂ with gentle shaking. After 5 min incubation, the cell suspension was filtered again through 100 µm filter into 50mL sterile cell culture plastic tubes (VWR International, Mississauga, Ontario, Canada) and placed on ice until it was 4° C. Thereafter, the cells were centrifuged at 1000 rpm for 5 min at 4° C and the supernatant was aspirated and cells were resuspended in the DME media (additive-free) and centrifuged for a 2nd time at 1000 rpm for 5 min at 4°C. The second centrifugation step was repeated twice. After completion of all centrifugation steps, the supernatant was aspirated and the cells were added to a Percoll gradient (prepared by adding 6.75 mL of 2X phosphate buffer saline (PBS), 8.25 mL of 1x PBS and 10 mL of Percoll) and again centrifuged at 4000 rpm for 10 min at 4° C. Finally, the supernatant was aspirated and cells were resuspended in DME media containing additives and the cells were adjusted to 0.5 millions/mL.

2.2.3.3 Determining the viability of hepatocytes

Cell viability was determined by using the trypan blue exclusion method. For this purpose, 50 μL of cells were diluted with 150 μL DME media and stained with 100 μL of 0.2% trypan blue solution. Each time, the cells were counted in 16 microscopic squares and the viable cells were expressed in million/mL excluding the dead cells. Cells were quantitated using a homocytometer.

2.2.3.4 Preparation of primary cultures

24-well plastic culture plates (VWR International: Mississauga, Ontario, Canada) precoated with collagen were used for seeding the cells. After viability assessments, the cells were added in an appropriate quantity of DME media supplemented with 10% fetal calf serum and antibiotics (penicillin/streptomycin, 1%). 0.25 million cells were added per well and the plates were incubated for 6 h at 37°C in a humidifier with 95% O₂ and 5% CO₂. After 6 h, media containing the dead cells was removed and cells were treated with drug in the presence or absence of 5% NL and HL serum in media.

2.2.3.5 Drug solutions

a. Stock solutions

1. A 2.5 $\mu\text{g}/\mu\text{L}$ concentration was prepared by dissolving 10 mg AM HCl in 4 mL of dimethyl sulfoxide (DMSO) solution.
2. A 10 $\mu\text{g}/\mu\text{L}$ concentration was prepared by dissolving 20 mg AM HCl in 2 mL of methanol.

b. Treatment (working) solutions

i) AM for use in control and serum pre-incubation treatments: 10 μL of AM (2.5 $\mu\text{g}/\mu\text{L}$) in DMSO was dissolved in 50 mL media to provide a final concentration of 500 ng/mL

ii) AM for coincubation with hepatocytes and rat sera: 2.5 μL of AM HCl (10 $\mu\text{g}/\mu\text{L}$) in methanol were added to 2.5 mL of NL or HL serum to provide a final concentration of 10 $\mu\text{g}/\text{mL}$ AM HCl. The mixture was vortex mixed for 30 s and incubated in a shaking water bath for 1h at 37°C to facilitate the association of AM with serum lipoproteins. The amount of methanol added to the serum did not exceed 0.1%. Afterwards the 2.5 mL of NL or HL serum AM mixture drug was added to 50 mL media so that the final drug and serum concentration in media were 500 ng/mL and 5% respectively.

c) Media preparation:

DME media was supplemented with 10% fetal calf serum, 1% penicillin/streptomycin antibiotic, 0.0063 mg/mL insulin, and 1M dexamethasone. The pH was adjusted to 7.4 using 1 M HCl or 10 M NaOH.

d. Collection of NL and HL serum

HL Rats received 1 g/kg P407 (0.13 g/mL in normal saline) *ip* about 36 h prior to the plasma collection[61]. The rats were allowed free access to water and food for these 36 h. In the NL group an equivalent volume of normal saline was injected on the day of collection of plasma samples. NL and HL blood was collected by

cardiac puncture in glass test tubes and kept at 4°C for 30 min. The serum was then separated from blood samples by centrifugation for 10 min at 2500g. These sera were then stored at -20°C until used

2.2.3.6 Hepatocytes-AM incubations

All experimental groups were treated with AM (500 ng/mL) for 0-72 h (n=6 wells for each time points). In serum treatment groups, cells were pre-incubated or co-incubated with NL or HL serum. In serum pre-incubation group (n=3 rats), NL hepatocytes were preincubated for 24 h at 37°C with media or 5% NL or HL serum in media. After 24 h, media containing serum was removed and treatment was initiated with drug incubated with media alone. For serum co-incubation groups (n=3 NL and n=3 HL rats), the AM serum mixture described above was added to the wells containing NL and HL hepatocytes. In the group containing no serum (n=6 NL and n=6 HL rats), AM in media (500 ng/mL) was co-incubated with NL or HL hepatocytes. At various time points from 0-72 h after drug treatment, experiments were terminated by addition of 0.5 mL 1N NaOH to each well and samples collected in Eppendorf tubes and stored at -30°C until analyzed for the concentration of AM remaining.

2.3 Effect of HL on the PK and pharmacodynamic aspects of (±)-KTZ

2.3.1 Stereospecific HPLC assay for the determination of KTZ enantiomers in biological specimens

To test some of the hypotheses regarding KTZ, assays were developed for its quantitation. One of these efforts involved development of a stereospecific liquid

chromatographic assay for determination of KTZ enantiomers in rat plasma using AM as internal standard (IS).

2.3.1.1 Instrumentation

The HPLC system consisted of a Waters 710B WISP auto-injector, Waters 510 pump (Waters, Milford, MA, USA), and a HP 1050 UV detector (Hewlett Packard, Palo Alto, CA, USA). The chromatographic data were collected and compiled by use of EZChrom software (Scientific Software, Pleasanton, CA, USA).

2.3.1.2 Chromatographic separation

The chromatographic separations of AM IS, and KTZ enantiomers were accomplished using a 250mm × 4.6mm ChiralPak AD column (Diacel Chemical Industries, LTD. NJ, USA) attached to a pre-column holder for PVDF-Cartridges 4-4 containing Lichrospher 100 Diol 5µm guard column (Merck, KGaA, Darmstadt, Germany). The mobile phase used was a 70:20:10 (V/V/V) mixture of hexane, absolute ethanol and 2-propanol to which 0.1% diethylamine had been added. The mobile phase was pumped isocratically at a flow rate of 1.5 mL/min. The UV wavelength was set at 240nm.

2.3.1.3 Preparation of stock solutions

A 100 mg/L stock solution of KTZ was prepared by dissolving 10 mg of (±)-KTZ in 100 mL methanol. A 100 mg/L stock solution of AM (IS) was prepared by dissolving 10 mg of AM HCl in 100 mL methanol. The stock solution of AM was

stored in -30°C while the KTZ solution was kept at 4°C. All working standard solutions were prepared daily by sequential dilution of stock solution in methanol.

2.3.1.4 Extraction procedures

a. Rat plasma, blood, buffer and fractions

AM (0.02 mL) was added to each 0.1 mL plasma sample in a 2 mL polypropylene microcentrifuge tube. To this, 0.3 mL of acetonitrile was added to precipitate the plasma proteins. Because methanol was present in the standard curve samples, an equivalent amount was added to the test samples as well (0.125 mL). The tubes were briefly vortex mixed (4 s) at high speed then subsequently centrifuged for 3 min at ~2500 g. The supernatants were carefully transferred to new glass tubes using Pasteur pipettes. Then 0.05 mL of 0.1 M HCl and 1 mL of hexane were subsequently added to each tube as a washing step. The tubes were then vortex mixed for 30 s and centrifuged at ~2500 g for 3 min. The organic hexane supernatant was carefully aspirated and then 0.075 mL of 0.1 M NaOH and 5 mL of TBME were added. The tubes were then vortex mixed again for 30 s and centrifuged at ~2500 g for 3 min. The organic layer was transferred to new glass tubes and evaporated to dryness in vacuo. The residues were reconstituted in 150 µL mobile phase of which 75-125 µL volumes were injected into the HPLC. For the assay of whole blood, buffer, blood-buffer, blood-diluted plasma mixtures, LPDP, TRL, LDL, and HDL from the plasma protein binding, blood: plasma ratio and plasma lipoprotein fractions determinations, standard curves were prepared from similar drug-spiked matrices.

b. Liver microsomes

Denatured microsomal media was used and spiked for standard curve preparation. Briefly, to the tubes containing 500 μL of microsomal incubation mixture and 1.5 mL of acetonitrile, 100 μL of IS in methanol (100 $\mu\text{g}/\text{mL}$ AM HCl stock) and 125 μL methanol were added. The tubes were briefly vortex mixed for 4 s at high speed then subsequently centrifuged for 3 min at ~ 2500 g. The supernatant was carefully transferred to new glass tubes. The tubes were rendered acidic using 1M HCl and then 2 mL of hexane was added. The tubes were vortex mixed for 30 s and centrifuged for 3 min. The organic supernatant was carefully aspirated, followed by the addition of 1M NaOH and 7 mL TBME. The tubes were then vortex mixed again for 30 s and centrifuged at ~ 2500 g for 3 min. The organic layer was transferred to new glass tubes and evaporated to dryness *in vacuo*. The residues were reconstituted in 150 μL mobile phase of which 75-125 μL volumes were injected into the HPLC. For standard curve construction, drug-free microsomal preparations were used and spiked with appropriate amounts of (\pm)-KTZ.

c. Liver homogenates

Liver homogenates were used and spiked for standard curve preparation. Briefly, to the tubes containing 400 μL of liver homogenate and 1.5 mL of acetonitrile, 100 μL of IS in methanol (100 $\mu\text{g}/\text{mL}$ AM stock) and 125 μL methanol was added. The tubes were briefly vortex mixed for 4 s at high speed then subsequently centrifuged for 3 min at ~ 2500 g. The supernatant was carefully

transferred to new glass tubes. The tubes were rendered acidic using 1M HCl and then 2 mL of hexane was added. The tubes were vortex mixed for 30 s and centrifuged for 3 min. The organic supernatant was carefully aspirated, followed by the addition of 1M NaOH and 7 mL TBME. The tubes were then vortex mixed again for 30 s and centrifuged at ~2500 g for 3 min. The organic layer was transferred to new glass tubes and evaporated to dryness *in vacuo*. The residues were reconstituted in 150 μ L mobile phase of which 75-125 μ L volumes were injected into the HPLC. For standard curve construction, drug-free liver homogenates were used and spiked with appropriate amounts of (\pm)-KTZ.

2.3.1.5 Calibration, accuracy and validation

Calibration curves were constructed using samples of 0.1 mL rat plasma. The curve ranged from 62.5-5000 ng/mL of each KTZ enantiomer. The ratio of measured drug to IS peak height and area was calculated and plotted vs. its nominal concentration. Owing to the wide range of concentrations, the calibration curve data were weighed by a factor of 1/KTZ enantiomer concentration. All standard curves and quality control samples were generated by spiking the drugs in the similar matrices as the samples.

Intraday accuracy and precision of the assay were determined using five sample replicates of 62.5, 125, 500 and 2500 ng/mL of each KTZ enantiomer. Rat plasma samples were assessed for interday accuracy and precision by repeating the assay on three separate days. For each daily run, concentrations were determined by comparison with a calibration curve prepared on the day of the analysis. Precision

was determined using percentage coefficient of variation (CV %) which was calculated as

$$CV\% \text{ interaday} = \frac{100 \times SD}{\text{mean measured concentration}}$$

and

$$CV\% \text{ interday} = \frac{CV\% \text{ run 1} + CV\% \text{ run 2} + CV\% \text{ run 3}}{3}$$

Bias was assessed using mean intra- or interday percentage error of the mean, which was calculated as:

$$\text{Mean \% error intraday} = 100 \times \frac{\text{measured concentration} - \text{expected concentration}}{\text{expected concentration}}$$

and

$$\text{Mean \% error interday} = \frac{\text{error\% run 1} + \text{error \% run 2} + \text{error\% run 3}}{3}$$

2.3.1.6 Assignment of KTZ enantiomer optical rotation and test for racemisation

The order of elution of (+) and (-) enantiomers were determined by collecting eluent fractions from repeated injections. There were ~25 injections made into the HPLC, with ~180 µg racemate per injection. After compiling the eluent fractions corresponding to each enantiomer, they were dried *in vacuo*, reconstituted in methanol and the optical rotation determined using a Perkin Elmer 241

polarimeter (PerkinElmer Life And Analytical Sciences, Waltham, Massachusetts, USA).

KTZ enantiomer fractions of 10000 ng each were collected. Each enantiomer fraction was divided into three aliquots, and then dried in vacuo. The contents of the tubes were extracted according to the procedure described above. The samples were reconstituted in 150 μ L of mobile phase, and 125 μ L was injected into the HPLC.

2.3.1.7 Assessment of chromatographic separation

The capacity factor (K') was calculated by use of the equation $K' = (t_r - t_m) / t_m$, where t_r and t_m are the retention times of the peak of interest and the non-retained peak (solvent front). The separation factor (α) was calculated as $\alpha = K'_J / K'_I$, where component J is the more strongly retained compound. The resolution factor (R_s) was calculated as $R_s = (t_{R,J} - t_{R,I}) / 0.5(W_{t,J} + W_{t,I})$, where W_t is the width at the base of the peak. The symmetry index was determined by first determining the peak width at 10% of peak height. The latter part of the width from time of peak height onwards was divided by the first part of the width up to the time of peak height.

2.3.1.8 Application of the assay method for measuring KTZ enantiomer concentrations in rat plasma *in vivo*

In order to assess the applicability of this method *in vivo*, two rats (250-300 g) were administered 10 mg/kg (\pm)-KTZ orally.

Serial blood samples were collected from a previously inserted jugular vein cannula at 0.5, 1, 2, 3, 4, 6, 8, 10 and 24 h post KTZ oral dose for the separation

of KTZ enantiomers. Plasma was separated by centrifugation of the blood at 2500 g for 3 min. The samples were kept at -30°C until assayed using the developed HPLC methods. Non-compartmental methods were used to calculate the PK parameters. The elimination rate constant (λ_z) was calculated by subjecting the plasma concentrations in the terminal phase to linear regression analysis. The $AUC_{0-\infty}$ was calculated using the combined log-linear trapezoidal rule from time 0 h postdose to the time of the last measured concentration, plus the quotient of the last measured concentration divided by λ_z . The C_{max} and T_{max} were determined visually.

2.3.2 Nonlinear stereoselective PK of KTZ in rat after administration of racemate

All study protocols were approved by the University of Alberta Health Sciences Animal Policy and Welfare Committee. Male Sprague–Dawley rats (Charles River, Quebec, Canada) with body wt ranging from 250 to 350g were used for PK, pharmacodynamic, and tissue distribution studies. All rats were housed in temperature controlled rooms with 12 h light per day. The animals were fed a standard rodent chow containing 4.5% fat (Lab Diet® 5001, PMI nutrition LLC, Brentwood, USA). Free access to food and water was permitted prior to the experiments.

2.3.2.1 Surgical procedures:

This is described above under 2.2.2.2.

2.3.2.2 Dosing and sample collection

A total of 27 male Sprague-Dawley rats (Charles River Canada) were included in the PK study. Rats were allocated into six groups: one group *iv* dosed with 10 mg/kg racemic KTZ (n=7) and five groups orally administered 10, 20, 40, 50 or 80 mg/kg racemic KTZ (n=3-4 each).

The KTZ *iv* dosing solution was prepared by dissolving powdered racemic compound in 9:1 polyethylene glycol 400: propylene glycol (10 mg/mL) [167]. The *iv* dose was injected over 2 min via the jugular vein cannula, immediately followed by injection of approximately 1 mL of sterile normal saline solution over the next two min. At the time of first sample withdrawal, the first 0.2 mL volume of blood was discarded. For oral dosing, KTZ (44 mg/mL) suspension was prepared. The tablets of (±)-KTZ were ground to a powder using a mortar and pestle, then dispersed in 1% methylcellulose. On the morning of the PK study, the rat groups received the desired dose by oral gavage. For both routes of administration, food was provided to animals 2 h after the dose administration.

Serial blood samples (0.15-0.25 mL) were collected at 0.5, 1, 2, 3, 4, 6, 8, 10 and 24 h postdose for oral dosing and at 0.08, 0.25, 0.75, 1, 1.5, 2, 3, 4, 5, 6, 8 and 10 h postdose for *iv* dosing into polypropylene microcentrifuge tubes. Heparin in normal saline (100 U/ml) was used to flush the cannula after each collection of blood. Plasma was separated by centrifugation of the blood at 2500 g for 3 min. The samples were kept at -30°C until assayed for KTZ enantiomers.

2.3.2.3 Microsomal incubations

Microsomal incubations were conducted using rat hepatocytes to understand stereospecific aspects of KTZ enantiomer metabolism.

a. Microsomal preparation

Four male Sprague-Dawley rats (Charles River Canada, Montreal, QC, Canada) were put under mild isoflurane anaesthesia and either their liver were removed and washed thoroughly in cold KC1 solution (1.15% W/V in distilled water). The liver was cut into pieces and homogenized separately in cold sucrose solution (0.25 M in distilled water) by using a homogenizer (5 g of tissues in 25 mL of sucrose). After homogenization, liver tissue was centrifuged at 10,000 rpm for 8 minutes in Optiseal propylene tubes using refrigerated ultracentrifuge (Beckman L-80 ultracentrifuge, Beckman instruments, Inc. Palo alto, Ca. USA). Then supernatants were transferred to new Optiseal propylene tubes and centrifuged again at 14,000 rpm for 10 minutes. Centrifugation continued again by transferring supernatants to new Optiseal propylene tubes and adding $\text{CaCl}_2 \cdot 2\text{H}_2\text{O}$ dihydrate 1M (10 up/mL supernatant) at 21,500 rpm for 15 more minutes. Then the pellets were resuspended in 1.15% KC1 solution and centrifuged at 21,500 rpm for 15 minutes. The pellets were collected in sucrose 0.25 M solution and stored at -80°C [184].

b. Assay of microsomal protein

The Lowry assay method is based on comparing the concentration of an unknown protein preparation with serial standard solutions of bovine serum albumin (BSA).

In order to assay the concentration of protein in microsomal preparations of liver and gut tissues, the following solutions were required:

Reagent A contained 1mL of CuSO_4 1% in distilled water, 1mL of sodium and potassium tartarate 2% in distilled water, and 20 mL of Na_2CO_3 anhydrous 10% in 0.5 M NaOH. Reagent B contained 1:10 diluted solution of Folin-phenol reagent in distilled water. Working standard solutions of BSA were prepared at the concentrations of 500, 400, 300, 200, 100, and 0 $\mu\text{g}/\text{mL}$ of BSA in distilled water from the stock solution of 500 $\mu\text{g}/\text{mL}$ (50 mg/100 H_2O).

To a number of clean test tubes containing 10 μL of microsomal preparation and 240 μL of distilled water (unknown concentration of protein) or 250 μL of each standard solution, 250 μL of reagent A were added and the tubes were incubated at room temperature for 10 minutes. In the next step and under continuous vortex mixing, 750 μL of reagent B was added to each of the test tubes and samples incubated at 50 °C for 10 more minutes. At the last step 200 μl of each mixture were transferred to a well in the ELISA plate and analyzed using an ELISA reader at 600 nm [185].

c. Total CYP 450 measurement

Hepatic microsomal CYP content was measured by a difference spectrum for the carbon monoxide-reduced form by the method of Omura and Sato [186]. Briefly, microsomal preparations were adjusted to 1 mg/mL protein with water, which was placed in sample cell. After recording the baseline, carbon monoxide was bubbled into the samples for 30-60 s to form the carbon oxide-CYP complex. Then, a few

milligrams of solid sodium thiocyanate were added to reduce the carbon monoxide-CYP complex. Solid sodium thiocyanate was also added to the reference cell. The absorbance of sample cell was scanned from 400 to 500 nm.

CYP content was calculated by the following equation:

$$\text{Cyp content (nmol/mg protein)} = \frac{OD450 - OD490}{91} \times 1000$$

d. Microsomal incubation studies:

Each 0.5 mL of incubate contained 1 mg/mL protein of the pooled liver microsomal preparation, 0.5-250 μ M (0.27 to 133 mg/L) of (\pm)-KTZ (dissolved in methanol), 1 mM NADPH, and 5 mM magnesium chloride hexahydrate dissolved in 0.5 M potassium phosphate buffer (pH=7.4). The volume of methanol added to each incubate with the addition of KTZ racemate was 0.8% v/v. The substrate was added to the liver microsomal suspensions and the oxidative reactions were started upon the addition of NADPH after a 5-min preequilibration period. All incubations were performed in quadruplicate in a 37°C water bath shaker for 15 min. Incubation conditions were optimized so that the rate of metabolism was linear with respect to incubation time and microsomal protein concentration. All microsomal incubations were stopped by the addition of three volumes of acetonitrile. The samples were then kept at -30°C until assayed for KTZ enantiomers. The rate of metabolism was calculated by measuring the rate of reduction in parent drug (substrate depletion).

2.3.2. Plasma protein binding

An erythrocyte vs. buffer or diluted plasma partitioning method was used for the determination of *in vitro* plasma protein binding of KTZ enantiomers in NL and HL plasma [187]. Briefly, NL and HL rats were anesthetised and blood was collected into heparinized tubes by cardiac puncture. The blood obtained from each rat was equally split between two different tubes. Plasma was separated from blood cells by centrifugation of the whole blood at 2500 g for 10 min. After removal of the plasma and buffy coat layer, the blood cells were washed with an equal volume of isotonic Sorensen's phosphate buffer (pH=7.4) and recentrifuged at 2500 g for 8 min. The washing step was repeated two more times after which the volume of erythrocytes in each of the tubes was measured. Either isotonic phosphate buffer (pH=7.4) or diluted plasma (1:10 NL and 1:20 HL in isotonic phosphate buffer) was then added to the blood cells to provide a hematocrit of 0.3 (buffer) or 0.4 (diluted plasma).

Stock solutions of (\pm)-KTZ (25 and 100 mg/mL) were prepared in methanol and added to the buffer-containing and diluted plasma-containing mixtures to allow a final concentration of approximately 10 or 40 mg/L of racemate. The volume of methanol added to each tube did not exceed 0.05% v/v. Tubes were incubated for 1 h in a 37°C water bath shaker.

At the conclusion of the incubation, replicates of 5 blood samples (50 μ L each) were set aside for assay with an additional 50 μ L of water added to each tube before freezing. For the remainder of the blood the plasma and buffer were

isolated by centrifugation for 10 min at 2500 g. Replicates of 5 samples of 100 μ L from each sample was set aside for assay. All samples were frozen at -30°C until assayed for KTZ enantiomer.

2.3.2.5 Determination of blood:plasma KTZ enantiomer ratios

Known amounts of (\pm)-KTZ in methanol were added to a heparinized tube containing freshly obtained rat blood from NL rats to provide a final concentration of 18 $\mu\text{g}/\text{mL}$ of racemate. The volume of methanol added was 5 $\mu\text{L}/\text{mL}$ of blood. The tube was placed in a shaking water bath at 37°C for 1 h. At that time, the tube was removed and 100 μl of blood was transferred to microcentrifuge tubes (n=5) containing 100 μL of water. The remaining blood was centrifuged at 2500g for 10min. A volume of 100 μL of the plasma layer was transferred to microcentrifuge tubes (n=5). Samples were kept frozen at -30°C until being assayed for KTZ enantiomer concentrations

2.3.3 Distribution of KTZ enantiomers within lipoprotein fractions of rat plasma.

2.3.3.1 Treatment of plasma samples

Pooled rat plasma was added to Beckman Ultraclear™ ultracentrifuge tubes in 3mL aliquots. A stock of (\pm)-KTZ (3000 $\mu\text{g}/\text{mL}$) was prepared in methanol. KTZ racemate was added such that the final concentration of racemate in plasma was 3000ng/mL. The final volume of methanol added to each plasma sample was known not to affect the plasma lipoprotein-lipid composition [188]. The plasma

aliquots were vortex mixed for 30s then incubated at 37°C for 60 min prior to separation of lipoprotein fractions.

2.3.3.2 Separation of lipoprotein components

NaBr density solutions (1.006 δ , 1.063 δ and 1.21 δ) were prepared by dissolving appropriate amounts of sodium chloride, sodium bromide and sodium hydroxide in water. The solutions were cooled to 4°C prior to preparation of the gradient. Three mL of the cooled, treated plasma samples, adjusted to a density of approximately 1.25 δ with sodium bromide, was added to an ultracentrifuge tube (Beckman Coulter: Fullerton, CA). Density solutions were carefully layered on top of the plasma in the order 1.21 δ , 1.063 δ then 1.006 δ . The tubes were balanced and placed into individual titanium buckets and capped. The buckets were loaded on a SW 41 Ti swinging bucket rotor (Beckman Coulter) and centrifuged at 40,000 rpm at 15°C for 18 h in a Beckman L8-80M Ultracentrifuge (Beckman Coulter) or a Beckman LE-80 Ultracentrifuge (Beckman Coulter). Upon completion, the tubes were removed and four distinct regions were observed and labelled. The layers correspond to the TG-rich lipoproteins (TRL) comprised of very low density lipoproteins and any CM present, LDL, HDL and the LPDP. These layers were removed using a Pasteur pipette and added to disposable glass test tubes and the volumes measured and recorded [189, 190]

3.3.4 The effect of increased lipoprotein levels on the stereoselective PK of (\pm)-KTZ in rat

All study protocols were approved by the University of Alberta Health Sciences Animal Policy and Welfare Committee. Male Sprague–Dawley rats (Charles

River, Quebec, Canada) with body wt ranging from 250 to 350 g were used for PK, pharmacodynamic, and tissue distribution studies. All rats were housed in temperature controlled rooms with 12 h light per day. The animals were fed a standard rodent chow containing 4.5% fat (Lab Diet® 5001, PMI nutrition LLC, Brentwood, USA). Free access to food and water was permitted prior to the experiments.

2.3.4.1 Induction of HL

This is described under 2.2.2.1

2.3.4.2 Surgical procedures

This is described under 2.2.2.2

2.3.4.3 Dosing and sample collection

A total of 64 male Sprague-Dawley rats (Charles River Canada) were included in the PK study. Rats were allocated into either NL or HL groups. Racemic KTZ was administered as 10 mg/kg *iv* (n = 8 each) or 40 mg/kg orally (n=24 each).

The KTZ *iv* dosing solution was prepared by dissolving powdered racemic compound in 9:1 polyethylene glycol 400: propylene glycol (10 mg/mL)[167]. The i.v. dose was injected over 2 min via the jugular vein cannula, immediately followed by injection of sterile normal saline solution. At the time of first sample withdrawal, the first 0.2 mL volume of blood was discarded. For oral dosing, (±)-KTZ (50 mg/mL) suspension was prepared. The tablets of (±)-KTZ were ground to a powder using a mortar and pestle, and then dispersed in 1% methylcellulose. On the morning of the PK study, the rat groups received the desired dose by oral

gavage. For both routes of administration, food was provided to animals 2 h after the dose administration.

Serial blood samples (0.15-0.25 mL) were collected at 0.08, 0.25, 0.75, 1, 1.5, 2, 4, 6 and 8 h post *iv* dosing into polypropylene microcentrifuge tubes. Heparin in normal saline was used to flush the cannula after each collection of blood. After the oral dosing, rats (n=6 for each group at each time point) were anaesthetized and exsanguinated by withdrawal of blood through cardiac puncture at 0.5, 1, 1.5, 3, 6 h post dose. Plasma was separated by centrifugation of the blood at 2500 *g* for 3 min. Liver specimens were collected at the same time. The samples were kept at -30°C until assayed for KTZ enantiomers.

2.3.4.4 Determination of blood:plasma KTZ enantiomer ratio

Known amounts of (\pm)-KTZ in methanol were added to a heparinized tube containing freshly obtained rat blood from HL rats to provide a final concentration of 18 $\mu\text{g}/\text{mL}$ of racemate. The volume of methanol added was 5 $\mu\text{L}/\text{mL}$ of blood. The tube was placed in a shaking water bath at 37°C for 1 h. At that time, the tube was removed and 100 μL of blood was transferred to microcentrifuge tubes (n=5) containing 100 μL of water. The remaining blood was centrifuged at 2500*g* for 10min. A volume of 100 μL of the plasma layer was transferred to microcentrifuge tubes (n=5). Samples were kept frozen at -30°C until being assayed for KTZ enantiomer concentrations

2.3.5 Simultaneous determination of MDZ and KTZ in plasma

An HPLC assay has been developed for simultaneous determination of MDZ and KTZ racemate in rat and human plasma using diazepam as IS.

2.3.5.1 Instrumentation

The HPLC system consisted of a Waters 710B WISP auto-injector, Waters 510 pump (Waters, Milford, MA, USA), and a HP 1050 UV detector (Hewlett Packard, Palo Alto, CA, USA). The chromatographic data were collected and compiled by use of EZChrom software (Scientific Software, Pleasanton, CA, USA).

2.3.5.2 Chromatographic separation:

The chromatographic separation of MDZ, KTZ and diazepam (IS) was accomplished using a Symmetry C18 analytical column, 3.5 μm particle size, 150 mm \times 4.6 mm (Waters, MA, USA) attached to a C18 2 cm \times 4.0 mm, 5 μm particle size guard column (Supelco, PA, USA). The mobile phase used was a 45:55 (V/V) mixture of acetonitrile: 15 mM KH_2PO_4 . The mobile phase was pumped isocratically at 1 mL/min. The UV wavelength was set at 220 nm.

2.3.5.3 Preparation of stock solutions

A 100 mg/L stock solution of KTZ was prepared by dissolving 10 mg of (\pm)-KTZ in 100 mL methanol. A 100 mg/L stock solution of MDZ was prepared by dilution of 2 mL of (5 mg/mL) MDZ to 100 mL with methanol. A 40 mg/L stock solution of diazepam was prepared by dilution of 2 mL of (5 mg/mL) diazepam to

250 mL with methanol. All stock solutions were kept at 4°C. All working standard solutions were prepared daily by sequential dilution of stock solution in methanol.

2.3.5.4 Extraction procedures

Diazepam (0.05 mL) was added to each 0.1 or 0.5 mL rat or human plasma sample, respectively in a glass test tube. To this, 0.2 mL of 0.1 N NaOH and 4 and 5 mL of diethyl ether were added, respectively. Because methanol was present in the standard curve samples, an equivalent amount was added to the test samples as well (0.2 mL). The tubes were vortex mixed (1 min) at high speed then subsequently centrifuged for 5 min at ~2500 g. The tubes were then covered and put into the -30 °C freezer for 5-7 min. The organic layer was transferred to new glass tubes and evaporated to dryness *in vacuo*. The residues were reconstituted in 200 µL mobile phase of which 75-125 µL volumes were injected into the HPLC.

2.3.5.5 Calibration, accuracy and validation

Calibration curves were constructed using samples of 0.1 mL rat plasma or 0.5 mL human plasma. The standard curve ranged from 25 to 25000 and 5 to 10000 ng/mL of KTZ racemate and MDZ in rat and human plasma, respectively. The ratio of measured drug to IS peak height and area was calculated and plotted vs. its nominal concentration. Owing to the wide range of concentrations, the calibration curve data were weighed by a factor of $1/\text{KTZ racemic}$ and $1/(\text{MDZ})^2$. All standard curves and quality control samples were generated by spiking the drugs in the similar matrices as the samples.

Intraday accuracy and precision of the assay were determined as described above (see 2.3.1.5) using five sample replicates of 62.5, 125, 500 and 2500 ng/mL of each KTZ enantiomer, 25, 100, 1000 and 10000 ng/mL of both KTZ racemate and MDZ in rat plasma and 5, 10, 100, 200 and 10000 ng/mL of both KTZ racemate and MDZ in human plasma. Human plasma was assessed for intraday validation only, but all rat plasma samples were assessed for interday accuracy and precision, by repeating the assay on three separate days. For each daily run, concentrations were determined by comparison with a calibration curve prepared on the day of the analysis.

2.3.5.6 Assessment of chromatographic separation:

This is described in 2.3.1.7

2.3.5.7 Application of assay method for measuring KTZ and MDZ concentrations in rat plasma *in vivo*

In order to assess the applicability of this method *in vivo*, two rats (250-300 g) were administered 40 mg/kg KTZ orally followed by 5 mg/kg MDZ *iv* after 1.5 h of oral dosing.

Serial blood samples were collected at 0.75h before and 0.083, 0.33, 0.67, 1, 1.5, 2, 3, 4, and 8 h post i.v. MDZ dose for the simultaneous determination of KTZ and MDZ. Plasma was separated by centrifugation of the blood at 2500 g for 3 min. The samples were kept at -30°C until assayed using the developed HPLC methods. Non-compartmental methods were used to calculate the PK parameters. The elimination rate constant (λ_z) was calculated by subjecting the plasma

concentrations in the terminal phase to linear regression analysis. The $t_{1/2}$ was calculated by dividing 0.693 by λz . The $AUC_{0-\infty}$ was calculated using the combined log-linear trapezoidal rule from time 0 h postdose to the time of the last measured concentration, plus the quotient of the last measured concentration divided by λz . The concentration at time 0 h after i.v. dosing was estimated by back extrapolation of the log-linear regression line using the first three measured plasma concentrations to time 0. The CL was calculated as the quotient of dose to $AUC_{0-\infty}$. The C_{max} and T_{max} were determined visually.

2.3.6 Effect of HL on KTZ-MDZ drug-drug interaction in rat

All study protocols were approved by the University of Alberta Health Sciences Animal Policy and Welfare Committee. Male Sprague–Dawley rats (Charles River, Quebec, Canada) with body wt ranging from 250 to 350g were used for PK, pharmacodynamic, and tissue distribution studies. All rats were housed in temperature controlled rooms with 12 h light per day. The animals were fed a standard rodent chow containing 4.5% fat (Lab Diet® 5001, PMI nutrition LLC, Brentwood, USA). Free access to food and water was permitted prior to the experiments.

2.3.6.1 Induction of HL:

As described in 2.2.2.1

2.3.6.2 Surgical procedures:

As described in 2.2.2.2

2.3.6.3 Dosing and sample collection

A total of 23 male Sprague-Dawley rats (Charles River Canada) were included in the PK drug interaction study. The rats were allocated into four groups, stratified by lipoprotein status and MDZ and KTZ dosage. The protocol included either single *iv* dose 5mg/kg MDZ treated rats or rats given 40 mg/kg oral KTZ followed by *iv* 5mg/kg MDZ, one and half hour later. For each of the groups there was a matching NL and HL group. Each group included 4-6 rats.

For oral KTZ dosing, KTZ (44 mg/mL) suspension was prepared. The tablets of (\pm)-KTZ were ground to a powder using a mortar and pestle, and then dispersed in 1% methylcellulose. For *iv* dosing, MDZ injectable solution (5 mg/mL) was used. On the morning of the PK study, NL and HL rat groups received the desired dose of either KTZ suspension in methyl cellulose or methyl cellulose only by oral gavage. One and a half hours later, the MDZ dose was injected over 1 min via the jugular vein cannula, immediately followed by injection of sterile normal saline solution. At the time of first sample withdrawal after *iv* dosing, the first 0.2 mL volume of blood was discarded.

Serial blood samples (0.15-0.25 mL) were collected at 0.75 h before and 0.08, 0.33, 0.67, 1, 1.5, 2, 3, 4 and 8h post *iv* dose into polypropylene microcentrifuge tubes. Heparin in normal saline (25 U/mL) was used to flush the cannula after each collection of blood. Plasma was separated by centrifugation of the blood at

2500 g for 3 min. The samples were kept at -30°C until assayed for KTZ and MDZ concentrations.

2.3.6.4 Determination of plasma protein binding of MDZ

The fu of MDZ was measured in NL and HL conditions in the presence and absence of KTZ using ultrafiltration (Centrifree[®], Amicon, Beverly, MA, USA). Briefly, NL and HL rat plasma were inoculated with MDZ injectable solution with and without methanolic stock solutions of (±)-KTZ (10 mg/mL) to allow a final concentration of approximately 10 and 27 mg/L, respectively. The volume of methanol added to each tube did not exceed 0.05% v/v. Tubes were incubated for 1 h in a 37°C water bath shaker. A volume of 1 mL of each tube was transferred to a Centrifree[®] apparatus (n=4), and the device was then placed in a fixed angle centrifuge rotor and spun at 2000 g for 10 min at 37 °C. Samples were then analyzed for MDZ concentrations.

2.4 Data analysis:

2.4.1 PK analysis:

Noncompartmental methods were used to calculate the PK parameters. The elimination rate constant (λ_z) was calculated by subjecting the plasma concentrations in the terminal phase to linear regression analysis. The $t_{1/2}$ was calculated by dividing 0.693 by λ_z . The $AUC_{0-\infty}$ was calculated using the combined log-linear trapezoidal rule from time 0 h postdose to the time of the last measured concentration, plus the quotient of the last measured concentration divided by λ_z . The concentration at time 0 h after *iv* dosing was estimated by back

extrapolation of the log-linear regression line using the first three measured plasma concentrations to time 0. The CL was calculated as the quotient of dose to $AUC_{0-\infty}$ and the steady state volume of distribution (V_{dss}) as $CL \times AUMC / AUC$, where AUMC is the area under the first moment plasma concentration vs. time curve, from time of dosing to infinity. The mean residence time (MRT) was determined as the quotient of AUMC to AUC. The oral F was calculated as follows:

$$F = \frac{\text{mean AUC oral}}{\text{mean AUC } iv} \times \frac{\text{Dose } iv}{\text{Dose oral}}$$

The mean blood CL of (+) and (-)-KTZ were estimated by dividing the respective mean plasma CL by the corresponding blood to plasma ratio. E was estimated, assuming negligible extrahepatic CL, by taking the quotient of blood CL divided by average hepatic blood flow of 55.2 mL/min/kg [191]. The gastrointestinal availability (fg) was calculated as $F = fg \times (1-E)$, where E is the E. The accumulation factors for AM in plasma were determined as the quotient of the last measured concentration to that 12 h after the first dose. For orally dosed rats the C_{max} and T_{max} were determined by visual examination of the data.

2.4.2 Calculation of fu

2.4.2.1 KTZ enantiomer determination

The calculation of the plasma unbound fraction (fu) for KTZ enantiomers in NL and HL plasma was determined using a series of equations outlined by

Schuhmacher et al [187]. The erythrocyte concentration of enantiomer in the erythrocyte–diluted plasma was determined by the following equation:

$$CE = \frac{CB - Cp(1 - HCT)}{HCT}$$

Where CB is the concentration of enantiomer in the blood cell–diluted plasma suspension, Cp is the concentration of enantiomer in the diluted plasma, and HCT is the hematocrit in the erythrocyte–diluted plasma sample. To estimate the erythrocyte concentration of enantiomer in the erythrocyte–buffer samples (CE*), the concentration of enantiomer in the blood cell–buffer suspension was substituted for CB, and the buffer concentration of enantiomer was substituted for Cp. The fu of enantiomers was determined by

$$f_u = \frac{\alpha \cdot P_p/P_b}{1 - [P_p/P_b \cdot (1 - \alpha)]}$$

Where α is the plasma-dilution factor. The partition coefficients for erythrocyte:diluted plasma (Pp) or buffer (Pb) are represented by the quotients CE/Cp and CE*/Cbuffer, respectively.

2.4.2.2 MDZ determination

The calculation of the MDZ fu in NL and HL plasma with or without KTZ was determined by dividing the MDZ concentration in the filtrate by that in the original solution.

2.4.3 Liver concentrations:

In determining KTZ liver distribution, because of the destructive study design, AUC could not be determined for individual rats in each group. For this purpose the Bailer method was used [192].

2.4.4 Lipoprotein fractionation

The partitioning of KTZ enantiomers was calculated using the measured concentrations in the fraction aliquots multiplied by the volumes obtained at the time of separation. The percentage recovered was determined by comparing the total mass recovered from all fractions to the total mass added to the plasma at the onset of the ultracentrifugation.

2.4.5 Hepatocytes

The AM remaining after exposure to the cells was expressed as percent remaining. The area under the percent AM remaining to be eliminated vs. time curve (ARE) was calculated using the linear trapezoidal rule.

2.5 Statistical analysis

2.5.1 PK studies

All compiled data were reported as mean \pm SD, unless otherwise indicated. Statistical analysis was performed using one or two way analysis of variance (ANOVA), Student's paired or unpaired t-tests as appropriate. The level of significance was set at $p=0.05$. Data analysis was performed using Microsoft Excel 2007, SPSS 16.0 and Sigma Plot 11. Bonferroni adjustment was applied as

necessary in cases where multiple comparisons were made using t-tests, with $p = 0.05/\text{number of comparisons being made}$.

2.5.2 Liver concentrations

AUC_{0-6 h} for (+) and (-)- KTZ in liver were determined. The SD of partial AUC was estimated to assess significance of differences. In this test, α was 0.05, the critical value of Z (Z_{crit}) for the 2-sided test after Bonferroni adjustment was 2.87, and the observed value for Z (Z_{obs}) was calculated as previously described [192]. The K_p were calculated for AUC and for postdistributive phase samples

2.5.3 Lipoprotein fraction distribution studies

All compiled data were expressed as means \pm SD of percentage unless otherwise indicated. Duncan's post hoc test was used to assess the significance of differences within lipoprotein fractions of each group. Student's paired or unpaired t-tests were used for statistical comparison between NL and HL groups and between enantiomers within each group. The level of significance was set at $p < 0.05$ for all comparisons.

2.5.4 Microsomal studies

Compiled data are expressed as mean \pm SD unless otherwise indicated. One way ANOVA, Duncan's Multiple Range post hoc test and Student paired or unpaired t-tests were used as appropriate to assess the significance of differences between groups. Microsoft Excel 2007 (Microsoft, Redmond WA) or SPSS version 12 (SPSS Inc., Chicago, IL) were used in statistical analysis of data. The level of significance was set at $p < 0.05$.

2.5.5 Hepatocytes

Compiled data are expressed as mean \pm SD. ARE was determined for all groups. The SD of partial ARE was estimated to assess significance of differences. In this test, α was 0.05, the critical value of Z (Zcrit) for the 2-sided test after Bonferroni adjustment was 2.82, and the observed value for Z (Zobs) was calculated as previously described [192].

3. Results

3.1 Effect of HL on PK and pharmacodynamic aspects of AM

3.1.1 Effect of HL on electrocardiographic changes associated with AM

As expected [193], P407 caused increases in both TG and total CHOL levels in rat plasma. Compared to NL rats, the HL rats showed considerable increases of 13.7- and 33.8-fold in the total CHOL and TG levels, respectively, by the end of the study.

The HL condition by itself had no effect on QT, QTc, PR or RR intervals in saline-control rats (Table 5). The increase in RR, PR and QTc intervals from baseline, respectively, was $-0.42 \pm 8.75\%$, $1.13 \pm 5.64\%$ and $0.95 \pm 1.47\%$ in NL saline-control rats vs $2.29 \pm 3.15\%$, $2.34 \pm 3.29\%$ and $4.36 \pm 5.74\%$ in HL. AM was found to prolong QT, QTc, PR and RR intervals in both NL and HL rats (Table 5). In general there were longer QT and QTc intervals in HL than in NL rats and in all dose groups significant differences were apparent after the last dose (Table 5; Figure 7). The QTc interval prolongation after the last dose compared to baseline in HL versus NL rats were $19.9 \pm 8.5\%$ versus $8.8 \pm 6.3\%$ for 25 mg/kg/d, $23.9 \pm 7.1\%$ versus $9.2 \pm 3.3\%$ for 50 mg/kg/d, and $86.8 \pm 18.2\%$ versus $51.3 \pm 22.0\%$ for the 100mg/kg/d treated rats. Similarly, after the last dose all AM-treated HL rats showed significant ($p < 0.05$) prolongations in PR interval compared to equivalently treated NL rats (Table 5); the increases in PR interval compared to baseline for the HL and NL rats were $12.4 \pm 3.9\%$ versus $5.54 \pm 3.9\%$ after 25 mg/kg/d, $14.5 \pm 9.0\%$ versus $5.80 \pm 3.3\%$ after 50 mg/kg/d, and $23.1 \pm 4.2\%$ versus $18.6 \pm 4.1\%$ after 100 mg/kg/d. Significant ($P < 0.01$) linear

correlations of moderate strength were present between the percent increase in QTc and PR intervals in both NL ($r^2=0.381$) and HL ($r^2=0.346$) rats. In evaluating the RR interval the data showed that, compared to baseline, similar magnitudes of prolongation were present in both the NL and HL rats. The 50 mg/kg/d treated HL rats differed in that there was a significantly higher increase in RR interval than in NL rats (Table 5).

The DEA concentrations were consistently lower than those of AM in plasma and heart, in both NL and HL rats (Table 5). Significant ($P<0.001$) and strong linear correlations were found between DEA and AM present in both NL and HL rats plasma ($r^2= 0.794$ and 0.950 , respectively) and heart ($r^2= 0.913$ for both NL and HL). In line with previous single dose studies [86, 97], throughout the study all AM treated HL rats had substantially higher AM plasma concentrations than equivalently treated NL rats (Table 5). In comparison, DEA plasma concentrations of AM-treated HL rats were only significantly ($p<0.05$) different from the equivalently treated NL rat groups 12 h after the last dose (Table 5). At the end of the study heart AM concentrations were significantly higher (>1.7 fold) in AM-treated HL rat groups than likewise treated NL rat groups ($p<0.05$; Figure 8). The heart concentrations of DEA in all groups showed a trend (>1.3 fold) towards increases in HL rats compared to NL rats, although the values were variable and statistical differences were only detected between the 100 mg/kg/d AM treated HL and NL rats (Table 5). A disproportionate increase in AM plasma and heart concentrations was noted 12 h after the last dose in NL and HL rat

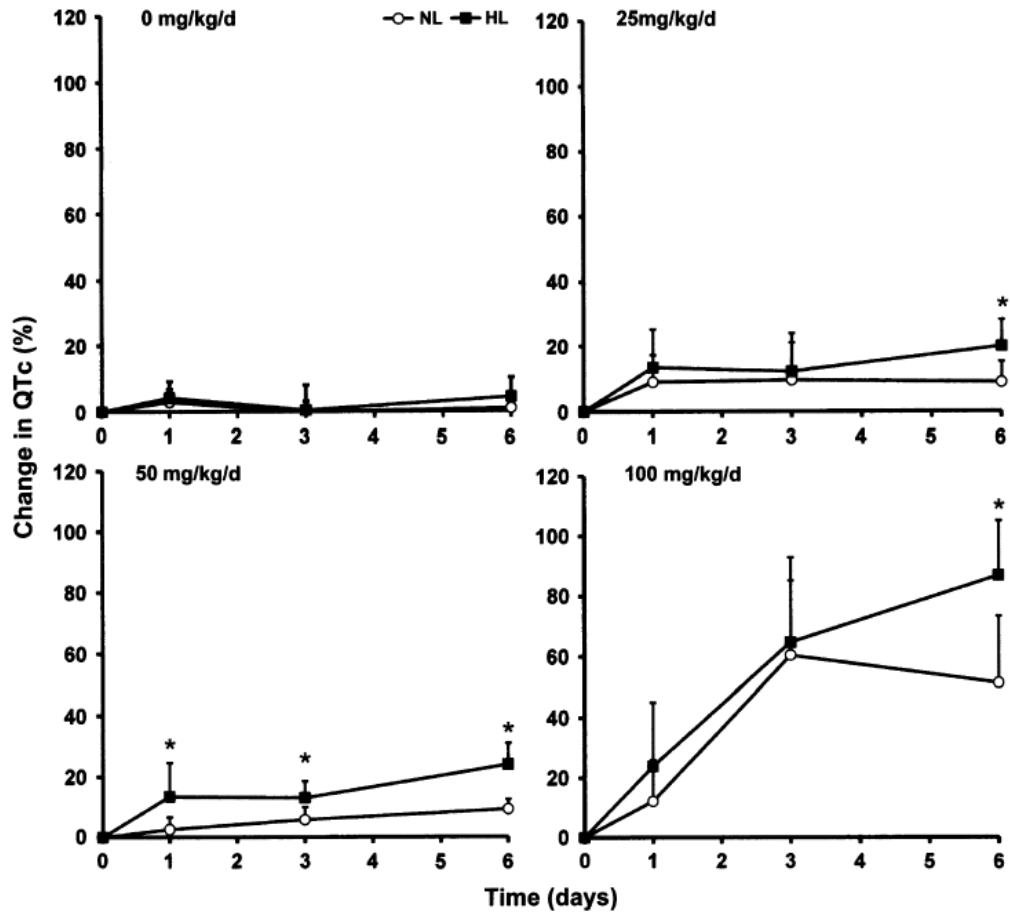


Figure 7: Percent change in QTc interval (mean \pm SD) in normolipidemic (NL) and hyperlipidemic (HL) rats after *iv* doses of 0, 25, 50 and 100 mg/kg/d amiodarone HCl on Days 1, 3 and 6 of the study. *Significant difference between HL and NL rats ($p < 0.05$).

Table 5: The ECG parameters, AM and DEA concentrations in plasma and heart, and CHOL and TG content of NL and HL saline control and AM-treated rats 12 h after the last dose

	Dose mg·kg ⁻¹ ·d ⁻¹															
	Saline Control				25				50				100			
	NL	HL	NL	HL	NL	HL	NL	HL	NL	HL	NL	HL	NL	HL		
QT (ms)	70.0 ± 5.90	70.0 ± 5.90	69.2 ± 4.10	71.5 ± 6.90	69.2 ± 4.20	66.6 ± 2.20	70.5 ± 4.50	68.5 ± 7.70	70.5 ± 4.50	66.6 ± 2.20	70.5 ± 4.50	68.5 ± 7.70	70.5 ± 4.50	68.5 ± 7.70		
	70.5 ± 6.0	73.5 ± 6.0	76.5 ± 5.70	87.6 ± 12.5*	74.6 ± 2.5	88.3 ± 5.9*	121 ± 16.8	146 ± 16.0*	121 ± 16.8	88.3 ± 5.9*	121 ± 16.8	146 ± 16.0*	121 ± 16.8	146 ± 16.0*		
QTc (ms)	130 ± 10.9	130 ± 10.7	129 ± 10.0	134 ± 14.1	126 ± 6.1	124 ± 6.1	134.1 ± 9.1	127 ± 13.5	134.1 ± 9.1	124 ± 6.1	134.1 ± 9.1	127 ± 13.5	134.1 ± 9.1	127 ± 13.5		
	131 ± 10.6	136 ± 9.6	140 ± 9.1	160 ± 21.4*	137 ± 5.6	154 ± 10.3*	200 ± 23.3	236 ± 17.3*	200 ± 23.3	154 ± 10.3*	200 ± 23.3	236 ± 17.3*	200 ± 23.3	236 ± 17.3*		
RR (ms)	156 ± 4.9	155 ± 5.8	155 ± 11.7	153 ± 12.5	150 ± 12.2	159 ± 10.2	152 ± 5.3	155 ± 9.4	152 ± 5.3	159 ± 10.2	152 ± 5.3	155 ± 9.4	152 ± 5.3	155 ± 9.4		
	156 ± 16.7	159 ± 6.0	163 ± 12.2	164 ± 19.9	162.0 ± 13.0	190 ± 14.3*	222 ± 30.3	233 ± 28.7	222 ± 30.3	190 ± 14.3*	222 ± 30.3	233 ± 28.7	222 ± 30.3	233 ± 28.7		
PR (ms)	56.3 ± 3.67	53.7 ± 2.70	54.1 ± 2.25	51.2 ± 2.87*	55.1 ± 3.92	55.7 ± 2.06	53.7 ± 3.78	53.8 ± 3.89	53.7 ± 3.78	55.7 ± 2.06	53.7 ± 3.78	53.8 ± 3.89	53.7 ± 3.78	53.8 ± 3.89		
	56.8 ± 1.73	54.9 ± 1.55	57.1 ± 3.26	57.5 ± 3.95	58.2 ± 3.87	63.8 ± 5.49*	63.6 ± 3.51	66.2 ± 4.81	63.8 ± 5.49*	63.8 ± 5.49*	63.6 ± 3.51	66.2 ± 4.81	63.6 ± 3.51	66.2 ± 4.81		
Total CHOL (mmol/L)	1.65 ± 0.14	23.5 ± 7.5*	1.62 ± 0.19	30.9 ± 11.2*	1.83 ± 0.24	31.2 ± 9.3*	2.95 ± 0.72	27.8 ± 11.6*	2.95 ± 0.72	31.2 ± 9.3*	2.95 ± 0.72	27.8 ± 11.6*	2.95 ± 0.72	27.8 ± 11.6*		
TGs (mmol/L)	1.82 ± 0.52	23.4 ± 11.0*	0.98 ± 0.32	31.7 ± 10.3*	0.75 ± 0.20	41.5 ± 13.1*	0.42 ± 0.15	20.9 ± 8.0*	0.75 ± 0.20	41.5 ± 13.1*	0.42 ± 0.15	20.9 ± 8.0*	0.42 ± 0.15	20.9 ± 8.0*		
AM Plasma (µg/mL)	0	0	0.395 ± 0.112	6.50 ± 2.26*	0.723 ± 0.149	16.9 ± 3.82*	3.60 ± 1.13	69.2 ± 21.7*	0.723 ± 0.149	16.9 ± 3.82*	3.60 ± 1.13	69.2 ± 21.7*	3.60 ± 1.13	69.2 ± 21.7*		
Heart (µg/g)	0	0	2.77 ± 2.26	5.12 ± 1.05*	7.38 ± 3.67	12.7 ± 5.04*	33.8 ± 17.9	85.3 ± 27.3*	7.38 ± 3.67	12.7 ± 5.04*	33.8 ± 17.9	85.3 ± 27.3*	33.8 ± 17.9	85.3 ± 27.3*		
DEA Plasma (µg/mL)	0	0	0.034 ± 0.008	0.095 ± 0.043*	0.107 ± 0.065	0.296 ± 0.124*	0.314 ± 0.096	2.22 ± 0.868*	0.107 ± 0.065	0.296 ± 0.124*	0.314 ± 0.096	2.22 ± 0.868*	0.314 ± 0.096	2.22 ± 0.868*		
Heart (µg/g)	0	0	0.447 ± 0.346	0.581 ± 0.292	2.54 ± 1.53	3.52 ± 5.41	10.7 ± 5.37	24.1 ± 12.7*	0.447 ± 0.346	0.581 ± 0.292	2.54 ± 1.53	3.52 ± 5.41	10.7 ± 5.37	24.1 ± 12.7*		

*Different from NL ($P < 0.05$).

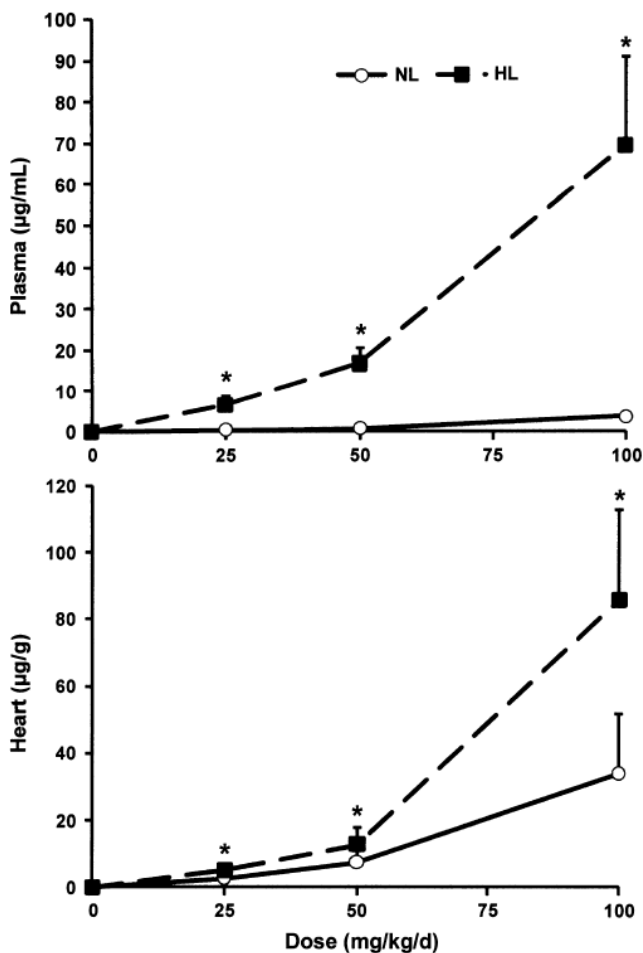


Figure 8: Amiodarone plasma and heart concentrations ($\mu\text{g/mL}$) in normolipidemic (NL) and hyperlipidemic (HL) rats 12 h after the last amiodarone HCl doses of 25, 50 or 100 mg/kg/d. * Significant difference between NL and HL rats, $p < 0.05$.

groups upon increasing the daily dose from 50 mg/kg/d to 100 mg/kg/d. Thus a two fold increase in the dose resulted in > 4 fold increase in AM plasma and heart trough concentrations in both NL and HL rats (Figure 8; Table 5). The same dose dependent nonlinear pattern was demonstrated in the effect (Table 5).

For the NL rats the accumulation factor for mean plasma concentrations, respectively, were 1.96 ± 0.58 , 1.59 ± 0.155 and 4.87 ± 1.60 for the 25, 50 and

100 mg/kg/d doses. The corresponding accumulation factors for HL rats were 8.08 ± 11.9 , 15.0 ± 17.6 and 27.5 ± 38.4 , respectively. In terms of ranking, the accumulation factor of the highest dose of NL rats was significantly higher than that of the lower doses in NL rats. There were no differences noted between accumulation factors of the HL rats.

There was a strong correlation noted between AM plasma concentrations and change in QTc interval, in both NL and HL rat groups (Figure 9). However, there was a large differential in the slope (~10-fold higher for NL) between the NL and HL animals. Similarly, there was a strong linear correlation between AM heart concentrations and change in QTc, although here the slopes were similar (Figure 9).

The relationships between total AM heart uptake and total AM plasma concentration for both NL and HL rat groups yielded strong correlations although with different slopes (NL=9.6; HL=1.3, Figure 10). These slope values closely matched those of the K_p of the heart previously observed for AM when given as single doses to NL (8.7) and HL (2.1)[97]. Strong positive and significant linear correlations were noted in the QT interval, plasma AM and heart AM concentrations vs. the plasma CHOL: TG ratios (Figure 11), for both NL and HL rats. The slopes of the relationships, however, were much higher for the HL rats.

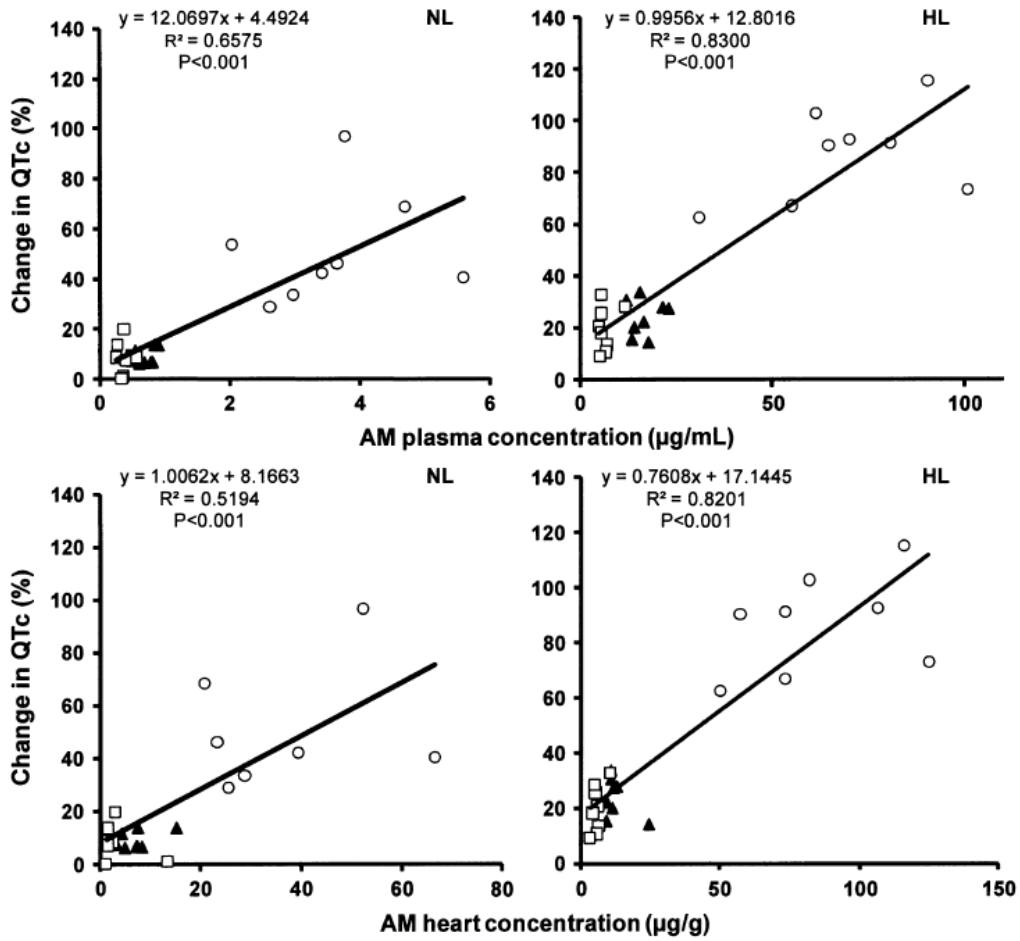


Figure 9: The correlation between % increase in QTc interval in normolipidemic (NL) and hyperlipidemic (HL) rats and amiodarone (AM) plasma or heart concentrations of all drug-treated rats at the time of heart collection. Open circles, closed triangles and open squares represent 100, 50 and 25 mg/kg/d AM dose groups, respectively.

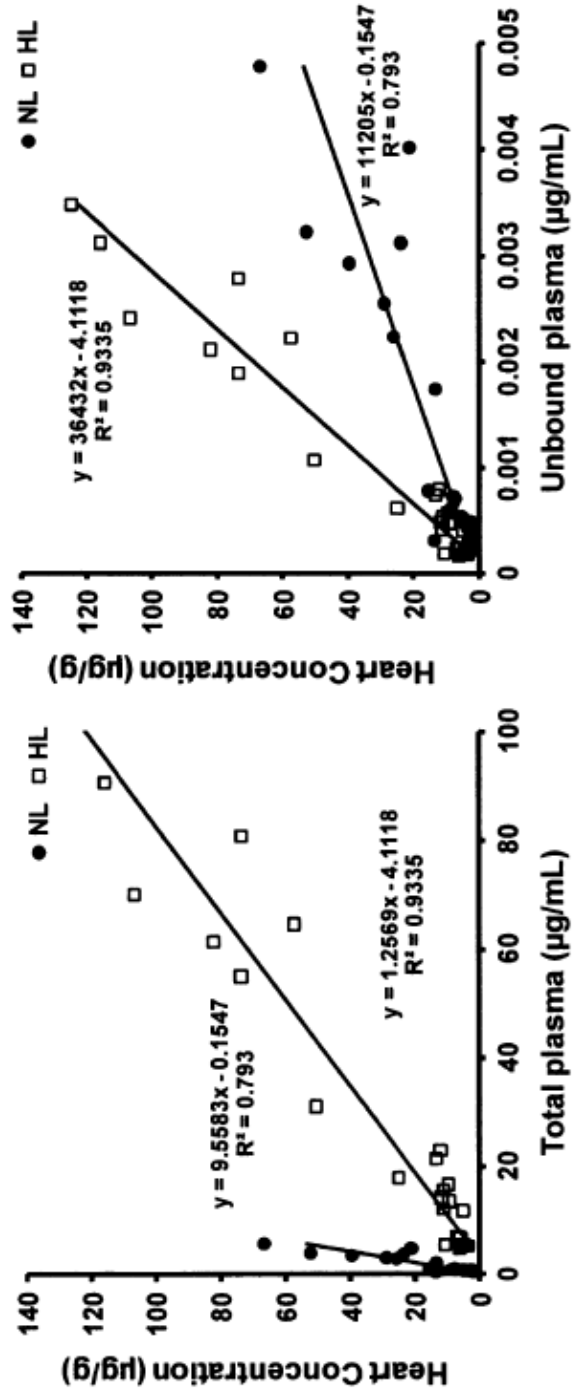


Figure 10: The correlation between heart and total or unbound plasma amiodarone concentrations in all drug-treated normolipidemic (NL) and hyperlipidemic (HL) rats

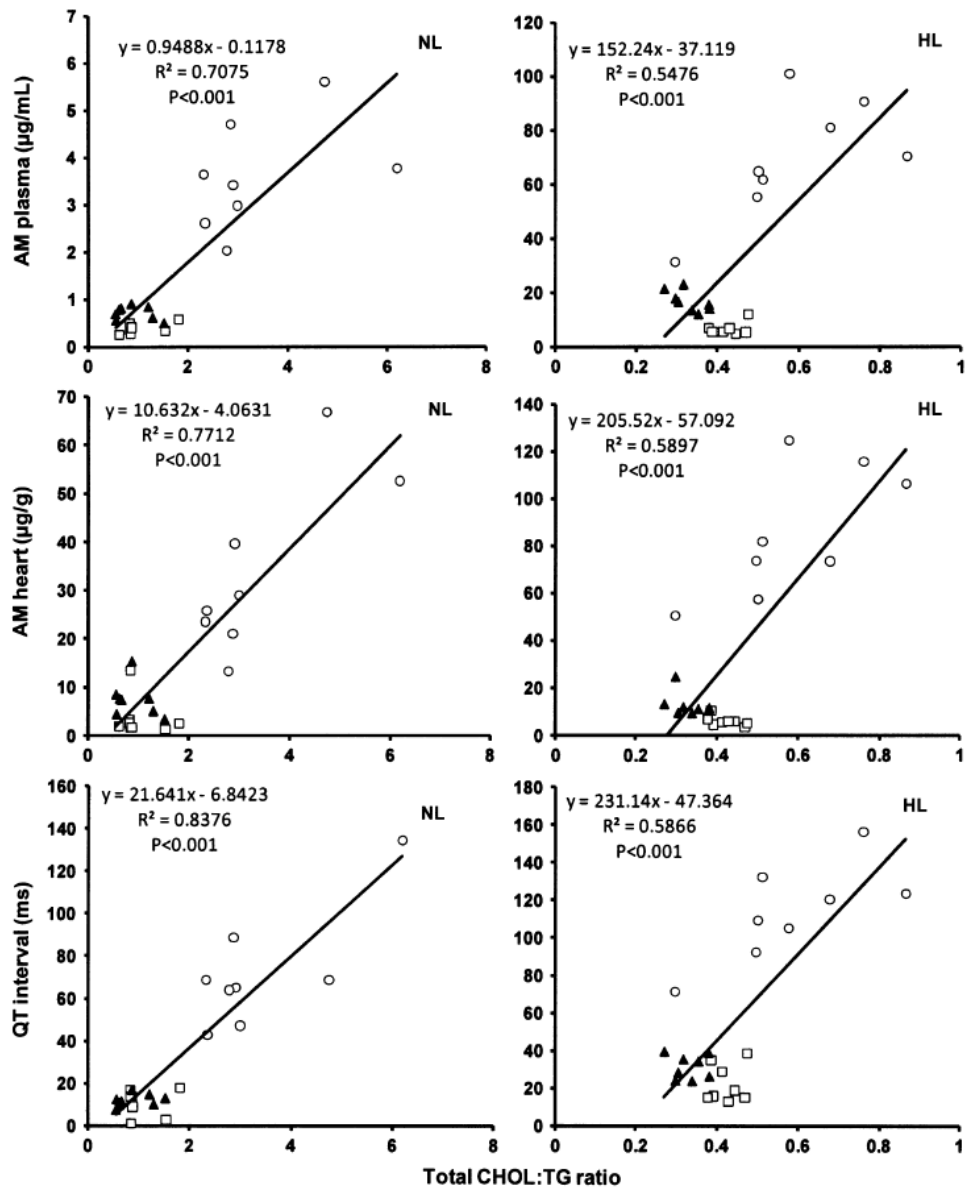


Figure 11: The correlation between plasma total cholesterol (CHOL) to triglyceride (TG) ratio with plasma amiodarone concentration, heart amiodarone concentration, and QT interval in normolipidemic (NL) and hyperlipidemic (HL) rats. Open circles, closed triangles and open squares represent 100, 50 and 25 mg/kg/d AM dose groups, respectively.

3.1.2 Effect of HL on AM metabolism by hepatocytes

3.1.2.1. Amount remaining vs. time plots

a. AM metabolism by hepatocytes from NL and HL rats, in the absence of rat sera.

Within 24 h of exposure of AM to hepatocytes, the rate of decline of drug from NL rat hepatocytes appeared to exceed that from HL rat hepatocytes. After 24 h, this difference dissipated (Figure 12). The area under the % AM recovering time curve from time 0 to 24 h was indeed significantly lower in hepatocytes from NL than HL rats (Figure 12).

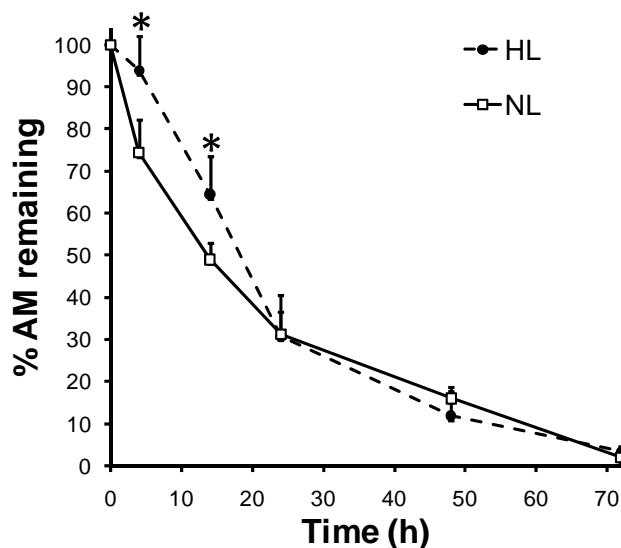


Figure 12: Amiodarone metabolism represented as % AM remaining vs. time curve. 500 mg/mL AM was exposed in regular cell media in the presence of hepatocytes from NL (open squares) and HL rats (closed circle) in the absence of serum. *Significant difference between NL and HL ($p < 0.05$)

b. AM metabolism in hepatocytes from NL and HL rats, in the presence and absence of rat sera.

In NL hepatocytes, control cells incubated with media and drug alone showed a decline of ~ 98% of initial AM concentration by 72 h post-incubation. The coincubation with 5% NL rat serum with the AM caused the decrease in AM to be less dramatic (~86%). Coincubation of 5% HL serum led to a significant attenuation of AM disappearance compared to both NL serum co-incubations and control groups, with a total decline of only ~30% being realized (Figure 13).

The experiment was also conducted in hepatocytes from HL rats. A similar trend was observed to that of NL hepatocytes. The control HL cells showed a decline in AM by ~99% within 72 h. NL serum coincubation caused AM to decline to only ~83%. HL serum coincubation significantly inhibited AM metabolism compared to both NL serum coincubation and control group with a total decline of ~25% of the initial AM concentration (Figure 14).

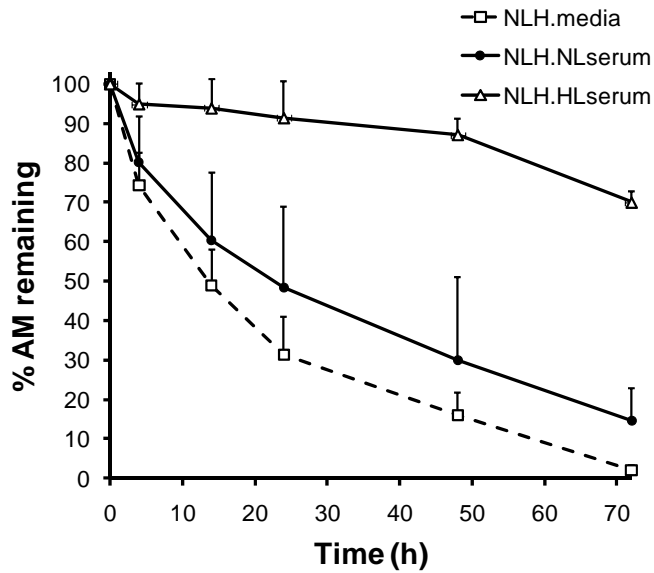


Figure 13: Amiodarone metabolism by NL hepatocytes (NLH) treated with media alone (open square) or co-incubated with 500 mg/mL AM within NL (closed circle) or HL (open triangle) serum (5%).

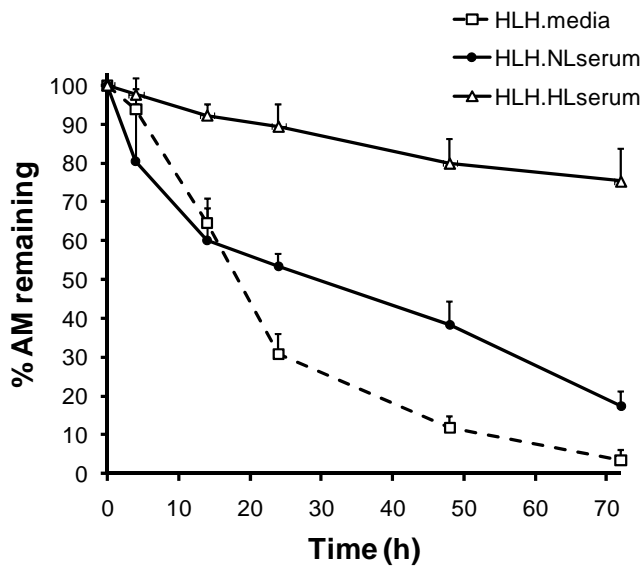


Figure 14: Amiodarone metabolism by HL hepatocytes (HLH) treated with media alone (open square) or co-incubated with 500 mg/mL AM within NL (closed circle) or HL (open triangle) serum (5%).

c. AM metabolism in hepatocytes from NL rats when preincubated rather than coincubated with cell media or rat serum (5%).

Hepatocytes from NL rats were preincubated with media only, or NL or HL serum (Figure 15). There was little difference in the amount remaining vs. time relationship between the cells preincubated with NL serum and media. However, HL serum pre-treatment resulted in a noticeable decrease in the apparent rate of AM metabolism. By 72 h the decline of AM in HL serum pretreated cells was only ~60% of the initial AM concentration compared to ~95% for the NL pre-treated and media only pretreated hepatocytes (Figure 15).

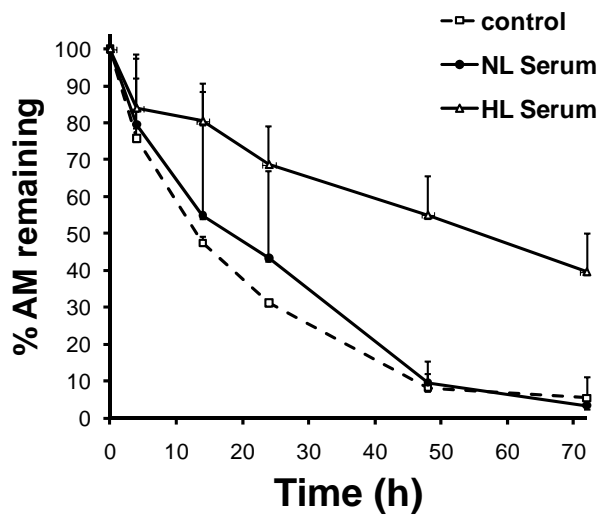


Figure 15: Amiodarone (500 mg/mL) metabolism by NL hepatocytes treated with media alone (open square), or preincubated with 5% NL (closed circle) or HL (open triangle) serum.

Compared to media alone, no significant difference was observed in the release of the lactate dehydrogenase (LDH) for up to 72 h in the presence or absence of NL or HL serum, indicating hepatocyte viability throughout the study.

3.1.2.2. Comparisons of the area under the percent AM remaining to be eliminated (ARE) vs. time curves

a. Influence of hepatocytes from HL or NL cells on AM metabolism in the absence of rat serum

There was no significant difference in the ARE of AM between the NL and HL hepatocytes over the time period from 0-72 h (Table 6). In comparing the partial ARE from 0-24, however, the ARE in the hepatocytes from HL rats (1630 ± 39.3 %·h) was significantly higher than that of the NL rat hepatocytes (1409 ± 57.2 %·h).

b. Comparison of the effect of sera treatments on the hepatocellular metabolism of AM.

These data are presented in Table 6. When incubated with DME media only, there were no significant differences in AM ARE between any of the groups (mean ARE 2000 to 2341 %·h). These could be considered to be the baseline or control values for each of the experimental groups.

The coincubation of NL serum led to a significant increase in the ARE in the NL hepatocytes compared to the incubations in the absence of the serum. A similar

increase was noted in the HL hepatocytes coincubated with NL serum, although this was not a significant change.

The addition of HL sera, whether it be as pre- or co-incubations, led to significant increases in the ARE in each of the groups compared to media only incubations. In addition, the coincubation with HL serum led to significantly higher ARE compared to the same type of cells coincubated with NL serum. Although both preincubated and coincubated NL hepatocytes had higher ARE when exposed to HL serum, the effect was significantly greater for the coincubated (6288 %·h) than the preincubated (4552 %·h) cells.

Table 6: Summary of the percent amount of drug remaining to be eliminated (ARE, %·h) from 0-72 h after exposure of cells to AM.

Hepatocytes	DME media only	NL serum	HL serum
<i>NL-co</i> ¹	2045±109	3080±133*	6288±126*†
<i>HL-co</i> ²	2341±79.7	3402±388	6149±154*†
<i>NL-pre</i> ³	2000±114	2317±321	4552±243*†‡

¹Hepatocytes from NL rats coincubated with AM in media or with 5% NL or HL sera.
²Hepatocytes from HL rats coincubated with AM in media or with 5% NL or HL sera.
³Hepatocytes from NL rats preincubated for 24 h with media or with 5% NL or HL sera. After 24 h the media was replaced with fresh rat sera-free media and drug was added.
*Significant difference from control group (p<0.006)
† Significant difference from NL serum (p<0.006)
‡Significant difference from the NL hepatocytes coincubated with HL serum (p<0.006)

3.2 Effect of HL on PK and pharmacodynamics aspects of KTZ

3.2.1 Development of an HPLC assay for the determination of KTZ enantiomers in rat plasma

a. Chromatography:

The IS and KTZ enantiomers eluted chromatographically at approximately 3.8, 11.9 and 15.6 min, respectively (Figure 16). From the polarimetry assessment, the dextro (+) enantiomer was found to be eluting first. KTZ enantiomer peaks showed baseline resolution and were symmetrical in appearance with no interferences from endogenous substances in plasma. The assay showed no observable racemization. The total analytical run time was 18 min.

The column capacity factors (K') for IS, (+)- and (-)- KTZ were calculated to be 0.3, 3.1, and 4.4 respectively. The column separation factor (α) and resolution factor for the KTZ enantiomers were calculated to be 1.4 and 2.3, respectively.

The average extraction recoveries in plasma of (+)-KTZ were 89.0 and 81.3% for the 250 and 1000 ng/mL concentrations, respectively. For the (-) enantiomer, extraction efficiencies were 83.7 and 79.8%, respectively, at concentrations of 250 and 1000 ng/mL. Highly linear relationships were noted between the analyte/IS peak height or area ratios and rat plasma enantiomer concentrations ranging from 62.5 to 5000 ng/mL. The mean r^2 for the three standard curves were 0.999 for each enantiomer (Figure 17).

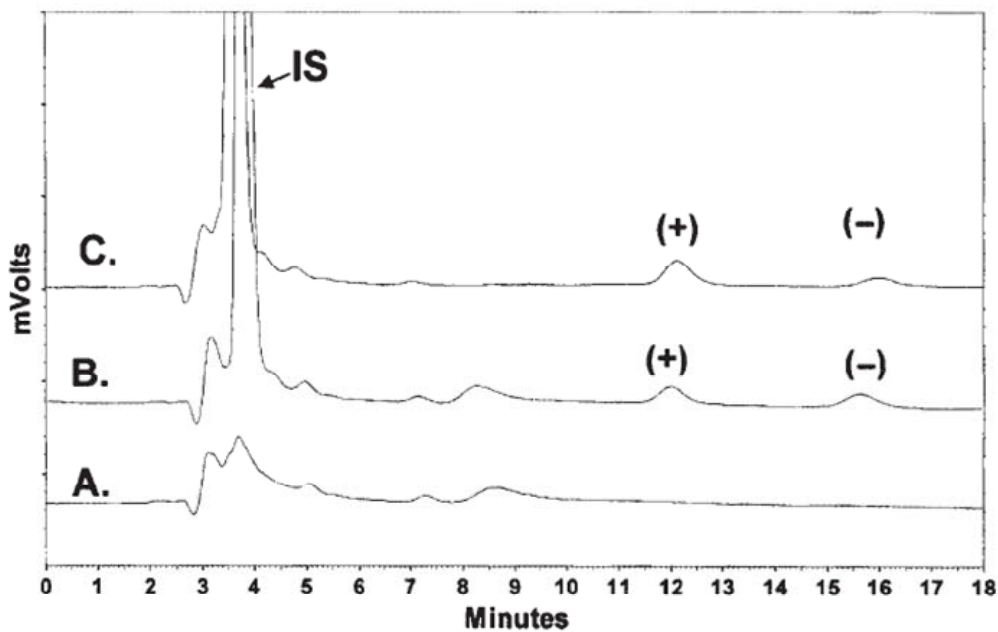


Figure 16: Chromatograms of A. blank rat plasma sample, B. rat plasma spiked with 2500 ng/mL of (\pm)-KTZ, C. rat plasma obtained after 2h of 10mg/kg KTZ racemate dose. Abbreviation: IS internal standard.

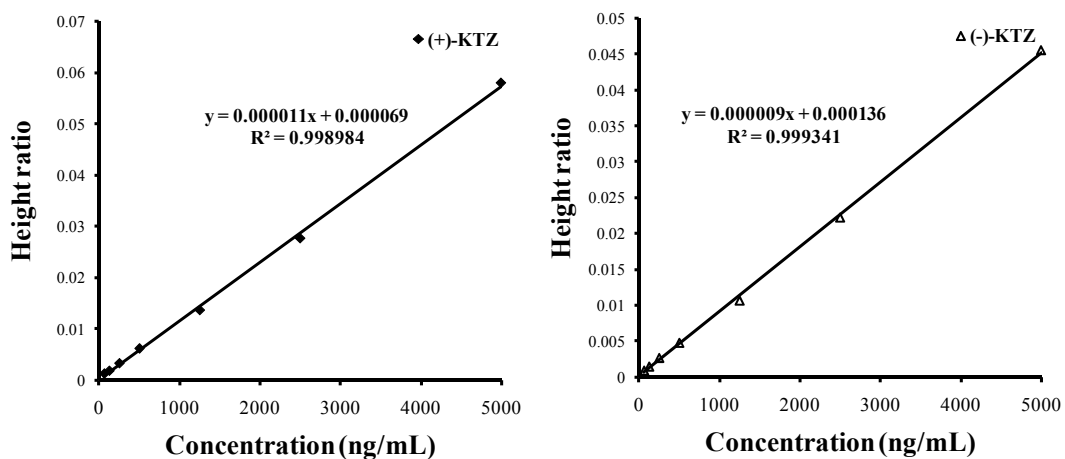


Figure 17: A representative standard curve of KTZ enantiomers in rat plasma (From 62.5-5000 ng/mL)

b. Assay validation:

The validation data showed the assay to be sensitive, accurate and precise, with the intraday and interday assessment CV% less than or equal to 19% and 10%, respectively for both enantiomers (Table 7). The mean interday error in rat plasma was less than 4% for both enantiomers. Since both CV% of interday and intraday assessment and interday mean error yielded values less than 20% at the lowest concentration tested, the lower limit of quantitation (LLQ) based on 100 μ L of rat plasma was found to be 62.5 ng/mL for each enantiomer.

c. Applicability of the assay:

In the rats dosed with (\pm)-KTZ orally, the concentrations of (+) enantiomer were much higher than those of (-)-KTZ (Figure 18). The C_{max} of the (+) enantiomer was 5246 and 1389 ng/mL for the 2 rats while those of the (-) enantiomer were 2424 and 614 ng/mL, respectively. The T_{max} for both enantiomers were similar, occurring at ~1h post dose in both rats. The KTZ enantiomer concentrations occurring after 4 h post dosing below the LLQ of 62.5 ng/mL, thus limiting the AUC calculation from 0 to 4 h postdose. The AUC_{0-4 h} for KTZ enantiomer concentrations in the 2 rats studied were 10596 and 2346 for the (+)-KTZ and 4404 and 945 ng.h/mL for the (-) KTZ.

Table 7: Validation data of ketoconazole enantiomers assay in 100 µL rat plasma

Expected enantiomer concentration ng/ml	KTZ enantiomer	Intra day mean±SD (intra day CV %)	Interday, mean±SD, ng/mL	Interday CV%	Interday mean error%		
62.5	(+)	63.9 ± 4.36 (6.8)	65.3±8.2 (12.5)	59.7±9.7 (16.2)	63.0±2.9	4.6	-0.8
	(-)	65.3±6.6 (10.0)	65.3±7.1 (10.8)	55.9±10.1 (18.0)	62.2±5.4	8.8	0.5
125	(+)	111±11.6 (10.4)	130±8.1 (6.2)	120.5±9.7 (8.0)	121±9.5	7.9	3.4
	(-)	111±21.3 (19.0)	130±13.7 (10.6)	111±3.5 (3.1)	118±11	9.3	6
500	(+)	476±17.9 (3.8)	530±15.3 (2.9)	517±24.1 (4.7)	508±28	5.5	-1.6
	(-)	921±28.7 (3.1)	529±18.4 (3.5)	524±29.0 (5.5)	505±38	7.6	-0.9
2500	(+)	2433±82.5 (3.4)	2522±44.1 (1.8)	2582±164 (6.4)	2512±72	3	-0.5
	(-)	2464±85.0 (3.5)	2515±36.3 (1.4)	2549±140 (5.5)	2510±43	1.7	-0.4

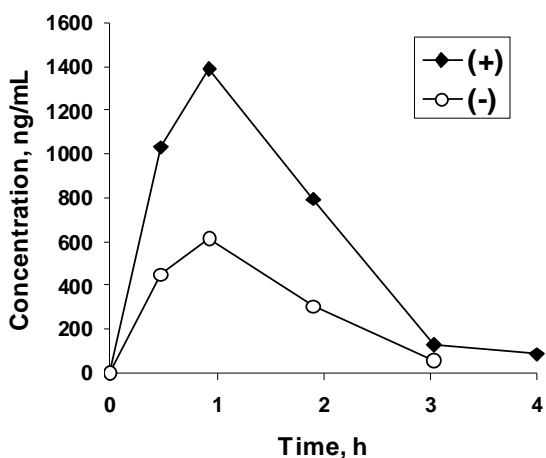
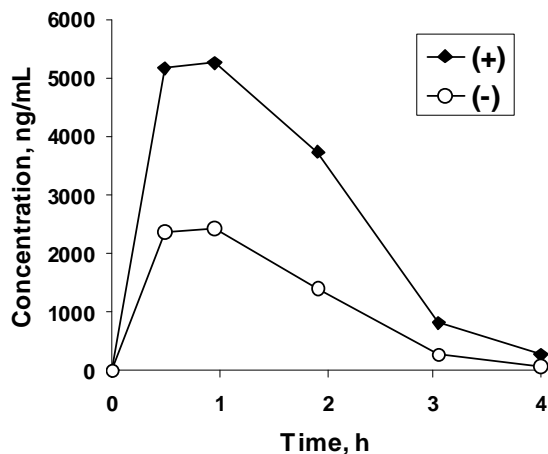


Figure 18: Plasma KTZ enantiomer concentrations versus time curves from 2 rats given an oral dose of 10mg/kg KTZ racemate. (+) KTZ enantiomer represented by closed diamonds and (-) KTZ enantiomer represented by open circles.

3.2.2 Determination of nonlinear stereoselective PK of KTZ in rat after administration of racemate

In general, after *iv* doses of 10 mg/kg (\pm)-KTZ, the plasma concentrations appeared to decline monoexponentially for both enantiomers, with mean $t_{1/2}$ of approximately 40 min (Figure 19, Table 8). However, in examining the individual concentration vs time plots, in some rats there was evidence of apparent convexity

in the latter concentration time points (Figure 19c). In all rats, the differences between enantiomers were significant with respect to $AUC_{0-\infty}$, CL and V_{dss} with overall mean (+):(-) KTZ ratios of 2.05, 0.47 and 0.56, respectively (Table 8).

As for *iv* doses, in all rats given oral doses (+)-KTZ plasma concentrations were significantly higher than (-)-KTZ with overall mean (+):(-) $AUC_{0-\infty}$ and C_{max} ratio of 2.36 and 2.19, respectively (Figure 20 and Table 8). For all of the doses, the median T_{max} was very similar between the two enantiomers. However, there seemed to be a trend towards longer T_{max} with higher dose levels. There were no significant differences between enantiomers within doses for the $t_{1/2}$, although the slope of log plasma concentration vs time for both enantiomers seemed to become shallower (ANOVA $p < 0.05$) as the dose increased (Table 8). Due to dose and perhaps a longer $t_{1/2}$, the KTZ enantiomers were detected for a longer duration of time at higher than lower doses (Figure 20). In all rats an AUC of at least 4 h was obtained, so the AUC_{0-4h} are displayed in Table 8 for comparison with $AUC_{0-\infty}$. In conjunction with the *iv* data, the F for the 10 mg/kg oral dose group were calculated to be 31.1% and 28.7% for the (+)- and (-)-KTZ, respectively.

The correlation between C_{max} or $AUC_{0-\infty}$ and dose showed a disproportional increase in plasma levels with escalating dose (Figure 21, Table 8). Three phases seemed to be present in the C_{max} vs. dose relationship, and two phases in the $AUC_{0-\infty}$ vs. dose profile. For both C_{max} and $AUC_{0-\infty}$, with the initial increases in dose the measures of plasma concentrations increased in an approximately linear fashion. Above these dose levels the nature of the relationship appeared to

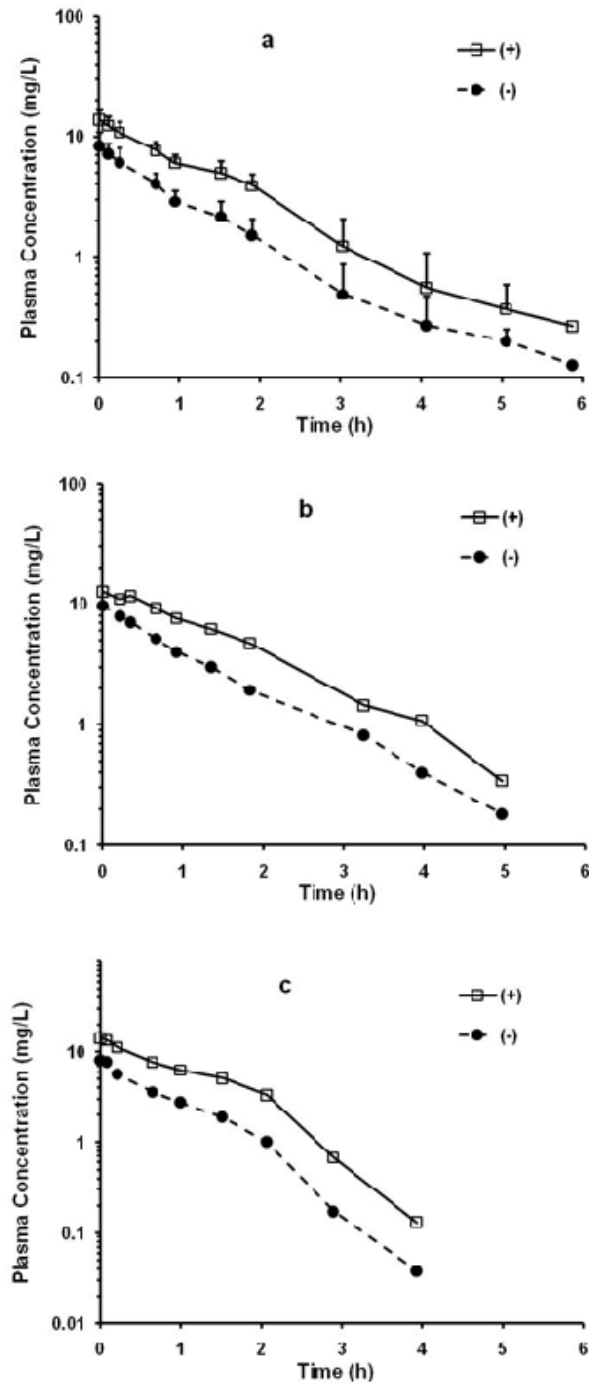


Figure 19: Plasma concentration vs. time plots of KTZ enantiomers after administration of 10 mg/kg of the racemate as *iv* doses. a.) mean \pm SD of all 7 rats, b.) an individual rat displaying monoexponential decline, c.) an individual rat displaying apparent nonlinearity in decline.

Table 8: Pharmacokinetic parameters (mean±SD) of ketoconazole enantiomers (KTZ) after *iv* and oral doses of racemate.

Racemate (mg/kg)	KTZ	AUC _{0-4h} (mg·h/L)	AUC ₀₋₈ (mg·h/L)	t _{1/2} (h)	C _{max} (mg/L)	t _{max} (h)	V _{dss} (L/Kg)	CL [†] (L/h/Kg)	MRT (h)
Intravenous dose									
10	(+)	17.29±4.25*	17.94±4.91*	0.661±0.259	–	–	0.707±0.075*	0.590±0.144*	1.25±0.259*
	(-)	8.45±2.67	8.72±2.90	0.615±0.258	–	–	1.27±0.196	1.26±0.390	1.07±0.246
Oral doses									
10	(+)	5.46±3.57*	5.59±3.63	0.580±0.060	2.72±1.72	0.930 (0.900-0.950)	–	2.36±1.32	1.54±0.095
	(-)	3.19±1.72	2.51±1.43	0.672±0.252	1.26±0.800	0.930 (0.900-0.950)	–	5.28±3.38	1.63±0.234
20	(+)	8.74±4.39*	9.70±5.21*	0.674±0.336	4.23±1.99*	1.87 (1.15-1.95)	–	3.22±3.02	1.90±0.616
	(-)	3.72±2.14	4.11±2.55	0.646±0.355	1.79±0.932	1.87 (0.333-1.95)	–	8.91±9.53	1.82±0.660
40	(+)	38.9±3.84*	56.8±18.4*	1.04±0.041	15.1±2.15*	1.53 (0.883-2.88)	–	0.802±0.237*	2.86±0.590*
	(-)	16.82±2.44	22.7±7.71	0.942±0.206	6.52±1.03	1.53 (0.883-2.88)	–	1.88±0.487	2.65±0.468
50	(+)	44.7±1.0*	71.8±18.7*	1.23±0.412	18.2±2.10*	1.91 (0.966-2.08)	–	0.738±0.217*	3.16±0.311
	(-)	20.1±4.64	27.0±13.0	1.07±0.279	8.22±0.889	1.91 (0.966-2.08)	–	2.24±1.08	3.71±0.493
80	(+)	56.3±8.49*	112±37.2*	2.02±0.892	20.7±3.11*	2.05 (1.95-2.07)	–	0.771±0.264*	5.22±2.34
	(-)	27.2±3.19	53.9±19.5	1.92±0.935	10.0±1.30	2.05 (1.95-2.07)	–	1.62±0.595	4.77±2.52

* Significant difference from corresponding (-) enantiomer

† CL/F for the oral doses.

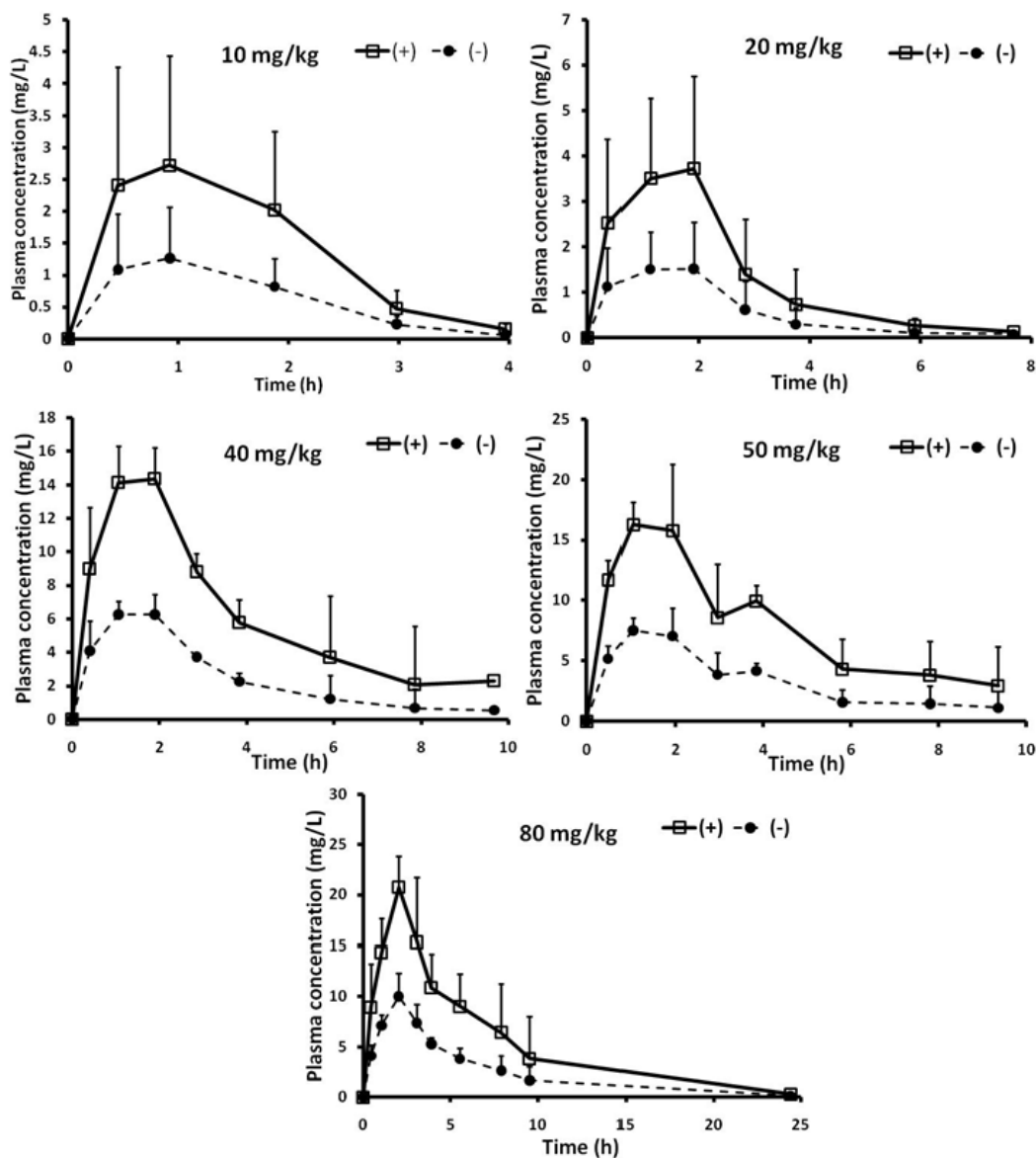


Figure 20: Mean (\pm S.D.) plasma concentration vs. time curves of ketoconazole enantiomers after oral racemic doses of 10, 20, 40, 50, or 80 mg/kg ($n=3-4$ rats per dose group).

change. From 20 to 40 mg/kg the 2-fold increase in dose resulted in 3.6 and 5.9 fold increases of the (+)-KTZ C_{max} and $AUC_{0-\infty}$ and 3.7 and 5.5 fold increases for the equivalent (-)-KTZ, respectively. Above these dose levels, the mean $AUC_{0-\infty}$ appeared to increase linearly with a different slope than lower doses. In

contrast to AUC, the C_{max} between 40 and 80 mg/kg doses tended to reach a plateau. For the dose-normalized AUC, a significant difference was noted between dose groups ($p < 0.05$, ANOVA).

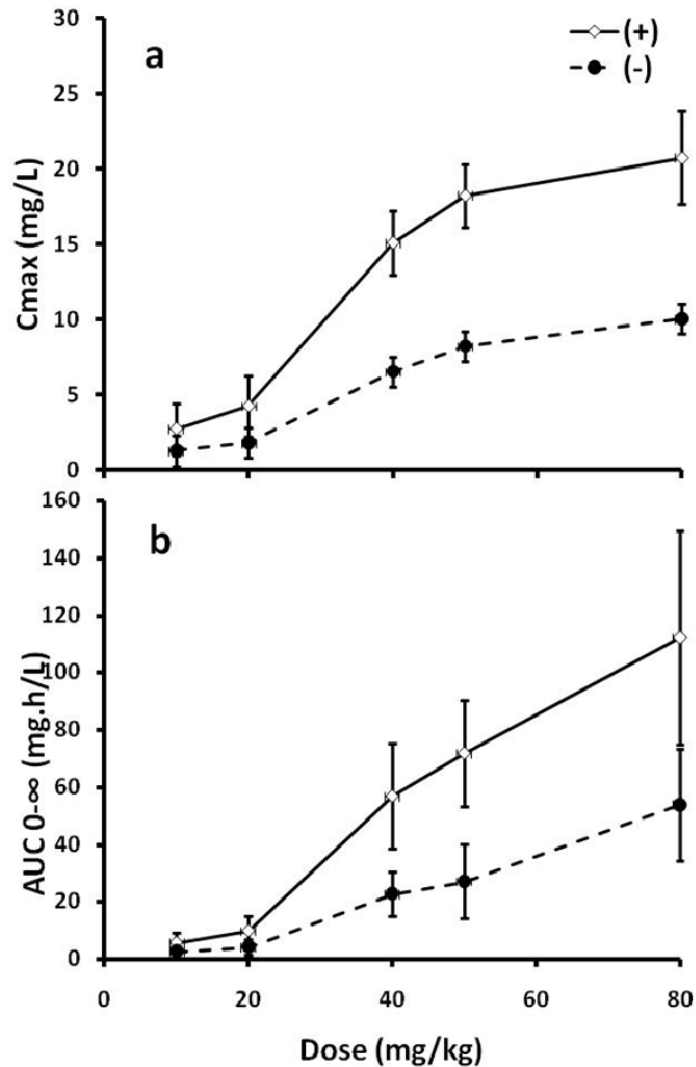


Figure 21: Relationship between the racemic ketoconazole oral doses and enantiomer a.) C_{max}, and b.) AUC.

Unlike the plasma concentrations, there was no evidence of stereoselectivity in the metabolism by hepatic microsomes. There were virtually superimposable velocities of disappearance of enantiomers observed along the concentration

ranges tested (Figure 22). Because this experiment was designed to examine only stereoselective metabolism using replicate samples of the same pooled microsomes, kinetic constants of metabolism are not reported.

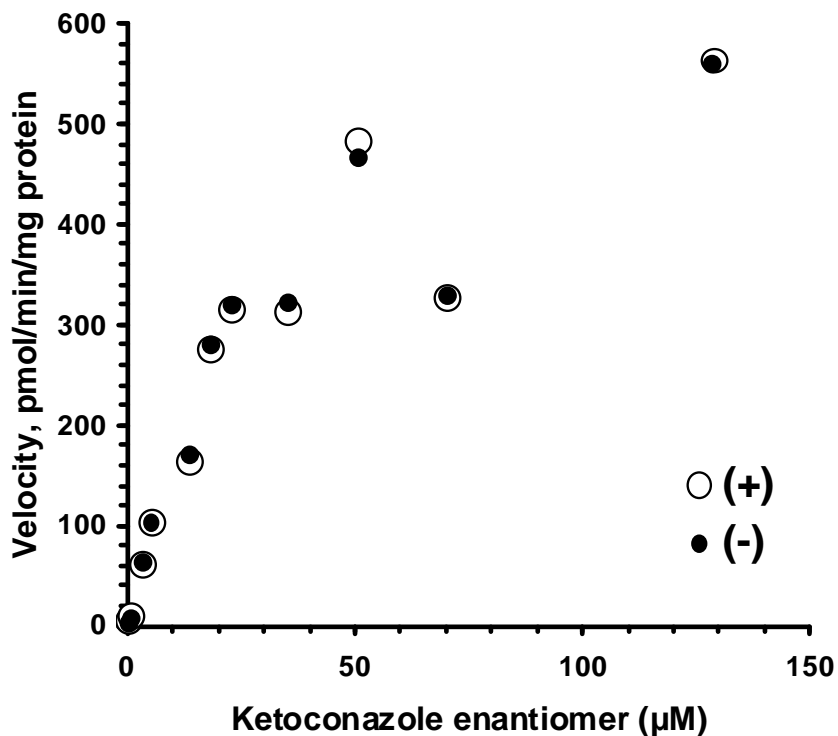


Figure 22: Mean rates of disappearance of ketoconazole enantiomers vs. enantiomer concentration in the presence of rat liver microsomes. Incubations were run over 15 min after being spiked with the racemate (n=2 to 4 per concentration).

Extensive plasma protein binding (>97%) was observed for both (+)-and (-)-KTZ in rat plasma. At lower KTZ concentrations (10 µg/mL of racemate), the fu for (+)-KTZ were found to be 0.64%±0.12% and 0.61%±0.10% for the two rats. In contrast, the respective (-)-KTZ fu were found to be 1.73%±0.30% and 1.90%±0.32%. At 40 µg/mL of racemate, the fu of (+)-KTZ in plasma from the

rats were $0.97\% \pm 0.29\%$ and $0.92\% \pm 0.30\%$ respectively. In comparison the (-)-KTZ fu were found to be $2.38\% \pm 0.65\%$ and $2.32\% \pm 0.88\%$. For both enantiomers at the higher concentrations of $40 \mu\text{g/mL}$, the unbound fraction were significantly higher compared to the lower concentration tested ($10 \mu\text{g/mL}$). Stereoselectivity was similar however for both concentrations, where the mean ratios of (-):(+) unbound enantiomer were 2.9 and 2.5 for the 10 and $40 \mu\text{g/mL}$ concentrations of racemate, respectively.

The mean blood:plasma ratios of (+)-and (-)-KTZ were 0.61 ± 0.039 and 0.64 ± 0.065 , respectively. This indicated minimal blood cell partitioning for KTZ enantiomers and its restriction to plasma within the blood matrix. The blood CL was calculated by dividing the plasma CL by the blood:plasma ratios, yielding mean blood CL of 0.976 and 1.97 L/h/kg for the (+)-and (-)-KTZ enantiomers, respectively. Using the reported mean hepatic blood flow in rat [191] and assuming that the majority of the CL of KTZ enantiomers is attributed to the liver, the E was estimated to be 0.30 and 0.60 for the (+)-and (-) enantiomers, respectively. The fg was calculated to be 0.44 and 0.72 for the (+) and (-) enantiomers respectively.

3.2.3 Influence of HL on in vitro distribution of KTZ enantiomers in rat plasma

As expected, HL caused significant increases in plasma TG and CHOL levels of 30.6 and 25.2-fold, respectively in P407 treated rat (Table 9). The total recovery from the spiked (\pm)-KTZ (3000 ng/mL) was about 80% in rat (Table 10). The presence of HL did not significantly affect the recovery of the KTZ enantiomers.

Table 9: The mean \pm SD cholesterol and triglyceride present in rat plasma

	Total cholesterol (mmol/L)	TriglycerideTG (mmol/L)
NL	1.55 \pm 0.10	2.08 \pm 0.15
HL	40.9 \pm 0.36*	62.2 \pm 4.89*
* $P < 0.05$ compared to NL		

After incubation with racemate, it was noted that KTZ enantiomers were most associated with LPDP in NL and HL plasma (Table 10). In NL rat plasma the LPDP fraction accounted for >98% of the (\pm)-KTZ recovered. In NL plasma negligible amounts of (\pm)-KTZ were measured in LDL and TRL lipoprotein fractions. In the HDL fraction KTZ concentrations were too low to measure (Figure 23). HL caused about 20% of the (\pm)-KTZ to migrate to each of the lipoprotein fractions, mostly to TRL followed by LDL and HDL (Figure 23).

Upon comparing KTZ enantiomers, both behaved similarly in NL rat plasma with greater than 98% of the recovered drug associated within the LPDP fraction. The levels within the HDL fraction were too low to measure for both enantiomers. On the other hand in HL plasma the (-)-KTZ enantiomer showed significant 1.2-fold lower LPDP and 1.5-fold higher TRL association levels than that of (+)-KTZ (Figure 24; Table 10).

Table 10: Association of (+)- and (-)-KTZ in each fraction of normolipidemic (NL) and hyperlipidemic (HL) rat plasma samples

Serum	Recovery in each fraction (%)			TRL	Total recovery (%)
	LPDP	HDL	LDL		
(+)-KTZ					
<i>NL</i>	78.0±5.83	n/a	1.03±0.320	0.421	79.5
<i>HL</i>	65.5±4.38	4.69±1.07	5.37±0.692	9.77±1.32	85.4
(-)-KTZ					
<i>NL</i>	77.5±3.17	n/a	0.470±0.341	0.628	78.6
<i>HL</i>	55.6±1.25	3.49±1.67	4.28±1.576	12.7±1.70	76.1

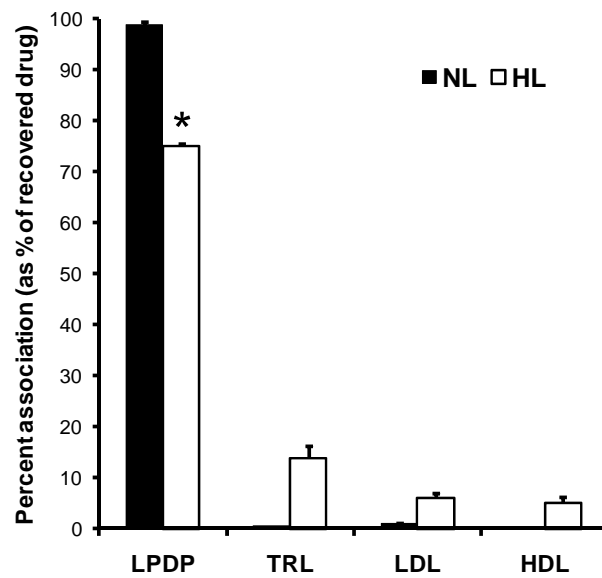


Figure 23: Association of (±)-KTZ (sum of the enantiomers) with lipoprotein fractions incubated with NL and HL rat plasma, expressed as percentage of total recovered drug.* denotes $p < 0.05$ between HL and NL

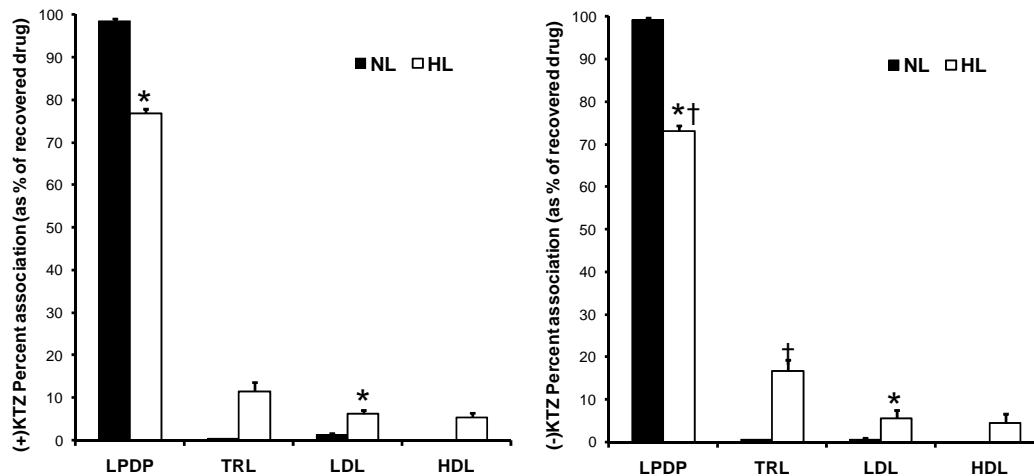


Figure 24: Association of (+)- and (-)-KTZ with lipoprotein fractions incubated with NL and HL rat plasma, expressed as percentage of total recovered drug. * denotes $p < 0.05$ between HL and NL. † denotes $p < 0.05$ difference between (+) and (-) enantiomers

3.2.4 The effect of HL on the PK of KTZ enantiomers in rat.

After *iv* administration of 10 mg/kg of (\pm)-KTZ, the plasma concentrations for both HL and NL rats declined monoexponentially for both enantiomers, with similar mean $t_{1/2}$ of ~ 40 min for NL and ~ 50 min for HL rats (Figure 25, Table 11). HL rats showed equivalent plasma concentrations, CL and $AUC_{0-\infty}$ to NL rats for both enantiomers (Figure 25). However, the V_{dss} of both enantiomers were significantly higher in HL rats (Table 11). Similar to what was previously reported for NL rats, (+)-KTZ showed significantly higher plasma concentrations than its antipode in HL states. Stereoselectivity in PK was altered in HL. The (+): (-) KTZ ratios of plasma $AUC_{0-\infty}$ were significantly lower in HL (2.11 ± 0.20 NL vs. 1.66 ± 0.11 HL), but significantly higher in HL for both CL (0.48 ± 0.044 NL vs. 0.60 ± 0.048 HL) and V_{dss} (0.56 ± 0.045 NL vs. 0.68 ± 0.083 HL).

Similar to *iv*, after oral doses there was no significant difference in the plasma AUC_{0-6h} , for either enantiomer between NL and HL animals (Figure 26). In NL rats the plasma and liver concentrations attained C_{max} at about 3 h, for each enantiomer. The T_{max} was reached earlier in the HL state, at 1.5 and 0.5 h postdose in plasma and liver, respectively compared to NL state. Liver concentrations were generally higher than equivalent plasma concentrations for both enantiomers in NL and HL rats (Figure 26, Table 12). In the liver, there were higher concentrations present at 1.5 and 3 h after dosing for both enantiomers in the NL rats, although before and after this time period there were no differences between the NL and HL animals (Figure 26). The differences between NL and HL

in KTZ liver concentrations were most prominent at 1.5 and 3 h after oral doses, for both enantiomers (Figure 26). The (-)-KTZ liver K_p in HL rats at each time point were significantly lower than those of NL rats. In contrast (+)-KTZ liver K_p showed no significant difference between NL and HL rats (Figure 27).

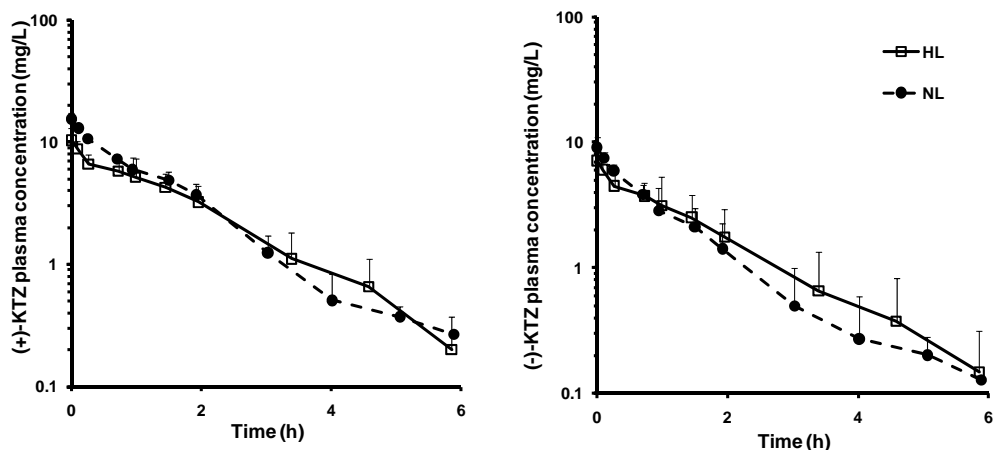


Figure 25: Mean (\pm S.D.) plasma concentrations vs. time plots of KTZ enantiomers in normal and hyperlipidemic rats after *iv* administration of 10 mg/kg of racemate.

The uptake of KTZ enantiomers by blood cells was minimal in NL, and in HL similarly low (blood to plasma ratio was 0.73 for each enantiomer). Therefore the mean enantiomer blood CL were calculated by dividing the respective mean plasma CL by the corresponding blood:plasma ratios in NL plasma. This yielded blood CL in NL rats of 1.0 and 2.1 L/h/kg for the (+) and (-)-KTZ, respectively.

Table 11: The pharmacokinetic parameters (mean \pm S.D.) of ketoconazole enantiomers (KTZ) in normal and hyperlipidemic rats after *iv* administration of 10 mg/kg of racemate.

	(+)KTZ		(-)KTZ	
	NL	HL	NL	HL
C₀	15.5 \pm 5.06 [†]	10.4 \pm 2.60 [†]	9.10 \pm 3.06	7.17 \pm 1.81
AUC_{0-6h}	17.1 \pm 4.62 [†]	13.9 \pm 3.79 [†]	8.22 \pm 2.84	8.55 \pm 2.51
AUC_{0-inf}	17.3 \pm 4.89 [†]	14.2 \pm 4.14 [†]	8.37 \pm 2.86	8.72 \pm 2.63
t_{1/2}	0.64 \pm 0.25	0.83 \pm 0.36	0.60 \pm 0.24	0.81 \pm 0.23
CL	0.61 \pm 0.15 [†]	0.74 \pm 0.20 [†]	1.31 \pm 0.39	1.25 \pm 0.38
V_{dss}	0.71 \pm 0.07* [†]	1.04 \pm 0.18 [†]	1.27 \pm 0.18*	1.56 \pm 0.29
MRT	1.21 \pm 0.26	1.47 \pm 0.38	1.03 \pm 0.25	1.32 \pm 0.33

*Significant difference between NL and HL (p<0.05)

[†]Significant difference between (+)- and (-)-KTZ enantiomers (p<0.05)

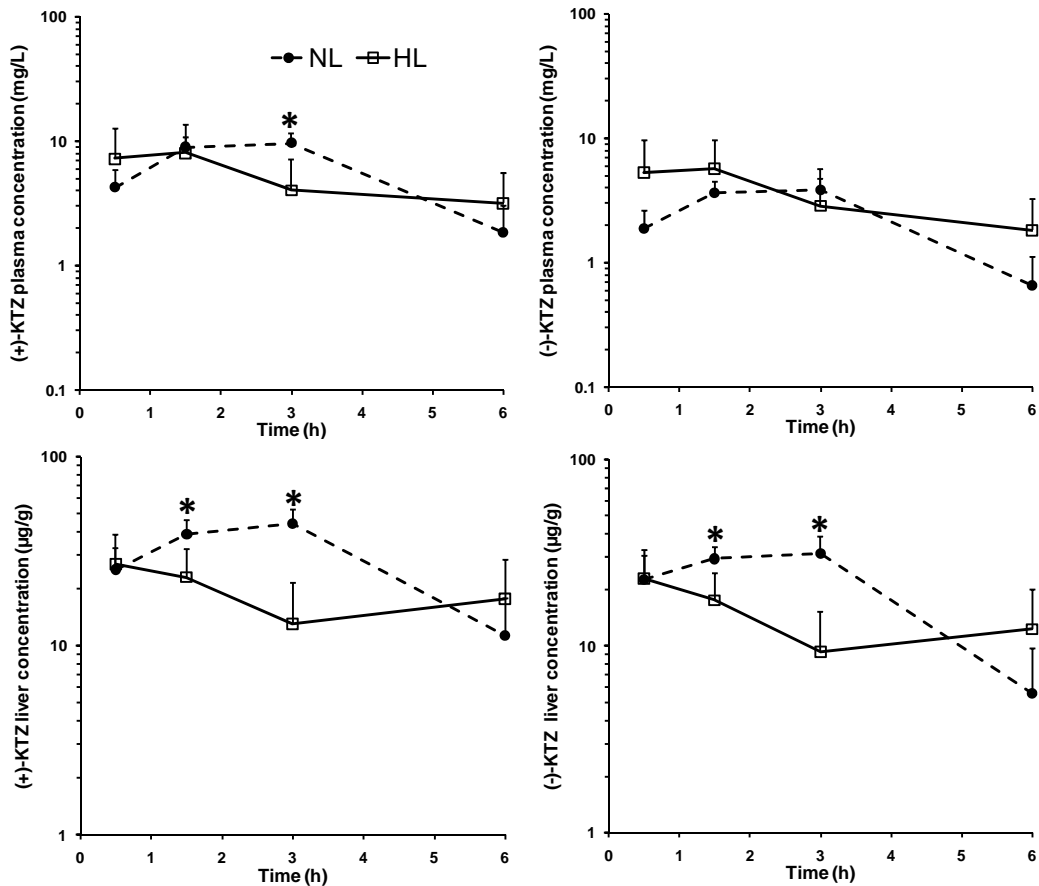


Figure 26: Mean (\pm S.D.) plasma and liver concentrations vs. time curves of KTZ enantiomers in normal and hyperlipidemic rats after oral administration of 40 mg/kg of racemate. * Significant difference between NL and HL ($p < 0.05$)

The corresponding values in HL rats were 1.01 and 1.70 L/h/kg, respectively. Using the reported mean hepatic blood flow rate in rat [191] and assuming that the majority of KTZ enantiomers CL is through liver, the extraction ratio (E) was estimated for (+) and (-)-KTZ to be 0.3 and 0.62 in NL and 0.31 and 0.52 in HL rats, respectively. It was not possible to calculate the bioavailability of the enantiomers, since different dose levels were administered for oral and iv regimens, and it was shown previously that the drug demonstrates a nonlinear relationship between dose and AUC.

Table 12: The area under the concentration time curve (mean±S.D.) of ketoconazole enantiomers in normal and hyperlipidemic rats after oral administration of 40 mg/kg of racemate

	(+)-KTZ		(-)-KTZ	
	NL	HL	NL	HL
Liver AUC_{0-6h} (mg·h/kg)	173±19.9†	97.4±24.4	121±13.5†	73.6±15.2†
Plasma AUC_{0-6h} (mg·h/L)	63.5±9.50	43.6±11.5	38.1±7.66	31.1±7.76

†Significant difference between liver and plasma AUC in the same lipidemic state (p<0.05)

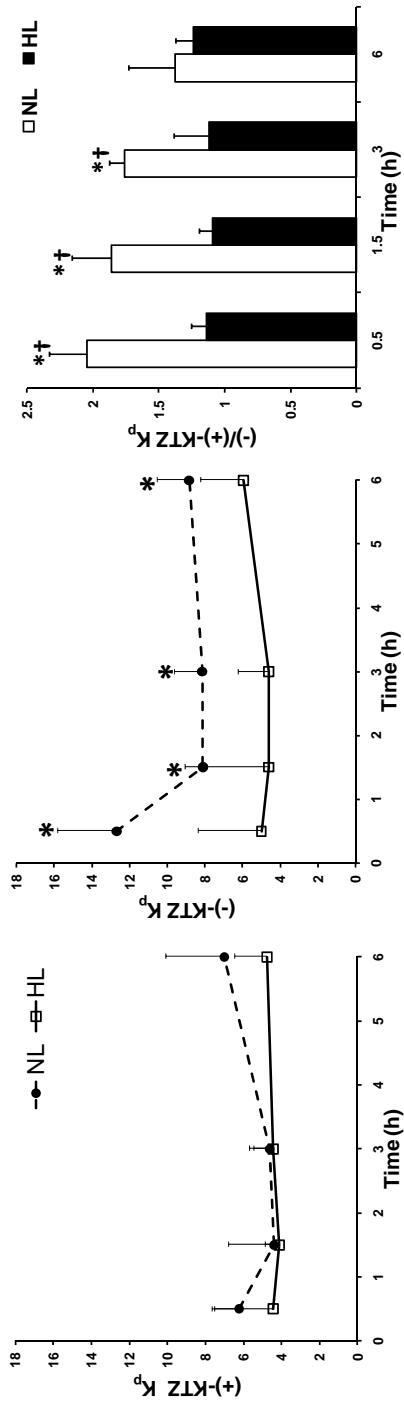


Figure 27: The mean (\pm S.D.) liver to plasma concentrations (K_p) of ketoconazole enantiomers vs. time plots and the (-):(+)-KTZ K_p ratio vs. time plots in normal and hyperlipidemic rats after oral administration of 40 mg/kg of racemate.

* Significant difference between NL and HL ($p < 0.05$)

† Significant difference between (+) and (-)-KTZ in the same lipidemic state

3.2.5 Development of an HPLC assay for the simultaneous determination of MDZ and KTZ in rat plasma

a. Chromatography

The MDZ, KTZ and IS eluted chromatographically at approximately 6.4, 7.5 and 9.1 min, respectively in rat plasma (Figure 28) and at approximately 7.2, 8.5 and 10.2 min, respectively in human plasma (Figure 29). All analyte peaks were symmetrical in appearance with baseline resolution with no interferences from endogenous substances in plasma. The total analytical run time was ~10 min. The column separation factor (α) and resolution factor for MDZ and KTZ were calculated to be 1.2 and 2, respectively. The column capacity factors (K') for MDZ, KTZ and IS were calculated to be 3.6, 4.3 and 5.5, respectively. The symmetry indexes were 1.2, 1.1 and 1.0 for the MDZ, KTZ and diazepam, respectively.

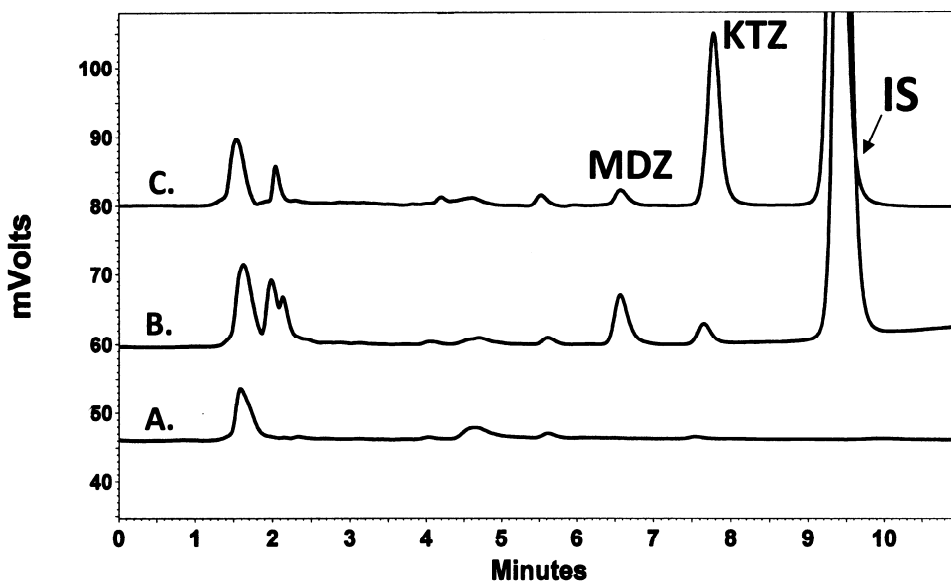


Figure 28: Chromatograms of A. blank rat plasma sample, B. rat plasma spiked with 1000 ng/mL of KTZ and MDZ, and C. rat plasma obtained after 1h of i.v. MDZ administration (1.5h of KTZ administration).

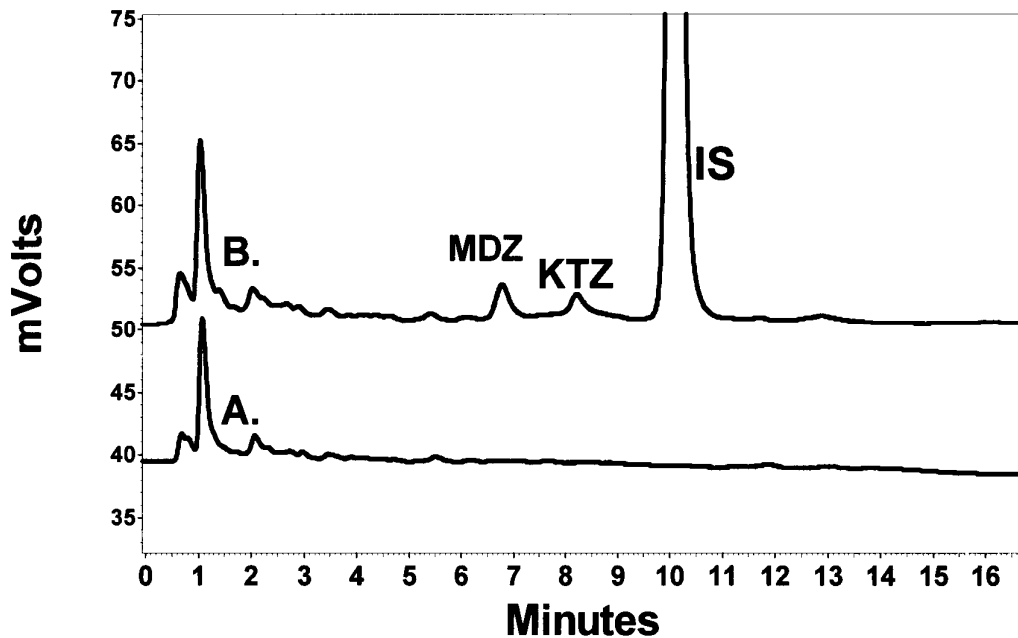


Figure 29: Chromatograms of A. blank human plasma sample, B. human plasma spiked with 100 ng/mL of KTZ and MDZ.

The recoveries of KTZ and MDZ and diazepam from plasma were complete (100%) in rat and human plasma. Highly linear relationships were noted between the peak height or area ratios of analyte/IS ranging from 25-25000 and 5 to 10000 ng/mL of rat and human plasma, respectively. The r^2 for human plasma was 0.999 and 0.9984 for MDZ and KTZ, respectively. The mean r^2 for the three standard curves in rat plasma were ≥ 0.999 for each drug (Figure 30).

b. Assay validation

The validation data showed the assay to be sensitive, accurate and precise, with the intraday and interday CV% less than or equal to 5.8 and 3.4%, respectively, for MDZ and KTZ (Table 13 and Table 14). The mean interday error in rat plasma was

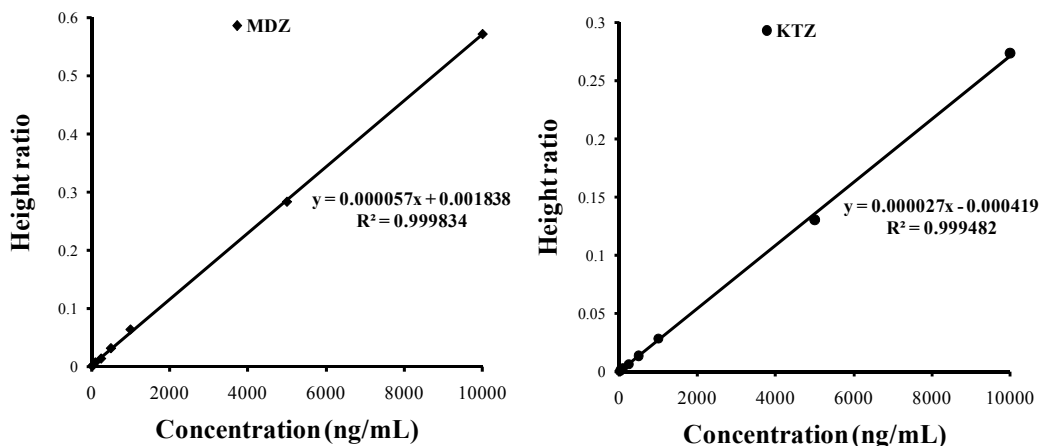


Figure 30: A representative standard curve of midazolam and ketoconazole assay in rat plasma (From 25-10000 ng/mL)

less than 13% for both drugs. The intraday CV% and % error of the mean were less than 13% for both drugs in human plasma (Table 13 and Table 14).

Since both CV% of interday and intraday assessment and interday mean error yielded values less than 20% at the lowest concentration tested, the lower limit of quantitation (LLQ) based on 100 μ L of rat plasma was found to be 25 ng/mL, and based on 500 μ L of human plasma, 5 ng/mL for both analytes.

c. Applicability of the assay

In rats dosed with 40 mg/kg KTZ orally followed 1.5 h later by 5 mg/kg MDZ i.v., KTZ plasma concentrations were higher than those of MDZ at all time points (Figure 31). The assay managed to measure both KTZ and MDZ concentrations up to 8 h post MDZ administration. Table 15 shows some PK parameters for both drugs.

Table 13: Validation data for midazolam in 100 µL rat plasma and 500 µL human plasma

Expected concentration ng/ml	Intraday mean±SD (Intraday CV%)	Interday mean±SD ng/mL	Interday CV%	Interday mean error%
Rat plasma				
25	24.8 ± 1.32 (5.32)	23.2±2.17 (2.18)	24.4±1.50 (6.13)	24.1±0.8
100	109±2.94 (2.70)	111±1.58 (1.42)	116±4.62 (3.98)	112±3.6
1000	1028±10.86 (1.06)	1034±15.2 (1.47)	1009±6.10 (0.61)	1023±13
10000	9665±49.7 (0.51)	9592±210 (2.19)	9499±70.5 (0.74)	9585±83
Human plasma				
5	5.62 ± 0.70 (12.3)			
10	10.5±1.24 (11.8)			
100	99.5±5.32 (5.3)			
200	207 ±3.09 (1.49)			
10000	9358 ±2.12 (2.26)			

Table 14: Validation data for ketoconazole in 100 µL rat plasma and 500 µL human plasma

Expected concentration ng/ml	Intraday mean±SD (Intraday CV %)	Intraday mean±SD ng/ml	Interday CV%	Interday mean error%
Rat plasma				
25	25.2 ± 1.52 (6.02)	27.2±3.86 (14.2)	27.4±2.07 (7.54)	26.6±1.2 4.6
100	103±2.40 (2.34)	96.6±3.95 (4.09)	109±2.32 (2.13)	103±6.0 5.8
1000	967±29.5 (3.06)	1025±18.0 (1.75)	1010±24.1 (6.99)	1001±30 3.0
10000	9900±425 (4.30)	10149±138 (1.35)	9854±78.6 (0.80)	9968±158 1.6
Human plasma				
5	4.53 ± 0.50 (10.9)			
10	10.8±0.92 (11.0)			
100	110±7.83 (7.14)			
200	196±12.3 (5.3)			
10000	10456±194 (1.86)			

Table 15: Plasma pharmacokinetic parameters of midazolam and ketoconazole after co-administration in individual rats

	Rat 1		Rat 2	
	KTZ	MDZ	KTZ	MDZ
AUC_{0-∞} (mg·h/L)	97.7	2.96	105	2.89
t_{1/2} (h)	1.40	3.43	0.83	4.46
CL (L/h/kg)	-	1.69	-	1.73
V_{dss} (L/kg)	-	2.66	-	4.53
C_{max} (mg/L)	18.8	-	26.5	-
T_{max} (h)	2.1	-	2.6	-

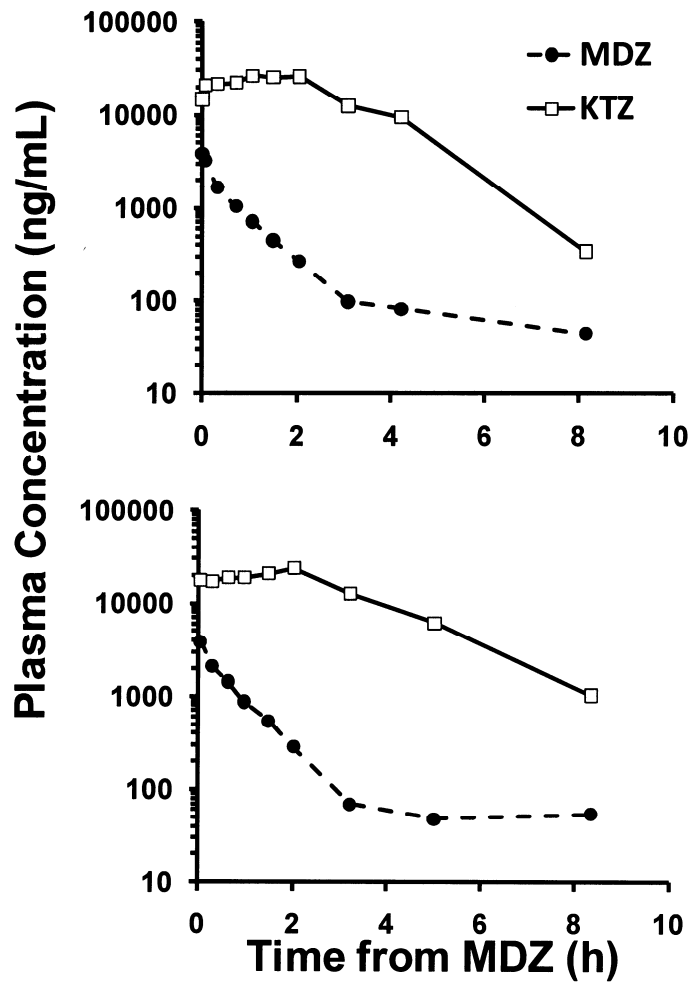


Figure 31: Plasma KTZ and MDZ concentration vs. time curve taken from 2 rats given 40 mg/kg KTZ orally followed 1.5 h later by 5 mg/kg MDZ i.v.

3.2.6 Effect of HL on KTZ-MDZ drug-drug interaction in rat

3.2.6.1 MDZ kinetics

In general, after *iv* doses of 5 mg/kg MDZ, the plasma concentrations declined multiexponentially (Table 16; Figure 32). In all rats MDZ was extensively (>98%) bound to plasma proteins.

a. Effect of KTZ on the kinetics of MDZ

Following the 40 mg/kg dose of (\pm)-KTZ, in the NL rats the CL of MDZ decreased by ~28% and the corresponding AUC_{0- ∞} increased by ~ 34%. Despite the difference, however, there was no significant difference between no KTZ and KTZ groups. KTZ also had no significant effect on Vd or on t_{1/2} in the NL rats (Table 16).

In the HL rats KTZ group, there were some significant changes noted in the kinetics of MDZ. Significant increases in the AUC (>2.2-fold) and lowering of the CL (56% decline) were observed. As for NL rats, no change in Vd or in t_{1/2} was noted. Hence, HL was found to accentuate the inhibitory effect of KTZ on MDZ kinetics.

b. Effect of HL on the kinetics of MDZ

In rats free of KTZ, HL was associated with a significant increase in the estimated C_{0h}, and decrease in V_c and f_u. In the presence of KTZ, however, HL caused significant changes in all parameters except for t_{1/2}. Significant increases were

observed in the AUC and C0h, and decreases in CL (31%), Vc (41%) , Vdss (48%) and fu (43%).

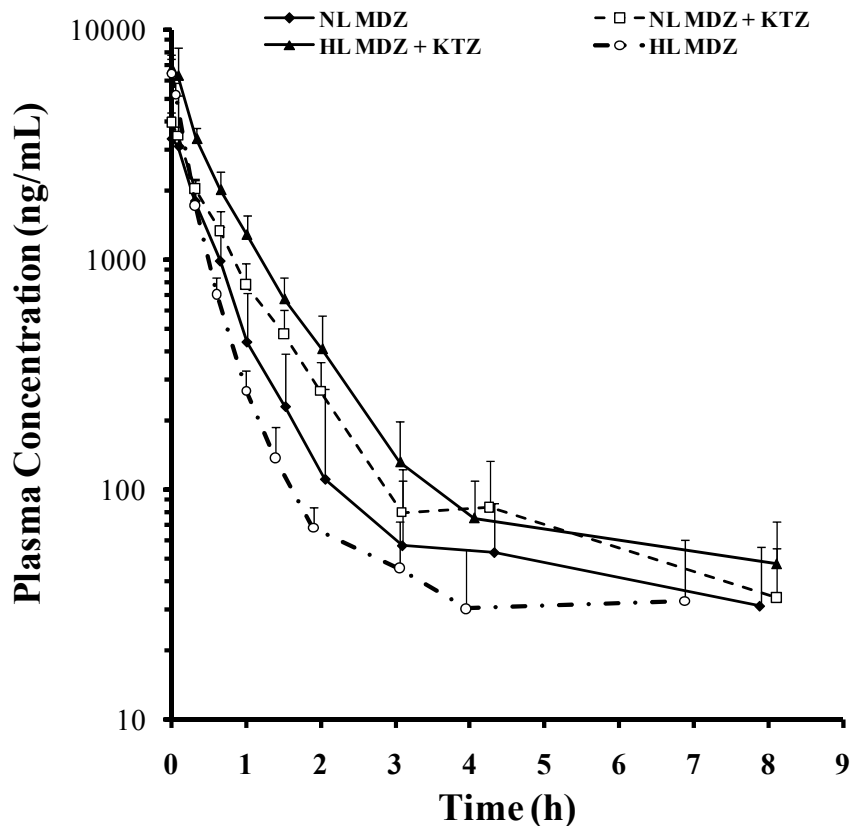


Figure 32: Plasma MDZ concentration-time profile in control normo (closed diamond) and hyperlipidemic (opened circle) rats and after 40 mg/kg (\pm)-KTZ oral pre-treatment in normo (open square) and hyperlipidemic (closed triangle) rats.

3.2.6.2. KTZ kinetics

KTZ displayed higher plasma concentrations than that those of MDZ at all time points in both NL and HL rats (Figure 33). There were no significant differences in the PK parameters of (\pm)-KTZ between NL and HL rats (Figure 33; Table 17).

Table 16: Effect of racemic ketoconazole (40mg/kg, po) on midazolam pharmacokinetics in NL and HL rats

	No KTZ		With KTZ	
	NL	HL	NL	HL
C₀ (mg/L)	3.94±0.878*	6.45±1.04	3.93±0.223*	6.78±1.01
AUC_{0-1last} (mg·h/L)	2.15±0.521	1.97±0.308†	2.72±0.476*	4.49±0.885
AUC_{0-inf} (mg·h/L)	2.41±0.597	2.06±0.338†	3.23±0.450*	4.78±0.979
t_{1/2} (h)	4.12±1.93	2.34±1.08	3.13±1.16	4.23±2.36
CL (L/h/kg)	2.17±0.458	2.48±0.445†	1.57±0.200*	1.08±0.223
V_{dss} (L/kg)	4.47±2.78	2.95±1.80	3.50±1.03*	1.82±0.576
V_c (L/kg)	1.32±0.263*	0.791±0.128	1.17±0.269*	0.695±0.197
fu (%)	1.97±0.38*	0.760±0.29	1.78±0.15*	1.02±0.21

*=different from HL in the same KTZ-treatment group (p<0.0125)

†=different from with KTZ in the same lipoprotein status group (p<0.0125)

Table 17: Ketoconazole pharmacokinetic parameters in NL and HL rats.

	NL	HL
C_{max} (mg/L)	23.5±6.44	19.6±8.05
AUC_{0-1last} (mg·h/L)	81.6±24.6	64.1±18.0
AUC_{0-inf} (mg·h/L)	84.0±25.2	69.1±25.1
T_{max} (h)	2.67±0.589	2.27±0.818

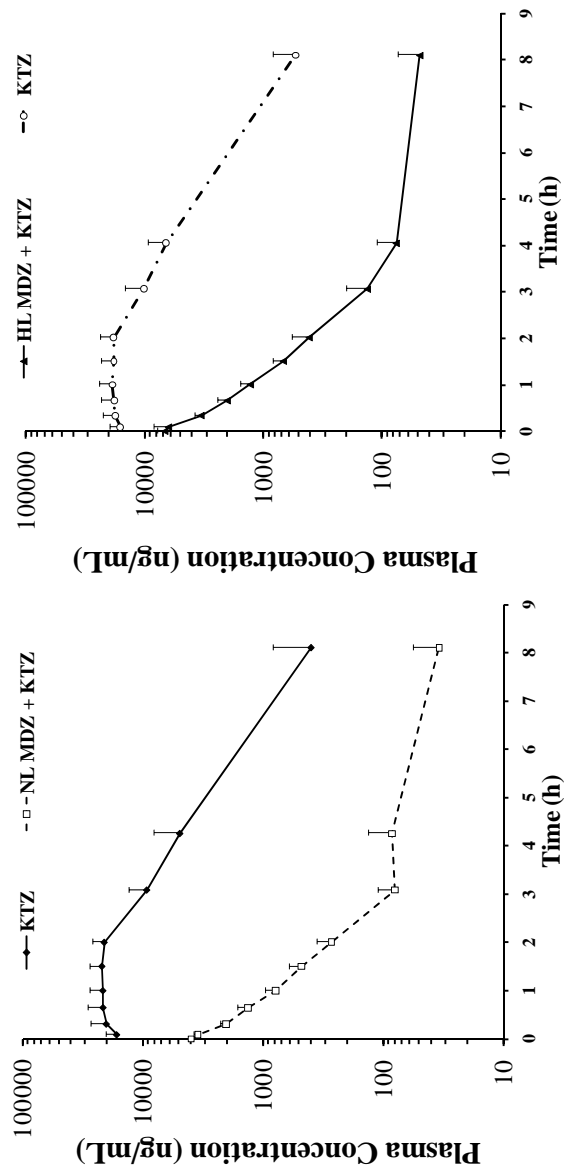


Figure 33: Comparative plasma concentration vs. time curves of oral (\pm)-ketoconazole (KTZ) and *iv* midazolam in the presence of ketoconazole (MDZ+KTZ). Left panel, profiles of the drugs in normolipidemic rats. Right panel, profiles of the drugs in hyperlipidemic rats.

4. Discussion

4.1 Effect of HL on PK and pharmacodynamic aspects of AM

4.1.1 Effect of HL on electrocardiographic changes associated with AM

The HL state is a precursor to cardiovascular disease, and as such is likely to be present in patients receiving AM. To induce HL here, P407 was used; its *ip* administration is known to cause a profound but reversible rise in circulating lipoprotein, particularly those of the very low density category [194]. Although lipoprotein concentrations are greatly increased, it does so with no apparent toxicity, and additionally, P407 provides one of the few rodent models of HL in which, with long term administration, atherosclerosis can be induced [44]. It has been shown to increase the plasma concentrations of several drugs including AM after single doses [86, 87, 97, 144], due to increased plasma lipoprotein binding and reduction in metabolism. In the rat AM has a moderate E , and as such a decrease in the f_u should be expected to cause either no change or a decrease in the tissue uptake of the drug. However, as was recently reported, in some tissues HL caused increases in AM concentrations, and notably, one of these tissues was the heart [97]. This was confirmed here in the present repeated dose study in which heart AM concentrations were higher in HL rats and where ECG changes were in line with the higher tissue concentrations (Table 5; Figure 8).

AM has been classified as a Vaughan-Williams class III antiarrhythmic agent. Such activity results in increases in atrial and ventricular refractoriness. It also depresses automaticity of the sinoatrial node, resulting in slowing of the heart rate. The drug also slows conduction and increases refractoriness of the AV node

[134]. These effects can be visualized by prolongation in the QTc, RR and PR intervals of the ECG. Some strong linear correlations were observed between AM heart concentrations and QTc interval prolongation in both NL and HL rats, with very similar slopes indicating similar effects at the level of the heart (Figure 9). However, although the relationship between AM total (bound+unbound) plasma concentrations and QTc interval prolongation was linear in both groups, the slope in NL rats was 10-fold higher than HL, suggesting heterogeneity in the heart uptake of the drug between the two groups (Figure 10). Since it is commonly believed that only the unbound drug is capable of traversing the cell membrane and exerting pharmacological activity, and since the drug had the same concentration vs. effect relationship at the level of the heart (Figure 9), the slopes of unbound concentration vs. heart uptake should match. It was possible to estimate the unbound AM plasma concentrations by multiplying previously obtained estimates of the f_u in NL (0.0853%) and HL (0.00345%) plasma by the total drug (bound+unbound) concentrations [86, 97]. In doing so it was clear that there was a difference in NL and HL slopes of unbound plasma AM concentrations and heart uptake, indicating that an additional factor besides f_u was involved in controlling uptake of AM into the heart (Figure 10).

It had been previously suggested that the cause of the increased heart concentrations of AM in HL rats was at least in part due to the influence of VLDL receptor mediated uptake of drug [97]. There are nine members of the LDL receptor family which comprise cell surface receptors that transport a number of lipoproteins, and lipoprotein encapsulated drug, into cells through endocytosis

[20]. The VLDL-R, which are a member of the LDL-R family, are abundantly expressed in fatty acid-active tissues (heart, muscle, adipose) and macrophages [27]. Unlike LDL-R, intracellular lipoproteins do not down regulate VLDL-R expression [21, 27]. It has been reported that in HL plasma, there is a substantial shift of drug and metabolite mostly from the lipoprotein-deficient plasma fractions to the CM and VLDL fractions, [61] which is in line with the high level of VLDL-R expression in heart.

The positive correlations (Figure 11) noted between the total CHOL: TG ratio and the QT interval and AM plasma and heart concentrations at first glance would appear to contradict the involvement of VLDL-R in the heart uptake of AM, because after CM they possess the lowest CHOL: TG ratio. It must be recognized, however, that it is not VLDL itself that is taken up by cells through the actions of VLDL-mediated endocytosis, but rather VLDL remnants, also called IDL [28]. The IDL particles are the product of the action of lipoprotein lipase, which facilitates the loss of TG from the VLDL particles. Further loss of TG from IDL particles causes them to become LDL particles. The VLDL-R also possess lipolytic activity and further aid in the transformation of VLDL to IDL [27]. Therefore the correlations observed between total CHOL: TG ratio versus QT interval and heart concentrations are still consistent with the uptake of AM into VLDL. In plasma, although the AM shift to VLDL is apparently greater than that to LDL fractions in HL plasma, the AM association with LDL is virtually identical in NL and HL plasma [61]. This suggests that the affinity of AM to LDL, with its higher CHOL: TG ratio, is greater than to VLDL. Therefore in

plasma which contains higher CHOL: TG ratios, more AM might be anticipated to be present in the LDL particles, which in turn might lead to a lower AM plasma fu and increased total (bound+unbound) AM concentrations in plasma, as was seen in these HL rats (Figure 11, upper panel).

It was apparent that the total CHOL: TG ratio was similar between the 25 and 50 mg/kg/d doses but higher with the 100 mg/kg/d dose (Figure 11). This pattern was similar for each of the NL and HL rats, suggesting that AM by itself may be affecting the lipid profile. It was previously reported that AM could significantly increase the CHOL and PL levels without altering the TG levels in rat, an increase that was thought to be dose dependant [195, 196]. Similar observations were made in human where long-term AM therapy resulted in a 17% increase in total CHOL [197].

The time of ECG parameters in saline-control rats came in accordance with those previously published (Tables 5 and 9) [181]. As anticipated, AM treatment resulted in PR, RR and QTc interval prolongations in both NL and HL rats. However, HL treated rats showed significantly more prominent PR and QTc prolongation than equivalently treated NL rats. This was not attributed to the HL condition as there was essentially no difference in ECG parameters between NL and HL AM-untreated rats (Table 5; Figure 7). Although there was only slight difference between RR interval prolongation among HL and NL AM treated rats, QT was still corrected for heart rate and QTc was calculated using both Bazett's [182] and Fridericia's [181] formulas for comparison. Whichever measure of QT

was used, the prolongation from baseline was essentially the same and yielded the same comparative statistical results, be it for NL or HL rats.

Examples of the effect of HL on the nature of the concentration vs. effect relationships have been reported for other drugs. For example a 31% decrease in nifedipine f_u and a significantly lower area under the unbound plasma concentration time curve was observed in P407 HL-treated rats compared to NL rats. Despite the lower area under the unbound concentration vs. time curve, a trend towards higher nifedipine-related reduction in mean arterial pressure was observed in HL [3]. Similarly, the nephrotoxicities of both CYA and amphotericin B, each of which are bound to lipoproteins, were enhanced by HL [106, 190]. In P407 HL rats given repeated doses of CYA, microscopic examination of stained kidney slices suggested more severe tubular and glomerular changes in HL rat kidneys than in NL ones [106]. In contrast, prostaglandin E1 and phenylephrine showed a reduced effect on the blood pressure of atherosclerotic-HL rabbits [198], although it should be noted that the extent of LDL association of prostaglandin is weak and limited [199, 200], and information regarding the binding of phenylephrine to lipoproteins is sparse.

Some nonlinearity in the dose vs. concentration data was apparent. The increase in AM plasma and heart concentrations was relatively linear between the 25 to 50 mg/kg/d dose levels (Figure 8). However, a greater than linear increase was apparent upon increasing the dose from 50 to 100 mg/kg/d. Such non linear behaviour in AM concentrations with escalating dose has been previously reported within these dose ranges after single *iv* doses [201]. The apparent

nonlinearity was accompanied by a similar pattern in the relationships between dose and ECG interval prolongation.

4.1.2 Effect of HL on AM metabolism using rat hepatocytes

Primary cultured hepatocytes are useful tools for investigations of drug metabolism, induction of drug metabolizing enzymes, and screening of cytotoxic and genotoxic compounds [202]. The present study determined the effect of serum lipoproteins on the hepatocellular metabolism of AM. It was previously reported that AM conversion to DEA was significantly decreased in HL liver microsomes [97]. This was explained by the observation that HL was associated with a down-regulation of microsomal CYP2C11 and CYP3A1/2, each of which was involved in the metabolism of the drug [97, 204].

In hepatocytes, similar results were obtained whereby AM declined more efficiently in control cells from NL rats vs. those from HL ones in the first 24 h after exposure of AM to the cells (Figure 14). However, the overall ARE_{0-72h} did not significantly differ between the NL and HL cells (Table 10). This may perhaps be explained by the CYP450 regaining its activity in the HL cells over time.

In the preincubation groups, where hepatocytes harvested from NL rats were treated with media only, or serum from NL or HL rats, a similar pattern was observed. Here the pretreatment with HL serum for 24 h caused a reduction in apparent metabolism of AM (Table 6; Figure 15). This is consistent with a

hypothesized reduction in CYP expression as a result of contact of lipoproteins with the hepatocytes.

With coincubation of serum and AM, two additional influences could possibly affect the metabolism of AM. The first is plasma protein binding, whereby lipoproteins in the media could potentially lead to less free drug being available for metabolism; over a 24 h incubation period a downregulation of CYP3A and 2C11 could also contribute to a reduction in metabolism of the drug. On the other hand, hepatocytes possess LDL-R. The presence of lipoproteins could lead to more LDL-bound drug, which might be more efficiently sequestered by the hepatocytes and lead to an increase in metabolism. This may be tempered however by the fact that AM has a high affinity for VLDL [61], and liver has much more LDL-R than VLDL-R [22, 27].

Coincubation of hepatocytes is associated with a number of contributory factors for consideration. AM is a highly lipophilic compound ($\log P=9$) and is known to possess extensive binding to NL and HL rats plasma that is increased further by HL [86]. On the other hand in HL AM predominantly shifts in its binding to the VLDL, and to a lesser extent, the LDL fraction [57]. Liver does not express VLDL-R but is rich in the LDL-R. It is known that in HL, there is a downregulation of LDL-R expression in hepatocytes (unpublished data from our laboratory, [202]).

The coincubation results showed that the presence of serum caused a decrease in metabolizing efficiency of the drug. The AM ARE of NL and HL coincubation

groups were 1.32- and 1.38-fold higher, respectively than the corresponding preincubation groups (Table 6). This could be explained by a decrease in fu afforded by the plasma proteins within the serum. Because NL and HL serum did not differ, this suggests that the enhanced association of drug with VLDL and LDL fractions was not sufficient to increase the uptake of the drug into hepatocytes and increase the metabolism the drug.

AM is a class III antiarrhythmic drug that is known for its hepatotoxicity at concentrations of 7.2 μ M or higher [203]. At subtoxic AM concentrations such as those chosen in this study (500 ng/mL) there was no significant change in LDH release in hepatocytes treated with AM dissolved in DMSO compared to DMSO alone for up to 96 h post AM incubation [203]. The DMSO or methanol used to dissolve the drug in this study did not exceed 0.1%. Finally, HL and NL serum caused no significant changes in LDH release up to 72 h compared to media alone.

4.2 Effect of HL on PK and pharmacodynamics aspects of KTZ

4.2.1 Development of an HPLC assay for the determination of KTZ enantiomers in rat plasma

KTZ is a lipophilic drug ($\log P=4.4$) and HL could potentially affect its PK. However, although it is chiral, there was no assay in the literature to quantitate its enantiomers. The described assay was capable of quantifying the enantiomers of KTZ in a biological specimen, rat plasma. The assay was sensitive and specific, affording baseline resolution of the enantiomers. For an analytical run of 20

samples, it took approximately 90 min to prepare the samples for injection into the HPLC. To our knowledge, this is the first stereospecific assay for KTZ in plasma. However, it is not the first method reported for separation of the KTZ enantiomers. The first HPLC separation utilized ChiralPak AS and ChiralCel OD columns with combinations of hexanes and alcohols with octanoic acid [203]. Although a chromatogram was not presented, the authors reported a baseline separation of KTZ enantiomers, albeit with a very long analysis time (~50 min). Similarly, Bernal et al reported that KTZ enantiomers were strongly retained (over 60 min) on both ChiralPak AD and Chiracel OD columns, using either hexane:ethanol or hexane:2-propanol as mobile phase [204]. Both authors reported better or similar resolution and a shorter analytical run (~7 min) upon using SFC [203, 204]. It was concluded by one group that SFC was the only technique that can provide appropriate enantiomeric separation for KTZ [204]. However, our HPLC method provided sensitive and precise means of measuring KTZ enantiomers with sufficient resolution and sensitivity for application in biological specimens. Although the analytical run time was somewhat longer than determined by SFC [204, 205], it was still entirely acceptable for an HPLC method (~18 min; Figure 16).

The current method provided resolution parameters that were quite comparable and in some ways superior to those calculated from or reported in previously for SFC using similar chiral columns. Thienpont et al reported an α of 1.3 and a resolution factor of 0.83. From the chromatograms presented by Bernal et al, an α of 1.6 and resolution factor of >2 were calculated [203, 205]. In both cases our

values of α and resolution factor were equivalent or superior. Both of the SFC methods were separation technique optimization and were not tested for quantification; neither standard curves nor validation data were reported.

A capillary electrophoresis technique has been reported which was capable of measuring KTZ enantiomers in pharmaceutical formulations and had superior separation qualities of a 3 min elution time and resolution factor > 2 . However, the stated lower limit of detection was 250 ng/mL for each enantiomer and there was no mention of extraction from biological fluids, limiting its application to drug solutions only [206].

Several non stereospecific analytical methods for the determination of KTZ in biological specimens have been reported. Using HPLC the non stereospecific LLQ of KTZ ranged from 62.5 ng/mL using fluorescence detection, to 100 ng/mL using UV detection, based on 100 μ L of human plasma [207, 208]. In canine plasma, a LLQ of 15 ng/mL was reported using HPLC and UV detection based on 100 μ L plasma [209]. In rat plasma the LLQ ranged from 2 ng/mL using LC/MS to more than 200 ng/mL using UV detection based on 100 μ L and 1 mL plasma, respectively [210, 211]. Thus our reported LLQ (62.5 ng/mL for each enantiomer) is within the ranges reported using HPLC and UV detection in biological specimens.

In working up the method, we found that there was a need to incorporate a hexane wash step to remove an interfering peak from plasma which eluted at the initial part of the (+)-KTZ peak. Hexane was an excellent solvent for this purpose, as it

caused virtually no extraction of KTZ enantiomers from the acetonitrile/aqueous phase. There was some loss of IS, but it did not have any adverse effects on linearity or validation parameters. We noticed that there was some noise in the baseline underlying the AM peak, but due to the excess of AM added, it similarly did not adversely affect KTZ enantiomer validation parameters. The optical rotation testing showed that (+)-KTZ is eluted first. This is in accordance with a reported preparative method for separation of KTZ enantiomers using the same HPLC column but different mobile phase [173, 212].

In vitro studies applying KTZ enantiomers to cytochrome P4503A4 using testosterone and methadone as substrates suggested stereoselective inhibition, wherein the (-)-KTZ enantiomer showed ~2 fold more inhibitory potency [173]. In our report based on C_{max} and AUC, we found that the plasma concentrations of (+)-KTZ were 2.1-2.4 fold higher than those of the (-)-KTZ, indicating a high level of stereoselectivity in KTZ PK in vivo after single oral doses. The T_{max} of the two enantiomers were similar indicating similar rates of absorption (Figure 17).

(±)-KTZ plasma concentrations are reported to be much lower than in tissues [210]. A previous report could not determine any measurable KTZ racemate plasma levels after 6 h of an iv administration of 5 mg/kg (±)-KTZ using nonstereospecific HPLC assay with 100 ng/mL LLQ based on 200 µL plasma [166]. Our method could quantify KTZ enantiomer concentrations for 4 h postdose using an oral dose of 10 mg/kg (±)-KTZ (Figure 17). It is of note that (±)-KTZ is associated with nonlinear CL [167, 168], and therefore with repeated

dosing it is likely that the time duration over which our assay could measure the drug would be longer than 4 h.

4.2.2 Determination of nonlinear stereoselective PK of KTZ in rat after administration of racemate

Although KTZ has been in clinical use for many years and is extensively used as a presumed inhibitor of CYP3A isoenzymes [213-215], it has been similarly widely overlooked that it is chiral and administered as the racemate of the two cis-isomers. Thus far the only stereoselective kinetic data that we know of in the literature is based on two rats which were used to illustrate applicability of the assay method. Similar to those rats, all rats, regardless of route of administration and dose, showed a high level of stereoselectivity in the plasma concentrations (Figure 19 and Figure 20; Table 8).

As reported for the sum of the two enantiomers, after iv administration a one compartment model was found to best conform to the data of each individual enantiomer [166, 167]. Each enantiomer had a V_{dss} reflective of a drug with substantial distribution to tissues. In addition, assuming that (\pm)-KTZ is mostly eliminated by the liver, the enantiomers had an estimated extraction ratio placing them in the low to moderate range. However, in each of these primary PK indices, marked stereoselectivity was noted. The CL and V_{dss} of (-) enantiomer were significantly higher than that of antipode. It is known that (\pm)-KTZ is strongly bound to rat plasma proteins over the concentration range 0.1 to 10 mg/L [167], and mostly metabolized [166, 168-170]. The cause of such enantioselectivity hence can be at the level of protein binding and/or hepatic metabolism. In the

plasma protein binding experiment it was observed that the f_u of the (-) enantiomer was higher than that of antipode. Although there was no evidence of stereoselective microsomal hepatic metabolism (Figure 22), in context with the PK data this must be viewed with some caution as it is not a cellular system, and is devoid of functional transport proteins. Nevertheless, the level of stereoselectivity in (-):(+) f_u at 10 and 40 $\mu\text{g/mL}$ racemate (2.5-2.7) was in line (1.8-2.1) with that in the V_{dss} and CL. Our findings for the enantiomer f_u , blood:plasma ratio and moderate E came in agreement with previously reported data for the sum of both enantiomers [167]. The degree of stereoselectivity in CL and V_{dss} was similar leading to essentially the same mean $t_{1/2}$ for each enantiomer.

After oral doses the KTZ enantiomers showed similar T_{max} values suggesting nonstereoselectivity in absorption rate (Table 8). The C_{max} and $AUC_{0-\infty}$ values for the enantiomers were consistent with the stereoselectivity observed in the *iv* dosed rats. The absolute F calculated for the two KTZ enantiomers after 10 mg/kg (\pm)-KTZ orally coincided with the racemate values reported by Remmel et al. with oral and *iv* doses of 5 mg/kg [166]. However, both of the estimates of F, especially for the (+) enantiomer, were lower than expected based on the values calculated from the *iv* data which assume complete hepatic elimination of drug [166, 170]. This suggests that a combination of other factors, including possibly incomplete absorption of parent drug, intestinal presystemic metabolism and perhaps transport of the enantiomers, occur.

The mean $t_{1/2}$ values reported for both KTZ enantiomers in this study were within the range of those reported previously for the sum of both enantiomers after racemic doses [166-168, 170]. In some of the rats given *iv* doses here, there was evidence of a greater slope of decline in the latter part of the concentration vs. time curves (Figure 19c). Such a profile is consistent with a saturable elimination process. Similar results were reported by Sjöberg et al for the racemate [168]. This was also reflected in the oral dose ranging study. Upon increasing the dose above 20 mg/kg, the dose vs. C_{max} and $AUC_{0-\infty}$ slopes of the two enantiomers tended to increase to a level higher than that at the dose range below 20 mg/kg. It is known that KTZ undergoes several metabolic biotransformations, including oxidation, scission and degradation of the imidazole ring, scission and degradation of the piperazine and dioxolane rings and oxidative O-dealkylation [169, 170]. Therefore, the initial change in slope at about 20 mg/kg can be explained by saturation of one or more of these metabolic pathways. The plateau in C_{max} with the highest oral dose levels seems to be due to saturable, nonlinear, plasma protein binding of KTZ enantiomers. Confirmation of saturation of this process was provided by the increases in the f_u of both enantiomers between 10 and 40 $\mu\text{g/mL}$ of racemate.

The mean F of the enantiomers were virtually identical. This was of interest because based on the *iv* dosing and assuming that most of the CL of KTZ occurs in the liver, it was suggested that the drug undergoes stereoselective hepatic extraction, and that the (-) enantiomer shows a moderate hepatic E . Hence, stereoselectivity in bioavailability would have been expected if the absorption of

the drug was passive and little extrahepatic metabolism occurred. Calculation of the f_g , however, indicated that there was stereoselectivity in the fraction of the drug available from the intestinal tract, which was opposite in direction to that imparted by the liver. This suggests possible stereoselectivity in extrahepatic mechanisms, such as intestinal metabolism or transport protein activity. It has been shown that stereoselectivity in metabolism may be opposite between CYP isoenzymes. One recent example of this was seen in rat for CYP3A1 and 2C11, where the direction of stereoselectivity for formation of desbutylhalofantrine enantiomer from HF was reversed [216]. Given that KTZ can inhibit a number of CYP enzymes [127], it is possible that the drug is metabolized by CYP enzymes other than the 3A isoforms. Also although most reports have used KTZ only as a probe for inhibition of Pgp, it has been shown to be an effective substrate for efflux at the level of the blood-brain barrier [217]. Further studies are required to definitively explain this issue.

The clinical use of (\pm)-KTZ has been more recently overshadowed by other azole antifungals due to its high incidence of drug-drug interactions and reported hepatotoxicity [218, 219]. Nevertheless, in drug development it is still frequently used as a probe to study the possibility of drug interactions due to its presumed, but not necessarily specific [127, 150, 220], ability to inhibit CYP3A isoforms. It is known that the enantiomers differ in their ability to bind to CYP isoforms, and that the (-) enantiomer is more potent against some strains of fungi [173].

Whether the enantiomers differ in their ability to cause toxicities remains to be determined.

4.2.3 Influence of HL on *in vitro* distribution of KTZ enantiomers in rat and human plasma

The pharmacological activity of a drug is governed by its PK and pharmacodynamics. Within this framework, the clinical relevance of protein binding has been frequently discussed [221, 222]. It was generally assumed that only free drug is capable of traversing biological barriers and interacting with receptors. Thus unbound drug plasma concentrations have been usually used in most PK, effect or toxicity correlations [223]. In that context albumin and α_1 -acid glycoprotein (AAG) were considered the most significant plasma proteins having preferential affinities for acidic and basic drugs, respectively [224]. However, recently this prevailing perception has been challenged, where cellular uptake, pharmacological activity and toxicity have been shown to be also affected by plasma lipoproteins binding [106, 225].

KTZ is a broad spectrum antifungal that is extensively (~97-99%) bound to plasma proteins [167]. It is a weak basic drug that binds mainly to albumin but does not bind to AAG in *in vitro* human serum [226]. In NL plasma, KTZ binds to the LPDP fraction with a negligible amount binding to the lipoprotein fraction (Figure 23). In the presence of HL rat serum ~ 20% of the total drug was shifted to the lipoprotein fractions mainly to TRL followed by LDL and HDL fractions (Figure 23). The KTZ shift from LPDP to the TRL fractions in rat exhibited some

stereoselectivity with the (-) enantiomer associating more with the TRL fraction than the (+) enantiomer.

Knowing that the (-) enantiomer has more antifungal potency and CYP inhibitory action [173], and that there is stereoselective PK, these observations could translate into PK and/or pharmacodynamic changes in HL .

4.2.4 The effect of HL on the PK of KTZ enantiomers in rat.

HL can affect the PK, metabolism and pharmacodynamics of a number of lipophilic drugs [17, 86]. This may occur through an alteration in the pattern of drug binding to plasma proteins due to a shift of lipophilic drug from lipoprotein deficient fractions to the more TG rich (VLDL and CM) and LDL [61, 102]. This is expected to result in a lower f_u in plasma with lower V_{dss} and CL (for drugs such as KTZ with low to moderate E) [86, 94]. On the other hand, lipoprotein-bound drugs may potentially experience a greater uptake by tissues through lipoprotein receptor-mediated mechanisms [97, 102, 106]. Because KTZ is lipophilic and its enantiomers possess low to moderate E, with extensive binding to plasma proteins, its PK were expected to be altered by HL. Such an effect of HL on KTZ PK was more into question after the shifting of KTZ from the LPDP fraction to lipoproteins VLDL and LDL. However, our study results indicated that the CL of the enantiomers was unchanged by HL. On the other hand, there was an increase in the V_{dss} of both enantiomers. The increase in V_{dss} may be suggestive of lipoprotein-receptor mediated uptake of the lipoprotein-bound drug to tissues after *iv* doses.

The uptake of KTZ enantiomers by liver was assessed after oral dosing, in which drug uptake by the organ is expected to be higher than after *iv* dosing due to first pass uptake. At all time points, KTZ liver concentrations were consistently higher than their corresponding plasma concentrations in both NL and HL, for both enantiomers (Figure 25). This is in accordance with previously published nonstereoselective data showing higher KTZ liver to plasma concentrations following oral administration of 150 mg/kg [210]. At some, but not all, time points after dosing, there were some significantly higher liver concentrations noted for the KTZ enantiomers in NL rats, with trends in AUC leaning in the same direction. Based on the K_p values, it was apparent that HL had a more profound effect on decreasing the liver uptake of the (-) enantiomer (Figure 27; Table 12). This may suggest a higher affinity of the (-) enantiomer for binding to lipoproteins than its antipode, which may have led to the change in the stereoselectivity ratios of AUC, CL and V_{dss} .

Based on the increase in V_{dss} in HL, a lipoprotein receptor uptake of KTZ enantiomer bound fractions would be expected to increase the liver concentrations in HL. However, the two enantiomers showed lower liver concentrations at 1.5 and 3 h after dosing (Figure 26), and a trend towards lower liver AUC_{0-6} in HL rats (Table 12). It is known that liver is rich in LDL-R and that HL can down-regulate those receptors, which could conceivably have led to the finding, but only if in NL the drug were extensively bound to lipoproteins. It is possible that the lower

hepatic uptake in HL during the absorption phase may be attributable to a lower f_u , the effect of which might outweigh any increase in lipoprotein receptor mediated uptake. We attempted to examine the plasma protein binding of the enantiomers in HL plasma using the erythrocyte binding technique. Unfortunately, unlike our experience with NL plasma, the technique led to inconsistent measures of f_u in the HL plasma, preventing us from estimating the plasma f_u of the enantiomers in HL. The use of ultrafiltration was found not to be feasible as KTZ was found to extensively bind to the filtration devices (Centrifree[®], Amicon, Beverly, MA, USA). Preincubating the Centrifree ultrafiltration devices with 5% Triton for 12 h overcame the extensive binding of the KTZ enantiomers to the filter. Unfortunately, though, the use of Triton interfered with our detection method for KTZ enantiomers and prevented measurement of the f_u in the HL plasma.

The induction of HL using P407 in rodents was first described by Johnston and coworkers [52, 227]. The polymer exerts its action through inhibiting plasma lipoprotein lipase and probably CHOL 7 α -hydroxylase [52]. This model of HL is attractive due to its rapid onset, low toxicity, reversibility and ability to induce atherosclerosis in rodents with repeated doses [44]. On the other hand, it causes an increase in lipoprotein levels which is considerably higher than clinically experienced by humans, and as such the findings of changes in PK such as those reported here should be considered exploratory rather than definitive in nature.

This study demonstrates the effect of elevated lipid levels on the PK and liver uptake of KTZ enantiomers. HL was found to increase V_{dss} of KTZ enantiomers,

to affect their stereoselectivity and to decrease the liver uptake of the more potent (-)-enantiomer and the liver concentrations of both enantiomers. KTZ drug interactions are attributed to its specific tissue binding to hepatic microsomal enzymes [228]. The drug is also potentially hepatotoxic, and can cause zone 3 necrosis hepatitis [229, 230]. Both of these factors have led to a limitation in its use as an antifungal drug. Whether a change in KTZ liver uptake caused by HL would affect the toxicity and/or its ability to modify drug-drug interactions remains to be determined.

4.2.5 Development of an HPLC assay for the simultaneous determination of MDZ and KTZ in plasma

HL resulted in shifting the KTZ enantiomers to plasma lipoprotein fractions and decreased the liver uptake of KTZ which may potentially result in affecting KTZ drug interaction potency. MDZ is often used as a probe for CYP3A inhibition studies. This encouraged us to develop an assay to simultaneously quantitate both drugs to decrease the blood sampling from rat and facilitate the PK study.

The described assay was capable of the simultaneous quantitation of KTZ and MDZ in plasma. It is simple, rapid, sensitive and efficient for PK studies involving both drugs with fewer numbers of blood samples taken from rats. The extraction solvents used by most of the HPLC reports for MDZ include using either diethyl ether [231, 232], ethyl acetate [233], n-hexane [234] or diethyl ether/methylene chloride [235]. while those used for KTZ extraction include the addition of just acetonitrile for protein precipitation [236], TBME and diethyl ether [237]. The combination of ACN: phosphate with different concentrations

and proportions were previously used for the determination of each drug alone [234, 238]. For the current method we found diethyl ether to be an ideal extraction solvent, and ACN:15 mM KH₂PO₄ (45:55, v/v) as a suitable mobile phase.

For the extraction procedures, this report used diazepam as an IS, and was based on the procedures described by Jurica et al. and Carrillo et al. for MDZ, with minor modifications [231, 232]. The rat and human plasma volumes required in our assay, however, were only 100 and 500 μ L compared to 450 μ L by Jurica et al. and 1 mL by Carrillo et al., respectively. This lower volume permits the use of serial blood sampling in studies involving a small animal species, the rat. The total samples preparation time was decreased by about 40 min. Additionally an improved lower limit of quantitation for MDZ (25 and 5 ng/mL based on 100 and 500 μ L rat and human plasma, respectively) was achieved compared to 50 ng/mL based on 450 μ L rat plasma [231] and 40 ng/mL based on 1 mL human plasma [232]. We must recognize however, that the other two assays were not focused on quantitation of MDZ and KTZ, but rather determination of MDZ and its hydroxylated metabolites.

The chromatographic run time reported for MDZ determination for other comparable assay methods range from 7.5 to 25 min [232, 239]. For KTZ run-times have ranged from 10 to over 20 min [209, 240]. Thus our analytical run time compares well to the reported ranges of the other methods. The sensitivity of our method represented in the LLQ of 25 and 5 ng/mL in rat and human plasma, respectively, compares favourably to that reported for both medications using HPLC systems [241-243]. It is demonstrated to be of use in the study of MDZ

and KTZ disposition in rat for up to 8 h after i.v. MDZ; this is similar to the available LCMS and LC-MS/MS methods [244, 245]. The published LC-MS/MS method for the simultaneous determination of MDZ and KTZ, although more sensitive with lower LLQ, did not state the volume of plasma assayed nor the IS used in the assay[244]. The LC/MS method described by Ogasawara et al., on the other hand, used a similar volume of 100 μ L plasma (from monkeys), and a commercially available IS (reserpine) [245].

One limitation of the described method is that it is non-stereoselective and measures the sum of the (+) and (-) KTZ enantiomer concentrations. This is potentially relevant because stereoselectivity in its PK and pharmacodynamics has been demonstrated [173]. In rats, the (+)-KTZ plasma concentrations were 2.5 fold higher than (-)-KTZ. In addition that (-)-KTZ displayed \sim 2 fold more inhibitory potency upon applying the enantiomers to human CYP3A4 supersomes using testosterone and methadone as substrates [173]. Despite this limitation, the assay is still of use because of the very low number of assays that can simultaneously measure both KTZ and MDZ. In cases where it is desired to determine knowledge of plasma concentrations of KTZ enantiomers, use of a separate stereoselective assay is needed. To date there is only one HPLC assay reported for stereospecific measurement of KTZ enantiomers. The assay was well suited for a PK study involving the interaction of (\pm)-KTZ and MDZ. The MDZ Cl in the presence of KTZ was found to be 28.5 and 28.9 mL/min/kg for the two rats, which is quite similar to a previously reported value of 29.8 mL/min/kg in presence of 20 mg/kg KTZ [244]. The $AUC_{0-\infty}$ of KTZ after 40 mg/kg oral

dosing for the two rats was quite close to the values obtained (~80 mg·h/L) after the summation of the two KTZ enantiomers and in absence of MDZ (Table 15).

Because doses of the drugs are typically lower in human than animal studies, in human subjects there is a need for greater assay sensitivity [241, 246, 247]. Furthermore, larger blood volumes can be drawn from humans than rats. Consequently a larger plasma volume of 500 µL plasma was used for human samples. As in rat, the extraction efficiency remained high (~100%) in the human plasma. Because in the human plasma there were some later eluting peaks at 12 and 13 min, an extended run time of 19 min was needed. As the validation data showed (Tables 13 and 14) the described method is potentially useful in examining human PK interactions involving MDZ and KTZ.

4.2.6 Effect of HL on KTZ-MDZ drug-drug interaction in rat

P407-induced HL in rat was shown to shift both enantiomers ~20% from the LPDP to the CHOL and TG-rich fractions. However, only V_{dss} was increased in HL rats after iv dosing. It was also noticed that liver uptake of the more potent (-)-KTZ enantiomer was decreased after oral dosing. This may have indicated a possible increased lipoprotein-mediated transport of the drug to extrahepatic tissues. Because there appeared to be a change in hepatic uptake of the (-)-KTZ enantiomer, there was a possibility that HL would affect the inhibitory potency and drug-drug interaction pattern of KTZ. After the development of the simultaneous assay for the determination of KTZ and MDZ in plasma, it became more feasible to devise a PK study to assess the effect of HL on the KTZ drug

interaction potency using MDZ as a probe and the rat as an animal model. The time points which showed maximum significant difference between NL and HL KTZ liver concentrations and uptake were 1.5 and 3h *po* (Figure 26 and Figure 27). Thus in the current study the CYP3A probe was administered 1.5h after KTZ pre-treatment.

CYP3A constitutes the most abundant subfamily in human liver and intestine [220, 248, 249]. It facilitates the biotransformation of approximately half of all currently used drugs [250] and its phenotyping has been reported as CYP3A4, CYP3A5, CYP3A7 and CYP3A43 isoenzymes in man [251] and CYP3A1 and CYP3A2 in rat [252]. These isoforms have similar amino acid sequences and different catalytic activity. Most of *in vivo* drug metabolism research relies on the total activity of CYP3A involving CYP3A4/5 in man and CYP3A2 in rat because they have similar substrate specificity [253]. Since most PK drug interactions occur when two drugs share a common CL pathway involving a drug metabolizing enzyme or transporter, the CYP3A family is frequently implicated in drug-drug interactions [244]. CYP3A-mediated inhibition of drug metabolism has been associated with some severe adverse effects prompting the withdrawal of some drugs from the market [254]. Consequently as part of safety assessment in drug development it is necessary to perform clinical drug interaction studies with CYP3A4 in mind [255].

KTZ, a broad spectrum azole antifungal used for systemic and local infections, is widely used as a prototypical inhibitor of CYP3A for such studies [255]. It is

commercially available as a racemic (1:1) mixture of enantiomers of the cis configuration. Stereoselective inhibition of CYP enzymes has been suggested, where the (-)-KTZ enantiomer displayed ~2 fold more inhibitory potency upon applying the enantiomers to human CYP3A4 supersomes using testosterone and methadone as substrates [173]. A recent study has also reported stereoselective PK and protein binding of KTZ enantiomers.

Midazolam is a short acting benzodiazepine which undergoes extensive hepatic and gastrointestinal pre-systemic extraction [241]. Its CL and F are primarily governed by CYP3A, and consequently, it is often used as a probe for measuring CYP3A activity [256]. Since MDZ is not a Pgp substrate, any interaction between midazolam and KTZ can be essentially attributed to effects on CYP3A [244, 257].

In NL rats, it was found that oral administration of KTZ caused a modest non-significant decrease in MDZ CL, and no effect on $t_{1/2}$. Using the reported MDZ blood to plasma ratio of 1 [258] and hepatic blood flow of 13.8 mL/min in a 250 g rat [191], the hepatic extraction of MDZ is that of a moderately-high extraction ratio (0.66) in NL rats. Given this, it might not be entirely surprising that the change in CL for NL rats was relatively insensitive to the coadministration of KTZ.

In the KTZ untreated group, HL resulted in a 61% decrease in MDZ fu; however this affected neither the CL nor the AUC of the drug compared to NL control rats (Table 16; Figure 32). The fact that there was a change in MDZ fu and V_{dss} in

HL, however, suggested strongly that the drug has the ability to bind to lipoproteins, something that has not been reported previously.

Based on our findings above that there was lower hepatic uptake of (-)-KTZ enantiomer in HL, we anticipated that there would be an attenuated inhibitory response of MDZ to KTZ coadministration in the HL rats. In contrast, in KTZ treated rats, HL accentuated the KTZ-MDZ drug interaction as evidenced by 31% decrease in MDZ CL compared to NL rats (Figure 32 and Table 16). This contradictory finding could be attributed to the fact that in HL two factors could have worked to lower the CL of MDZ. This includes the decrease in f_u of MDZ, which was not anticipated as MDZ was not shown previously to bind to lipoproteins. In addition, in HL it had been shown that CYP3A could be down-regulated.

Most reported studies of the drug interactions between KTZ and MDZ have been able to follow the MDZ profile *in vivo* for only 2 or 4 h due to lack of a sensitive analytical assay which may mask the real terminal phase of the drug and affect some other PK parameters [259, 260]. The only other paper reporting this drug interaction up to 8 h had only data of 2 rats, and statistical analysis could not be reported [244].

KTZ exhibited higher plasma concentrations than MDZ at all time points (Figure 33). HL did not affect the CL, AUC, C_{max} or T_{max} of (\pm)-KTZ after oral administration (Table 17). This comes in accordance with the previously reported behaviour of each enantiomer in NL and HL state after oral and *iv* dosing. MDZ

did not affect KTZ PK parameters. The AUC and Cmax of the sum of KTZ enantiomers matched well to the values that were reported in Tables 8 and 17.

5. Conclusion

HL results in an increase in the plasma lipoproteins and can affect the PK, pharmacodynamics and toxicity of lipoprotein-bound medications. AM and KTZ are lipophilic compounds of log P 9 and 4.3 respectively. It had been shown that AM could bind to lipoproteins, and it was possible that the same was true for KTZ. Therefore, this formed the rationale for the studies completed and presented as part of this thesis.

HL was already known to increase AM AUC, decrease its CL and Vd, and increase its heart uptake in the P407 rat HL model after a single AM dose [86, 97]. Our repeat dose study [see section 3.1.1] found that HL similarly increased AM plasma concentrations and heart concentrations but also caused an increased ECG potency. The increase in heart concentration was greater than could be accounted for based on the estimate of unbound drug concentrations in plasma. We believe that VLDL-R mediated uptake of the VLDL-bound AM had contributed to the higher than expected heart concentrations.

Despite the increase in AM liver uptake in HL, its overall CL was lower [97]. In liver microsomal preparations, HL was shown to downregulate CYP3A1/2 and CYP2C11. It was found that HL caused reduced AM metabolism in rat hepatocytes. The presence of serum lipoproteins with AM decreased metabolism further, possibly by decreasing the fraction of drug available for entry into the hepatocytes due to an increase in serum protein binding.

KTZ is a chiral lipophilic drug. In our studies, we have developed the first separation and determination of KTZ enantiomers in biological specimens. The

method was sensitive and specific, with a lower limit of quantitation of 62.5 ng/mL. This proved sufficient for use in PK studies involving rats.

Utilizing this method to explore the PK of each enantiomer, we have reported the stereoselective PK of KTZ enantiomers in rat plasma. Stereoselectivity in plasma concentrations of KTZ enantiomers can be attributed to enantioselectivity in plasma protein binding, although other unknown mechanisms as transporters enantioselectivity and tissue uptake maybe involved as well. In agreement with previous reports for (\pm)-KTZ, both KTZ enantiomers showed nonlinearity with increasing racemic doses in rat, presumably due to a combination of saturation of some metabolic pathways and plasma protein binding.

Based on the lipophilicity of KTZ, we decided to explore the effect of HL on its *in vitro* distribution towards plasma lipoproteins. We found that the P407 induced HL rat model resulted in a shift of ~20% KTZ from LPDP to lipoprotein rich fractions. It was mainly towards VLDL and LDL fractions. The (-) enantiomer was found to be more significantly influenced than antipode by HL. Knowing that the (-) enantiomer has more antifungal potency and CYP inhibitory action [173], and that there is stereoselective PK, these observations could translate into PK and/or pharmacodynamic changes in HL .

The previous results have encouraged us to study the effect of elevated lipid levels on the PK and liver uptake of KTZ enantiomers. In these studies HL was found to increase V_{dss} of KTZ enantiomers, to affect their stereoselectivity and to decrease the liver uptake of the more potent (-)-enantiomer and the liver

concentrations of both enantiomers. KTZ drug interactions are attributed to its specific tissue binding to hepatic microsomal enzymes [228]. Also, the drug is potentially hepatotoxic, and can cause zone 3 necrosis hepatitis [229, 230]. Both of these factors have led to a limitation in its use as an antifungal drug. Whether a change in KTZ liver uptake caused by HL would affect the toxicity remains to be determined.

Based on the pharmacokinetic and hepatic uptake findings it was decided to go further and to explore the effect of HL and the decreased KTZ liver uptake on KTZ drug-drug interactions. MDZ was chosen for such interaction due to its known use as a CYP3A probe. We initially sought to use two assays to measure both KTZ and MDZ, but fortuitously developed a method that could simultaneously determine both drugs. Using this method we conducted our drug-drug interaction study in NL and HL rats, where we have found that HL resulted in a more pronounced KTZ inhibition of MDZ CL. This was partially due to the involvement of an additive CL inhibitory factor through the decrease of MDZ fu and to the possible CYP inhibitory activity imparted by the HL state.

In conclusion, HL was shown to have a various effects on the pharmacokinetics and pharmacodynamics of AM and KTZ. Given the prevalence of HL in many societies, the findings could be of relevance in explaining unexplained dose versus effect outcomes in HL patients receiving such lipoprotein-bound drugs.

6. Future direction

HL was found to affect not only the pharmacokinetics of AM but also its pharmacodynamics. We have shown that in heart, AM uptake is dependent on other factors in addition to the fu. Further studies are required to explore the mechanisms behind the increased heart uptake despite the lower fu. Specific experiments to determine the exact role of VLDL-R and their regulations in HL should be performed.

Further our hepatocyte studies focused on the effects of lipoproteins on the metabolism of AM. A worthy objective of future study would be to examine AM uptake by these cells, as a consequence of the involvement of LDL-R receptors .

HL was also evident to decrease the fu of MDZ, pointing out the possibility of MDZ-lipoprotein binding. Further studies can be explored to determine whether or not MDZ bind to lipoproteins and if so to which fraction.

Finally, since HL was shown to potentiate the KTZ-MDZ drug-drug interaction, determining the effect of HL on the antifungal activity of both enantiomers could be also studied.

7. Bibliography

- [1] S.E. Schober, M.D. Carroll, D.A. Lacher, R. Hirsch, High serum total cholesterol--an indicator for monitoring cholesterol lowering efforts: U.S. adults, 2005-2006, NCHS Data Brief (2007) 1-8.
- [2] K.M. Wasan, N.A. Looije, Emerging pharmacological approaches to the treatment of obesity, *J Pharm Pharm Sci* 8 (2005) 259-271.
- [3] L.A. Eliot, F. Jamali, Pharmacokinetics and pharmacodynamics of nifedipine in untreated and atorvastatin-treated hyperlipidemic rats, *J Pharmacol Exp Ther* 291 (1999) 188-193.
- [4] K.M. Wasan, D.R. Brocks, S.D. Lee, K. Sachs-Barrable, S.J. Thornton, Impact of lipoproteins on the biological activity and disposition of hydrophobic drugs: implications for drug discovery, *Nat Rev Drug Discov* 7 (2008) 84-99.
- [5] D.S. Fredrickson, An international classification of hyperlipidemias and hyperlipoproteinemias, *Ann Intern Med* 75 (1971) 471-472.
- [6] D.S. Fredrickson, R.S. Lees, A system for phenotyping hyperlipoproteinemia, *Circulation* 31 (1965) 321-327.
- [7] J. DiPiro, R.L. Talbert, G.C. Yee, G.R. Matzke, B.G. Wells, L.M. Posey, *Pharmacotherapy a pathophysiologic approach*, sixth ed., The McGraw-Hill Companies, 1999.
- [8] T.A. Manolio, T.A. Pearson, N.K. Wenger, E. Barrett-Connor, G.H. Payne, W.R. Harlan, Cholesterol and heart disease in older persons and women. Review of an NHLBI workshop, *Ann Epidemiol* 2 (1992) 161-176.
- [9] M.A. Austin, Epidemiology of hypertriglyceridemia and cardiovascular disease, *Am J Cardiol* 83 (1999) 13F-16F.

- [10] H.N. Ginsberg, Y. Arad, I.J. Goldberg, Pathophysiology and therapy of hyperlipidemia., in: In Cardiovascular Pharmacology, Antoaccio MJ(ed). 3 edn. Raven: New York, 1990, pp. 485-513.
- [11] J. Genest, J. Frohlich, G. Fodor, R. McPherson, Recommendations for the management of dyslipidemia and the prevention of cardiovascular disease: summary of 2003 update, CMAJ 169 (2003) 921-924.
- [12] D. Steinberg, Hypercholesterolemia and inflammation in atherogenesis: two sides of the same coin, Mol Nutr Food Res 49 (2005) 995-998.
- [13] J.E. Hall, Guyton and Hall text book of medical physiology, Eleventh ed., EISERVIER SAUNDERS, 2001.
- [14] MRC/BHF Heart Protection Study of cholesterol lowering with simvastatin in 20, 536 high-risk individuals: a randomised placebo-controlled trial, Lancet 360 (2002) 7-22.
- [15] G.A. Kaysen, New insights into lipid metabolism in chronic kidney disease: what are the practical implications?, Blood Purif 27 (2009) 86-91.
- [16] Y.J. Wang, J.B. Sun, F. Li, S.W. Zhang, Hyperlipidemia intensifies cerulein-induced acute pancreatitis associated with activation of protein kinase C in rats, World J Gastroenterol 12 (2006) 2908-2913.
- [17] J.P. Patel, D.R. Brocks, The effect of oral lipids and circulating lipoproteins on the metabolism of drugs, Expert Opin Drug Metab Toxicol 5 (2009) 1385-1398.
- [18] H. Shen, P. Howles, P. Tso, From interaction of lipidic vehicles with intestinal epithelial cell membranes to the formation and secretion of chylomicrons, Adv Drug Deliv Rev 50 Suppl 1 (2001) S103-125.
- [19] R.E. Olson, Discovery of the lipoproteins, their role in fat transport and their significance as risk factors, J Nutr 128 (1998) 439S-443S.

- [20] N.S. Chung, K.M. Wasan, Potential role of the low-density lipoprotein receptor family as mediators of cellular drug uptake, *Adv Drug Deliv Rev* 56 (2004) 1315-1334.
- [21] S. Takahashi, J. Sakai, T. Fujino, H. Hattori, Y. Zenimaru, J. Suzuki, I. Miyamori, T.T. Yamamoto, The very low-density lipoprotein (VLDL) receptor: characterization and functions as a peripheral lipoprotein receptor, *J Atheroscler Thromb* 11 (2004) 200-208.
- [22] M.M. Hussain, D.K. Strickland, A. Bakillah, The mammalian low-density lipoprotein receptor family, *Annu Rev Nutr* 19 (1999) 141-172.
- [23] J. Gliemann, Receptors of the low density lipoprotein (LDL) receptor family in man. Multiple functions of the large family members via interaction with complex ligands, *Biol Chem* 379 (1998) 951-964.
- [24] M.S. Brown, J.L. Goldstein, A receptor-mediated pathway for cholesterol homeostasis, *Science* 232 (1986) 34-47.
- [25] J.C. Webb, D.D. Patel, M.D. Jones, B.L. Knight, A.K. Soutar, Characterization and tissue-specific expression of the human 'very low density lipoprotein (VLDL) receptor' mRNA, *Hum Mol Genet* 3 (1994) 531-537.
- [26] A. Nykjaer, T.E. Willnow, The low-density lipoprotein receptor gene family: a cellular Swiss army knife?, *Trends Cell Biol* 12 (2002) 273-280.
- [27] S. Takahashi, J. Sakai, T. Fujino, I. Miyamori, T.T. Yamamoto, The very low density lipoprotein (VLDL) receptor--a peripheral lipoprotein receptor for remnant lipoproteins into fatty acid active tissues, *Mol Cell Biochem* 248 (2003) 121-127.
- [28] Y.G. Niu, D. Hauton, R.D. Evans, Utilization of triacylglycerol-rich lipoproteins by the working rat heart: routes of uptake and metabolic fates, *J Physiol* 558 (2004) 225-237.

- [29] A. Saito, S. Pietromonaco, A.K. Loo, M.G. Farquhar, Complete cloning and sequencing of rat gp330/"megalin," a distinctive member of the low density lipoprotein receptor gene family, *Proc Natl Acad Sci U S A* 91 (1994) 9725-9729.
- [30] J.R. Leheste, B. Rolinski, H. Vorum, J. Hilpert, A. Nykjaer, C. Jacobsen, P. Aucouturier, J.O. Moskaug, A. Otto, E.I. Christensen, T.E. Willnow, Megalin knockout mice as an animal model of low molecular weight proteinuria, *Am J Pathol* 155 (1999) 1361-1370.
- [31] S.K. Moestrup, S. Cui, H. Vorum, C. Bregengard, S.E. Bjorn, K. Norris, J. Gliemann, E.I. Christensen, Evidence that epithelial glycoprotein 330/megalin mediates uptake of polybasic drugs, *J Clin Invest* 96 (1995) 1404-1413.
- [32] S.K. Moestrup, The alpha 2-macroglobulin receptor and epithelial glycoprotein-330: two giant receptors mediating endocytosis of multiple ligands, *Biochim Biophys Acta* 1197 (1994) 197-213.
- [33] E.I. Christensen, H. Birn, P. Verroust, S.K. Moestrup, Membrane receptors for endocytosis in the renal proximal tubule, *Int Rev Cytol* 180 (1998) 237-284.
- [34] G. Zheng, D.R. Bachinsky, I. Stamenkovic, D.K. Strickland, D. Brown, G. Andres, R.T. McCluskey, Organ distribution in rats of two members of the low-density lipoprotein receptor gene family, gp330 and LRP/alpha 2MR, and the receptor-associated protein (RAP), *J Histochem Cytochem* 42 (1994) 531-542.
- [35] R.C. Kowal, J. Herz, J.L. Goldstein, V. Esser, M.S. Brown, Low density lipoprotein receptor-related protein mediates uptake of cholesteryl esters derived from apoprotein E-enriched lipoproteins, *Proc Natl Acad Sci U S A* 86 (1989) 5810-5814.
- [36] U. Beisiegel, W. Weber, G. Ihrke, J. Herz, K.K. Stanley, The LDL-receptor-related protein, LRP, is an apolipoprotein E-binding protein, *Nature* 341 (1989) 162-164.
- [37] J. Herz, The LDL receptor gene family: (un)expected signal transducers in the brain, *Neuron* 29 (2001) 571-581.

[38] M. Trommsdorff, M. Gotthardt, T. Hiesberger, J. Shelton, W. Stockinger, J. Nimpf, R.E. Hammer, J.A. Richardson, J. Herz, Reeler/Disabled-like disruption of neuronal migration in knockout mice lacking the VLDL receptor and ApoE receptor 2, *Cell* 97 (1999) 689-701.

[39] M. Shiomi, T. Ito, The Watanabe heritable hyperlipidemic (WHHL) rabbit, its characteristics and history of development: a tribute to the late Dr. Yoshio Watanabe, *Atherosclerosis* 207 (2009) 1-7.

[40] J.C. Russell, Evaluating micro- and macro-vascular disease, the end stage of atherosclerosis, in rat models, *Methods Mol Biol* 573 (2009) 17-44.

[41] T. Mashimo, H. Ogawa, Z.H. Cui, Y. Harada, K. Kawakami, J. Masuda, Y. Yamori, T. Nabika, Comprehensive QTL analysis of serum cholesterol levels before and after a high-cholesterol diet in SHRSP, *Physiol Genomics* 30 (2007) 95-101.

[42] K. Fujinami, K. Kojima, K. Aragane, J. Kusunoki, Postprandial hyperlipidemia in Zucker diabetic fatty fa/fa rats, an animal model of type II diabetes, and its amelioration by acyl-CoA:cholesterol acyltransferase inhibition, *Jpn J Pharmacol* 86 (2001) 127-129.

[43] L.S. Srivastava, M. Kashyap, G. Perisutti, C.Y. Chen, Induction of hyperlipidemia by human thyroid stimulating hormone immunization in rabbits, *Experientia* 33 (1977) 593-595.

[44] W.K. Palmer, E.E. Emeson, T.P. Johnston, The poloxamer 407-induced hyperlipidemic atherogenic animal model, *Med Sci Sports Exerc* 29 (1997) 1416-1421.

[45] X.M. Liu, F.H. Wu, [Comparison of animal models of hyperlipidemia], *Zhong Xi Yi Jie He Xue Bao* 2 (2004) 132-134.

[46] M. De Castro, A.P.M. Veiga, M.R. Pacheco, Plasma lipid profile of experimentally induced hyperlipidemic New Zealand white rabbit is not affected by resveratrol, *The journal of applied research* 9 (2009) 18-22.

- [47] S. Morishita, T. Saito, Y. Mishima, A. Mizutani, Y. Hirai, S. Koyama, M. Kawakami, [Strains and species differences in experimental hyperlipidemia], *Nippon Yakurigaku Zasshi* 87 (1986) 259-264.
- [48] H.L. Newmark, K. Yang, M. Lipkin, L. Kopelovich, Y. Liu, K. Fan, H. Shinozaki, A Western-style diet induces benign and malignant neoplasms in the colon of normal C57Bl/6 mice, *Carcinogenesis* 22 (2001) 1871-1875.
- [49] B.H. Cho, T.L. Smith, J.R. Park, F.A. Kummerow, Effects of estrogen-induced hyperlipidemia on the erythrocyte membrane in chicks, *Lipids* 23 (1988) 853-856.
- [50] S. Gustafson, C. Vahlquist, L. Sjoblom, A. Eklund, A. Vahlquist, Metabolism of very low density lipoproteins in rats with isotretinoin (13-cis retinoic acid)-induced hyperlipidemia, *J Lipid Res* 31 (1990) 183-190.
- [51] X. Prieur, T. Huby, H. Coste, F.G. Schaap, M.J. Chapman, J.C. Rodriguez, Thyroid hormone regulates the hypotriglyceridemic gene APOA5, *J Biol Chem* 280 (2005) 27533-27543.
- [52] T.P. Johnston, W.K. Palmer, Mechanism of poloxamer 407-induced hypertriglyceridemia in the rat, *Biochem Pharmacol* 46 (1993) 1037-1042.
- [53] S.Y. Yousufzai, M. Siddiqi, 3-Hydroxy-3-methylglutaric acid and triton-induced hyperlipidemia in rats, *Experientia* 32 (1976) 1178-1179.
- [54] S. Goldfarb, Rapid increase in hepatic HMG CoA reductase activity and in vivo cholesterol synthesis after Triton WR 1339 injection, *J Lipid Res* 19 (1978) 489-494.
- [55] T.P. Johnston, The P-407-induced murine model of dose-controlled hyperlipidemia and atherosclerosis: a review of findings to date, *J Cardiovasc Pharmacol* 43 (2004) 595-606.
- [56] D.N. Brindley, J.C. Russell, Animal models of insulin resistance and cardiovascular disease: some therapeutic approaches using JCR:LA-cp rat, *Diabetes Obes Metab* 4 (2002) 1-10.

- [57] M.H. Hofker, B.J. van Vlijmen, L.M. Havekes, Transgenic mouse models to study the role of APOE in hyperlipidemia and atherosclerosis, *Atherosclerosis* 137 (1998) 1-11.
- [58] J.C. Escola-Gil, O. Jorba, J. Julve-Gil, F. Gonzalez-Sastre, J. Ordonez-Llanos, F. Blanco-Vaca, Pitfalls of direct HDL-cholesterol measurements in mouse models of hyperlipidemia and atherosclerosis, *Clin Chem* 45 (1999) 1567-1569.
- [59] C. Li, W.K. Palmer, T.P. Johnston, Disposition of poloxamer 407 in rats following a single intraperitoneal injection assessed using a simplified colorimetric assay, *J Pharm Biomed Anal* 14 (1996) 659-665.
- [60] P.E. Schurr, J.R. Schultz, T.M. Parkinson, Triton-induced hyperlipidemia in rats as an animal model for screening hypolipidemic drugs, *Lipids* 7 (1972) 68-74.
- [61] A. Shayeganpour, S.D. Lee, K.M. Wasan, D.R. Brocks, The influence of hyperlipoproteinemia on in vitro distribution of amiodarone and desethylamiodarone in human and rat plasma, *Pharm Res* 24 (2007) 672-678.
- [62] L. Dory, P.S. Roheim, Rat plasma lipoproteins and apolipoproteins in experimental hypothyroidism, *J Lipid Res* 22 (1981) 287-296.
- [63] T.G. Cole, I. Kuisk, W. Patsch, G. Schonfeld, Effects of high cholesterol diets on rat plasma lipoproteins and lipoprotein-cell interactions, *J Lipid Res* 25 (1984) 593-603.
- [64] W.K. Palmer, E.E. Emeson, T.P. Johnston, Poloxamer 407-induced atherogenesis in the C57BL/6 mouse, *Atherosclerosis* 136 (1998) 115-123.
- [65] T.P. Johnston, Y. Li, A.S. Jamal, D.J. Stechschulte, K.N. Dileepan, Poloxamer 407-induced atherosclerosis in mice appears to be due to lipid derangements and not due to its direct effects on endothelial cells and macrophages, *Mediators Inflamm* 12 (2003) 147-155.

[66] M. Blay, J. Peinado-Onsurbe, J. Julve, V. Rodriguez, J.A. Fernandez-Lopez, X. Remesar, M. Alemany, Anomalous lipoproteins in obese Zucker rats, *Diabetes Obes Metab* 3 (2001) 259-270.

[67] M.S. Benedetti, R. Whomsley, I. Poggesi, W. Cawello, F.X. Mathy, M.L. Delporte, P. Papeleu, J.B. Watelet, Drug metabolism and pharmacokinetics, *Drug Metab Rev* 41 (2009) 344-390.

[68] C.Y. Wu, L.Z. Benet, Predicting drug disposition via application of BCS: transport/absorption/ elimination interplay and development of a biopharmaceutics drug disposition classification system, *Pharm Res* 22 (2005) 11-23.

[69] R.D. Toothaker, P.G. Welling, The effect of food on drug bioavailability, *Annu Rev Pharmacol Toxicol* 20 (1980) 173-199.

[70] C. Miles, P. Dickson, K. Rana, C. Lippert, D. Fleisher, CCK antagonist pre-treatment inhibits meal-enhanced drug absorption in dogs, *Regul Pept* 68 (1997) 9-14.

[71] D.R. Sullivan, The clinical and nutritional implications of lipid-lowering drugs that act in the gastrointestinal tract, *Curr Opin Lipidol* 16 (2005) 39-45.

[72] D. Fleisher, C. Li, Y. Zhou, L.H. Pao, A. Karim, Drug, meal and formulation interactions influencing drug absorption after oral administration. Clinical implications, *Clin Pharmacokinet* 36 (1999) 233-254.

[73] H. Lange, R. Eggers, J. Bircher, Increased systemic availability of albendazole when taken with a fatty meal, *Eur J Clin Pharmacol* 34 (1988) 315-317.

[74] O.M. Alhamami, Delay in gastric emptying rate enhances bioavailability of sodium salicylates in rabbit, *Arch Pharm Res* 30 (2007) 1144-1148.

[75] V.H. Sunesen, R. Vedelsdal, H.G. Kristensen, L. Christrup, A. Mullertz, Effect of liquid volume and food intake on the absolute bioavailability of danazol, a poorly soluble drug, *Eur J Pharm Sci* 24 (2005) 297-303.

[76] C. Tschanz, W.W. Stargel, J.A. Thomas, Interactions between drugs and nutrients, *Adv Pharmacol* 35 (1996) 1-26.

[77] L. Williams, D.P. Hill, Jr., J.A. Davis, D.T. Lowenthal, The influence of food on the absorption and metabolism of drugs: an update, *Eur J Drug Metab Pharmacokinet* 21 (1996) 201-211.

[78] P.H. Marathe, D.S. Greene, G.D. Kollia, R.H. Barbhaiya, Evaluation of the effect of food on the pharmacokinetics of avitriptan, *Biopharm Drug Dispos* 19 (1998) 381-394.

[79] I. Bekersky, D. Dressler, Q.A. Mekki, Effect of low- and high-fat meals on tacrolimus absorption following 5 mg single oral doses to healthy human subjects, *J Clin Pharmacol* 41 (2001) 176-182.

[80] Y. Kido, S. Hiramoto, M. Murao, Y. Horio, T. Miyazaki, T. Kodama, Y. Nakabou, Epsilon-polylysine inhibits pancreatic lipase activity and suppresses postprandial hypertriacylglyceridemia in rats, *J Nutr* 133 (2003) 1887-1891.

[81] W.N. Charman, C.J. Porter, S. Mithani, J.B. Dressman, Physiochemical and physiological mechanisms for the effects of food on drug absorption: the role of lipids and pH, *J Pharm Sci* 86 (1997) 269-282.

[82] L.J. Naylor, V. Bakatselou, J.B. Dressman, Comparison of the mechanism of dissolution of hydrocortisone in simple and mixed micelle systems, *Pharm Res* 10 (1993) 865-870.

[83] N.R. Calafato, G. Pico, Griseofulvin and ketoconazole solubilization by bile salts studied using fluorescence spectroscopy, *Colloids Surf B Biointerfaces* 47 (2006) 198-204.

[84] C. Crevoisier, J. Handschin, J. Barre, D. Roumenov, C. Kleinbloesem, Food increases the bioavailability of mefloquine, *Eur J Clin Pharmacol* 53 (1997) 135-139.

[85] X. Meng, P. Mojaverian, M. Doedee, E. Lin, I. Weinryb, S.T. Chiang, P.R. Kowey, Bioavailability of amiodarone tablets administered with and without food in healthy subjects, *Am J Cardiol* 87 (2001) 432-435.

[86] A. Shayeganpour, A.S. Jun, D.R. Brocks, Pharmacokinetics of amiodarone in hyperlipidemic and simulated high fat-meal rat models, *Biopharm Drug Dispos* 26 (2005) 249-257.

[87] D.R. Brocks, K.M. Wasan, The influence of lipids on stereoselective pharmacokinetics of halofantrine: Important implications in food-effect studies involving drugs that bind to lipoproteins, *J Pharm Sci* 91 (2002) 1817-1826.

[88] M.P. McIntosh, C.J. Porter, K.M. Wasan, M. Ramaswamy, W.N. Charman, Differences in the lipoprotein binding profile of halofantrine in fed and fasted human or beagle plasma are dictated by the respective masses of core apolar lipoprotein lipid, *J Pharm Sci* 88 (1999) 378-384.

[89] D.R. Brocks, J.W. Toni, Pharmacokinetics of halofantrine in the rat: stereoselectivity and interspecies comparisons, *Biopharm Drug Dispos* 20 (1999) 165-169.

[90] C.J. Porter, S.A. Charman, W.N. Charman, Lymphatic transport of halofantrine in the triple-cannulated anesthetized rat model: effect of lipid vehicle dispersion, *J Pharm Sci* 85 (1996) 351-356.

[91] C.T. Ueda, M. Lemaire, G. Gsell, K. Nussbaumer, Intestinal lymphatic absorption of cyclosporin A following oral administration in an olive oil solution in rats, *Biopharm Drug Dispos* 4 (1983) 113-124.

[92] J.P. Patel, H.M. Korashy, A.O. El-Kadi, D.R. Brocks, Effect of bile and lipids on the stereoselective metabolism of halofantrine by rat everted-intestinal sacs, *Chirality* 22 (2010) 275-283.

[93] A. Shayeganpour, D.A. Hamdy, D.R. Brocks, Effects of intestinal constituents and lipids on intestinal formation and pharmacokinetics of desethylamiodarone formed from amiodarone, *J Pharm Pharmacol* 60 (2008) 1625-1632.

[94] D.R. Brocks, S. Ala, H.M. Aliabadi, The effect of increased lipoprotein levels on the pharmacokinetics of cyclosporine A in the laboratory rat, *Biopharm Drug Dispos* 27 (2006) 7-16.

[95] S.K. Teo, M.R. Scheffler, K.A. Kook, W.G. Tracewell, W.A. Colburn, D.I. Stirling, S.D. Thomas, Effect of a high-fat meal on thalidomide pharmacokinetics and the relative bioavailability of oral formulations in healthy men and women, *Biopharm Drug Dispos* 21 (2000) 33-40.

[96] L.A. Eliot, R.T. Foster, F. Jamali, Effects of hyperlipidemia on the pharmacokinetics of nifedipine in the rat, *Pharm Res* 16 (1999) 309-313.

[97] A. Shayeganpour, H. Korashy, J.P. Patel, A.O. El-Kadi, D.R. Brocks, The impact of experimental hyperlipidemia on the distribution and metabolism of amiodarone in rat, *Int J Pharm* 361 (2008) 78-86.

[98] N. Sugioka, K. Haraya, Y. Maeda, K. Fukushima, K. Takada, Pharmacokinetics of human immunodeficiency virus protease inhibitor, nelfinavir, in poloxamer 407-induced hyperlipidemic model rats, *Biol Pharm Bull* 32 (2009) 269-275.

[99] A.J. Humberstone, C.J. Porter, G.A. Edwards, W.N. Charman, Association of halofantrine with postprandially derived plasma lipoproteins decreases its clearance relative to administration in the fasted state, *J Pharm Sci* 87 (1998) 936-942.

[100] J. Wojcicki, V. Sulzyc-Bielicka, J. Kutrzeba, B. Gawronska-Szklarz, M. Drozdziak, Z. Sterna, Studies on the pharmacokinetics and pharmacodynamics of propranolol in hyperlipidemia, *J Clin Pharmacol* 39 (1999) 826-833.

[101] G. Dutkiewicz, J. Wojcicki, B. Gawronska-Szklarz, Pharmacokinetics of phenytoin in hyperlipidemia, *Eur J Pharm Sci* 4 (1996) 33-37.

[102] J.P. Patel, J.G. Fleischer, K.M. Wasan, D.R. Brocks, The effect of experimental hyperlipidemia on the stereoselective tissue distribution, lipoprotein association and microsomal metabolism of (+/-)-halofantrine, *J Pharm Sci* 98 (2009) 2516-2528.

[103] K.M. Wasan, P.H. Pritchard, M. Ramaswamy, W. Wong, E.M. Donnachie, L.J. Brunner, Differences in lipoprotein lipid concentration and composition modify the plasma distribution of cyclosporine, *Pharm Res* 14 (1997) 1613-1620.

[104] S. Kanduru, in: Further investigations into the effects of hyperlipidemia on the biodisposition and nephrotoxicity of cyclosporine A. Master of Science in Faculty of Pharmacy and Pharmaceutical Sciences, University of Alberta, Edmonton, 2009, pp. 157.

[105] K.M. Wasan, A.L. Kennedy, S.M. Cassidy, M. Ramaswamy, L. Holtorf, J.W. Chou, P.H. Pritchard, Pharmacokinetics, distribution in serum lipoproteins and tissues, and renal toxicities of amphotericin B and amphotericin B lipid complex in a hypercholesterolemic rabbit model: single-dose studies, *Antimicrob Agents Chemother* 42 (1998) 3146-3152.

[106] H.M. Aliabadi, T.J. Spencer, P. Mahdipoor, A. Lavasanifar, D.R. Brocks, Insights into the effects of hyperlipoproteinemia on cyclosporine A biodistribution and relationship to renal function, *Aaps J* 8 (2006) E672-681.

[107] B.D. Wilson, M.L. Lippmann, Pulmonary accumulation of amiodarone and N-desethylamiodarone. Relationship to the development of pulmonary toxicity, *Am Rev Respir Dis* 141 (1990) 1553-1558.

[108] K. Vadie, G. Lopez-Berestein, D.R. Luke, Disposition and toxicity of amphotericin-B in the hyperlipidemic Zucker rat model, *Int J Obes* 14 (1990) 465-472.

[109] A.M. Gardier, D. Mathe, X. Guedeney, J. Barre, C. Benvenuti, N. Navarro, L. Vernillet, D. Loisançe, J.P. Cachera, B. Jacotot, et al., Effects of plasma lipid levels on blood distribution and pharmacokinetics of cyclosporin A, *Ther Drug Monit* 15 (1993) 274-280.

[110] K.D. Peteherych, K.M. Wasan, Effects of lipoproteins on cyclosporine A toxicity and uptake in LLC-PK1 pig kidney cells, *J Pharm Sci* 90 (2001) 1395-1406.

- [111] J.P. Patel, D.R. Brocks, Effect of experimental hyperlipidemia on the electrocardiographic effects of repeated dose halofantrine, *British journal of pharmacology* (In press).
- [112] M.J. Zamek-Gliszczyński, K.A. Hoffmaster, K. Nezasa, M.N. Tallman, K.L. Brouwer, Integration of hepatic drug transporters and phase II metabolizing enzymes: mechanisms of hepatic excretion of sulfate, glucuronide, and glutathione metabolites, *Eur J Pharm Sci* 27 (2006) 447-486.
- [113] D.J. Liska, The detoxification enzyme systems, *Altern Med Rev* 3 (1998) 187-198.
- [114] X. Zhang, Q.Y. Zhang, D. Liu, T. Su, Y. Weng, G. Ling, Y. Chen, J. Gu, B. Schilling, X. Ding, Expression of cytochrome p450 and other biotransformation genes in fetal and adult human nasal mucosa, *Drug Metab Dispos* 33 (2005) 1423-1428.
- [115] D.F. Tierney, Lung metabolism and biochemistry, *Annu Rev Physiol* 36 (1974) 209-231.
- [116] H.T. Yao, Y.W. Chang, S.J. Lan, C.T. Chen, J.T. Hsu, T.K. Yeh, The inhibitory effect of polyunsaturated fatty acids on human CYP enzymes, *Life Sci* 79 (2006) 2432-2440.
- [117] V. Hirunpanich, B. Sethabouppha, H. Sato, Inhibitory effects of saturated and polyunsaturated fatty acids on the cytochrome P450 3A activity in rat liver microsomes, *Biol Pharm Bull* 30 (2007) 1586-1588.
- [118] V. Hirunpanich, J. Katagi, B. Sethabouppha, H. Sato, Demonstration of docosahexaenoic acid as a bioavailability enhancer for CYP3A substrates: in vitro and in vivo evidence using cyclosporin in rats, *Drug Metab Dispos* 34 (2006) 305-310.
- [119] C.C. Li, C.K. Lii, K.L. Liu, J.J. Yang, H.W. Chen, DHA down-regulates phenobarbital-induced cytochrome P450 2B1 gene expression in rat primary hepatocytes by attenuating CAR translocation, *Toxicol Appl Pharmacol* 225 (2007) 329-336.

[120] M.S. Kim, S. Wang, Z. Shen, C.J. Kochansky, J.R. Strauss, R.B. Franklin, S.H. Vincent, Differences in the pharmacokinetics of peroxisome proliferator-activated receptor agonists in genetically obese Zucker and Sprague-Dawley rats: implications of decreased glucuronidation in obese Zucker rats, *Drug Metab Dispos* 32 (2004) 909-914.

[121] H. Xiong, K. Yoshinari, K.L. Brouwer, M. Negishi, Role of constitutive androstane receptor in the in vivo induction of Mrp3 and CYP2B1/2 by phenobarbital, *Drug Metab Dispos* 30 (2002) 918-923.

[122] S.K. Gupta, L.Z. Benet, High-fat meals increase the clearance of cyclosporine, *Pharm Res* 7 (1990) 46-48.

[123] A.J. McLean, P.J. McNamara, P. duSouich, M. Gibaldi, D. Lalka, Food, splanchnic blood flow, and bioavailability of drugs subject to first-pass metabolism, *Clin Pharmacol Ther* 24 (1978) 5-10.

[124] A.J. McLean, C. Isbister, A. Bobik, F.J. Dudley, Reduction of first-pass hepatic clearance of propranolol by food, *Clin Pharmacol Ther* 30 (1981) 31-34.

[125] R. Mantyla, H. Allonen, J. Kanto, T. Kleimola, R. Sellman, Effect of food on the bioavailability of labetalol, *Br J Clin Pharmacol* 9 (1980) 435-437.

[126] S. Noble, D. Faulds, Saquinavir. A review of its pharmacology and clinical potential in the management of HIV infection, *Drugs* 52 (1996) 93-112.

[127] M.E. Elsherbiny, A.O. El-Kadi, D.R. Brocks, The metabolism of amiodarone by various CYP isoenzymes of human and rat, and the inhibitory influence of ketoconazole, *J Pharm Pharm Sci* 11 (2008) 147-159.

[128] V. Hirunpanich, K. Murakoso, H. Sato, Inhibitory effect of docosahexaenoic acid (DHA) on the intestinal metabolism of midazolam: in vitro and in vivo studies in rats, *Int J Pharm* 351 (2008) 133-143.

[129] L. Xu, Y. Liu, T. Wang, Y. Qi, X. Han, Y. Xu, J. Peng, X. Tang, Development and validation of a sensitive and rapid non-aqueous LC-ESI-

MS/MS method for measurement of diosgenin in the plasma of normal and hyperlipidemic rats: a comparative study, *J Chromatogr B Analyt Technol Biomed Life Sci* 877 (2009) 1530-1536.

[130] C. Funk, The role of hepatic transporters in drug elimination, *Expert Opin Drug Metab Toxicol* 4 (2008) 363-379.

[131] M.E. Elsherbiny, A.O. El-Kadi, D.R. Brocks, in: The effect of hyperlipidemia on P-glycoprotein activity in porcine and rat renal cell line model in CSPS Conference, Vancouver, BC, Canada, 2010.

[132] G.C. Yee, G. Mills, R. Schaffer, T.P. Lennon, M.S. Kennedy, H.J. Deeg, Renal cyclosporine clearance in marrow transplant recipients: age-related variation, *J Clin Pharmacol* 26 (1986) 658-661.

[133] M.D. Delle Monache, A. Gigliozzi, A. Benedetti, L. Marucci, A. Bini, C. Francia, E. Papa, E. Di Cosimo, F. Fraioli, A.M. Jezequel, D. Alvaro, Effect of pharmacological modulation of liver P-glycoproteins on cyclosporin A biliary excretion and cholestasis: a study in isolated perfused rat liver, *Dig Dis Sci* 44 (1999) 2196-2204.

[134] S.J. Connolly, Evidence-based analysis of amiodarone efficacy and safety, *Circulation* 100 (1999) 2025-2034.

[135] G.V. Naccarelli, D.L. Wolbrette, J.T. Dell'Orfano, H.M. Patel, J.C. Luck, Amiodarone: what have we learned from clinical trials?, *Clin Cardiol* 23 (2000) 73-82.

[136] J.W. Mason, L.M. Hondeghem, B.G. Katzung, Block of inactivated sodium channels and of depolarization-induced automaticity in guinea pig papillary muscle by amiodarone, *Circ Res* 55 (1984) 278-285.

[137] B.N. Singh, Amiodarone: the expanding antiarrhythmic role and how to follow a patient on chronic therapy, *Clin Cardiol* 20 (1997) 608-618.

[138] S.D. Kramer, J.C. Gautier, P. Saudemon, Considerations on the potentiometric log P determination, *Pharm Res* 15 (1998) 1310-1313.

- [139] T.E. Morey, C.N. Seubert, M.J. Raatikainen, A.E. Martynyuk, P. Druzgala, P. Milner, M.D. Gonzalez, D.M. Dennis, Structure-activity relationships and electrophysiological effects of short-acting amiodarone homologs in guinea pig isolated heart, *J Pharmacol Exp Ther* 297 (2001) 260-266.
- [140] M.R. Lalloz, P.G. Byfield, R.M. Greenwood, R.L. Himsworth, Binding of amiodarone by serum proteins and the effects of drugs, hormones and other interacting ligands, *J Pharm Pharmacol* 36 (1984) 366-372.
- [141] R. Latini, A. Bizzi, M. Cini, E. Veneroni, S. Marchi, E. Riva, Amiodarone and desethylamiodarone tissue uptake in rats chronically treated with amiodarone is non-linear with the dose, *J Pharm Pharmacol* 39 (1987) 426-431.
- [142] P.A. Wyss, M.J. Moor, M.H. Bickel, Single-dose kinetics of tissue distribution, excretion and metabolism of amiodarone in rats, *J Pharmacol Exp Ther* 254 (1990) 502-507.
- [143] E.G. Giardina, M. Schneider, M.L. Barr, Myocardial amiodarone and desethylamiodarone concentrations in patients undergoing cardiac transplantation, *J Am Coll Cardiol* 16 (1990) 943-947.
- [144] S.D. Beder, M.H. Cohen, G. BenShachar, Time course of myocardial amiodarone uptake in the piglet heart using a chronic animal model, *Pediatr Cardiol* 19 (1998) 204-211.
- [145] P. Sermsappasuk, M. Baek, M. Weiss, Kinetic analysis of myocardial uptake and negative inotropic effect of amiodarone in rat heart, *Eur J Pharm Sci* 28 (2006) 243-248.
- [146] A. Soyama, N. Hanioka, Y. Saito, N. Murayama, M. Ando, S. Ozawa, J. Sawada, Amiodarone N-deethylation by CYP2C8 and its variants, CYP2C8*3 and CYP2C8 P404A, *Pharmacol Toxicol* 91 (2002) 174-178.
- [147] S. Nattel, M. Davies, M. Quantz, The antiarrhythmic efficacy of amiodarone and desethylamiodarone, alone and in combination, in dogs with acute myocardial infarction, *Circulation* 77 (1988) 200-208.

- [148] J.M. Trivier, C. Libersa, C. Belloc, M. Lhermitte, Amiodarone N-deethylation in human liver microsomes: involvement of cytochrome P450 3A enzymes (first report), *Life Sci* 52 (1993) PL91-96.
- [149] G. Fabre, B. Julian, B. Saint-Aubert, H. Joyeux, Y. Berger, Evidence for CYP3A-mediated N-deethylation of amiodarone in human liver microsomal fractions, *Drug Metab Dispos* 21 (1993) 978-985.
- [150] A. Shayeganpour, A.O. El-Kadi, D.R. Brocks, Determination of the enzyme(s) involved in the metabolism of amiodarone in liver and intestine of rat: the contribution of cytochrome P450 3A isoforms, *Drug Metab Dispos* 34 (2006) 43-50.
- [151] L. Becquemont, M. Neuvonen, C. Verstuyft, P. Jaillon, A. Letierce, P.J. Neuvonen, C. Funck-Brentano, Amiodarone interacts with simvastatin but not with pravastatin disposition kinetics, *Clin Pharmacol Ther* 81 (2007) 679-684.
- [152] D.M. Rotstein, D.J. Kertesz, K.A. Walker, D.C. Swinney, Stereoisomers of ketoconazole: preparation and biological activity, *J Med Chem* 35 (1992) 2818-2825.
- [153] H. Vanden Bossche, L. Koymans, H. Moereels, P450 inhibitors of use in medical treatment: focus on mechanisms of action, *Pharmacol Ther* 67 (1995) 79-100.
- [154] J.J. Sheets, J.I. Mason, Ketoconazole: a potent inhibitor of cytochrome P-450-dependent drug metabolism in rat liver, *Drug Metab Dispos* 12 (1984) 603-606.
- [155] M. Pasanen, T. Taskinen, M. Iscan, E.A. Sotaniemi, M. Kairaluoma, O. Pelkonen, Inhibition of human hepatic and placental xenobiotic monooxygenases by imidazole antimycotics, *Biochem Pharmacol* 37 (1988) 3861-3866.
- [156] I. Schuster, The interaction of representative members from two classes of antimycotics--the azoles and the allylamines--with cytochromes P-450 in steroidogenic tissues and liver, *Xenobiotica* 15 (1985) 529-546.

[157] H.M. Korashy, A. Shayeganpour, D.R. Brocks, A.O. El-Kadi, Induction of cytochrome P450 1A1 by ketoconazole and itraconazole but not fluconazole in murine and human hepatoma cell lines, *Toxicol Sci* 97 (2007) 32-43.

[158] I. Velikinac, O. Cudina, I. Jankovic, D. Agbaba, S. Vladimirov, Comparison of capillary zone electrophoresis and high performance liquid chromatography methods for quantitative determination of ketoconazole in drug formulations, *Farmaco* 59 (2004) 419-424.

[159] A.D. Rodrigues, G.G. Gibson, C. Ioannides, D.V. Parke, Interactions of imidazole antifungal agents with purified cytochrome P-450 proteins, *Biochem Pharmacol* 36 (1987) 4277-4281.

[160] A.D. Rodrigues, D.F. Lewis, C. Ioannides, D.V. Parke, Spectral and kinetic studies of the interaction of imidazole anti-fungal agents with microsomal cytochromes P-450, *Xenobiotica* 17 (1987) 1315-1327.

[161] S. Abel, D. Russell, R.J. Taylor-Worth, C.E. Ridgway, G.J. Muirhead, Effects of CYP3A4 inhibitors on the pharmacokinetics of maraviroc in healthy volunteers, *Br J Clin Pharmacol* 65 Suppl 1 (2008) 27-37.

[162] Y. Fan, R. Rodriguez-Proteau, Ketoconazole and the modulation of multidrug resistance-mediated transport in Caco-2 and MDCKII-MDR1 drug transport models, *Xenobiotica* 38 (2008) 107-129.

[163] Y.C. Huang, J.L. Colaizzi, R.H. Bierman, R. Woestenborghs, J. Heykants, Pharmacokinetics and dose proportionality of ketoconazole in normal volunteers, *Antimicrob Agents Chemother* 30 (1986) 206-210.

[164] T.K. Daneshmend, D.W. Warnock, Clinical pharmacokinetics of systemic antifungal drugs, *Clin Pharmacokinet* 8 (1983) 17-42.

[165] J.G. Baxter, C. Brass, J.J. Schentag, R.L. Slaughter, Pharmacokinetics of ketoconazole administered intravenously to dogs and orally as tablet and solution to humans and dogs, *J Pharm Sci* 75 (1986) 443-447.

- [166] R.P. Rimmel, K. Amoh, M.M. Abdel-Monem, The disposition and pharmacokinetics of ketoconazole in the rat, *Drug Metab Dispos* 15 (1987) 735-739.
- [167] D. Matthew, B. Brennan, K. Zomorodi, J.B. Houston, Disposition of azole antifungal agents. I. Nonlinearities in ketoconazole clearance and binding in rat liver, *Pharm Res* 10 (1993) 418-422.
- [168] P. Sjoberg, L. Ekman, T. Lundqvist, Dose and sex-dependent disposition of ketoconazole in rats, *Arch Toxicol* 62 (1988) 177-180.
- [169] R. Heel, Ketoconazole: pharmacological profile, in: *Ketoconazole in the management of fungal disease*, Adis press, Balgowlah, Australia, Levine HB, 1982, pp. 55-76.
- [170] E.W. Gascogaine, G.J. Barton, M. Micheals, W. Meuldermans, J. Heykants, The kinetics of ketoconazole in animals and man, *Clinical Research Reviews* 1 (1981) 177-187.
- [171] F. Jamali, R. Mehvar, F.M. Pasutto, Enantioselective aspects of drug action and disposition: therapeutic pitfalls, *J Pharm Sci* 78 (1989) 695-715.
- [172] D.R. Brocks, F. Jamali, Stereochemical aspects of pharmacotherapy, *Pharmacotherapy* 15 (1995) 551-564.
- [173] S. Dilmaghanian, J.G. Gerber, S.G. Filler, A. Sanchez, J. Gal, Enantioselectivity of inhibition of cytochrome P450 3A4 (CYP3A4) by ketoconazole: Testosterone and methadone as substrates, *Chirality* 16 (2004) 79-85.
- [174] D.R. Brocks, Drug disposition in three dimensions: an update on stereoselectivity in pharmacokinetics, *Biopharm Drug Dispos* 27 (2006) 387-406.
- [175] H. Lu, Stereoselectivity in drug metabolism, *Expert Opin Drug Metab Toxicol* 3 (2007) 149-158.

- [176] M.S. Brown, J.L. Goldstein, Drugs used in the treatment of hyperlipoproteinemias, in: Goodman and Gilman's; The pharmacological basis of therapeutics, 1990, pp. 874-896.
- [177] J. Genest, J. Frohlich, G. Fodor, R. McPherson, Recommendations for the management of dyslipidemia and the prevention of cardiovascular disease: summary of the 2003 update, *Cmaj* 169 (2003) 921-924.
- [178] H.R. Kim, S. Gil, K. Andrieux, V. Nicolas, M. Appel, H. Chacun, D. Desmaele, F. Taran, D. Georjin, P. Couvreur, Low-density lipoprotein receptor-mediated endocytosis of PEGylated nanoparticles in rat brain endothelial cells, *Cell Mol Life Sci* 64 (2007) 356-364.
- [179] P. Gershkovich, D. Shtainer, A. Hoffman, The effect of a high-fat meal on the pharmacodynamics of a model lipophilic compound that binds extensively to triglyceride-rich lipoproteins, *Int J Pharm* 333 (2007) 1-4.
- [180] A. Shayeganpour, V. Somayaji, D.R. Brocks, A liquid chromatography-mass spectrometry assay method for simultaneous determination of amiodarone and desethylamiodarone in rat specimens, *Biomed Chromatogr* 21 (2007) 284-290.
- [181] E.A. Leite, A. Grabe-Guimaraes, H.N. Guimaraes, G.L. Machado-Coelho, G. Barratt, V.C. Mosqueira, Cardiotoxicity reduction induced by halofantrine entrapped in nanocapsule devices, *Life Sci* 80 (2007) 1327-1334.
- [182] E.C. Costa, A.A. Goncalves, M.A. Areas, R.G. Morgabel, Effects of metformin on QT and QTc interval dispersion of diabetic rats, *Arq Bras Cardiol* 90 (2008) 232-238.
- [183] P.O. Seglen, Preparation of isolated rat liver cells, *Methods Cell Biol* 13 (1976) 29-83.
- [184] M.M. Barakat, A.O. El-Kadi, P. du Souich, L-NAME prevents in vivo the inactivation but not the down-regulation of hepatic cytochrome P450 caused by an acute inflammatory reaction, *Life Sci* 69 (2001) 1559-1571.

- [185] O.H. Lowry, N.J. Rosebrough, A.L. Farr, R.J. Randall, Protein measurement with the Folin phenol reagent, *J Biol Chem* 193 (1951) 265-275.
- [186] T. Omura, R. Sato, The carbon monoxide-binding pigment of liver microsomes. I. Evidence for Its Hemoprotein Nature, *J Biol Chem* 239 (1964) 2370-2378.
- [187] J. Schuhmacher, K. Buhner, A. Witt-Laido, Determination of the free fraction and relative free fraction of drugs strongly bound to plasma proteins, *J Pharm Sci* 89 (2000) 1008-1021.
- [188] K.M. Wasan, M. Ramaswamy, M.P. McIntosh, C.J. Porter, W.N. Charman, Differences in the lipoprotein distribution of halofantrine are regulated by lipoprotein apolar lipid and protein concentration and lipid transfer protein I activity: in vitro studies in normolipidemic and dyslipidemic human plasmas, *J Pharm Sci* 88 (1999) 185-190.
- [189] K.M. Wasan, S.M. Cassidy, M. Ramaswamy, A. Kennedy, F.W. Strobel, S.P. Ng, T.Y. Lee, A comparison of step-gradient and sequential density ultracentrifugation and the use of lipoprotein deficient plasma controls in determining the plasma lipoprotein distribution of lipid-associated nystatin and cyclosporine, *Pharm Res* 16 (1999) 165-169.
- [190] K.M. Wasan, J.S. Conklin, Enhanced amphotericin B nephrotoxicity in intensive care patients with elevated levels of low-density lipoprotein cholesterol, *Clin Infect Dis* 24 (1997) 78-80.
- [191] B. Davies, T. Morris, Physiological parameters in laboratory animals and humans, *Pharm Res* 10 (1993) 1093-1095.
- [192] A.J. Bailer, Testing for the equality of area under the curves when using destructive measurement techniques, *J Pharmacokinet Biopharm* 16 (1988) 303-309.
- [193] A. Shayeganpour, D.A. Hamdy, D.R. Brocks, Pharmacokinetics of desethylamidarone in the rat after its administration as the preformed metabolite,

and after administration of amiodarone, *Biopharm Drug Dispos* 29 (2007) 159-166.

[194] K.M. Wasan, R. Subramanian, M. Kwong, I.J. Goldberg, T. Wright, T.P. Johnston, Poloxamer 407-mediated alterations in the activities of enzymes regulating lipid metabolism in rats, *J Pharm Pharm Sci* 6 (2003) 189-197.

[195] B. Padmavathy, S.N. Devaraj, H. Devaraj, Effect of amiodarone, an antiarrhythmic drug, on serum and liver lipids and serum marker enzymes in rats, *Indian J Biochem Biophys* 29 (1992) 522-524.

[196] W.M. Wiersinga, M. Broenink, Amiodarone induces a dose-dependent increase of plasma cholesterol in the rat, *Horm Metab Res* 23 (1991) 94-95.

[197] P.T. Pollak, M.H. Tan, Elevation of high-density lipoprotein cholesterol in humans during long-term therapy with amiodarone, *Am J Cardiol* 83 (1999) 296-300, A297.

[198] R.J. Cenedella, W.G. Crouthamel, G.G. Bierkamper, D.P. Westfall, Alteration of drug pharmacodynamics by hyperlipidemia, *Arch Int Pharmacodyn Ther* 218 (1975) 299-311.

[199] L.D. Bergelson, E.M. Manevich, J.G. Molotkovsky, G.I. Muzya, M.A. Martynova, The interaction of prostaglandins with high-density lipoproteins: a non-equilibrium model of ligand-receptor interaction, *Biochim Biophys Acta* 921 (1987) 182-190.

[200] E.M. Manevich, G.I. Muzya, N.V. Prokazova, J.G. Molotkovsky, V.V. Bezuglov, L.D. Bergelson, Interaction of prostaglandin E1 with human high density lipoproteins, *FEBS Lett* 173 (1984) 291-294.

[201] S.J. Weir, C.T. Ueda, Amiodarone pharmacokinetics. I. Acute dose-dependent disposition studies in rats, *J Pharmacokinet Biopharm* 14 (1986) 601-613.

[202] J.A. Cuthbert, P.E. Lipsky, Mitogenic stimulation alters the regulation of LDL receptor gene expression in human lymphocytes, *J Lipid Res* 31 (1990) 2067-2078.

[203] A. Thienpont, J. Gal, C. Aeschlimann, G. Felix, Studies on stereoselective separations of the azole antifungal drugs ketoconazole and itraconazole using HPLC and SFC on silica-based polysaccharides., *Analisis* 27 (1999) 713-718.

[204] J.L. Bernal, L. Toribio, M.J. del Nozal, E.M. Nieto, M.I. Montequi, Separation of antifungal chiral drugs by SFC and HPLC: a comparative study, *J Biochem Biophys Methods* 54 (2002) 245-254.

[205] J.L. Bernal, M.J. del Nozal, L. Toribio, M.I. Montequi, E.M. Nieto, Separation of ketoconazole enantiomers by chiral subcritical-fluid chromatography, *J Biochem Biophys Methods* 43 (2000) 241-250.

[206] M. Castro-Puyana, A.L. Crego, M.L. Marina, Enantiomeric separation of ketoconazole and terconazole antifungals by electrokinetic chromatography: Rapid quantitative analysis of ketoconazole in pharmaceutical formulations, *Electrophoresis* 26 (2005) 3960-3968.

[207] K.B. Alton, Determination of the antifungal agent, ketoconazole, in human plasma by high-performance liquid chromatography, *J Chromatogr* 221 (1980) 337-344.

[208] K.H. Yuen, K.K. Peh, Simple high-performance liquid chromatographic method for determination of ketoconazole in human plasma, *J Chromatogr B Biomed Sci Appl* 715 (1998) 436-440.

[209] M.V. Vertzoni, C. Reppas, H.A. Archontaki, Optimization and validation of a high-performance liquid chromatographic method with UV detection for the determination of ketoconazole in canine plasma, *J Chromatogr B Analyt Technol Biomed Life Sci* 839 (2006) 62-67.

[210] C.M. Riley, M.O. James, Determination of ketoconazole in the plasma, liver, lung and adrenal of the rat by high-performance liquid chromatography, *J Chromatogr* 377 (1986) 287-294.

- [211] Q. Huang, G.J. Wang, J.G. Sun, X.L. Hu, Y.H. Lu, Q. Zhang, Simultaneous determination of docetaxel and ketoconazole in rat plasma by liquid chromatography/electrospray ionization tandem mass spectrometry, *Rapid Commun Mass Spectrom* 21 (2007) 1009-1018.
- [212] J. Gal , C. Aeschlimann, G. Felix, HPLC separation of stereoisomers of Ketoconazole, miconazole and itraconazole on the ChiralPak AD chiral stationary phase, Fourth International Symposium on Chiral Discrimination, Montreal, Canada (1993) Abstract 130.
- [213] V.J. Sekar, E. Lefebvre, M. De Pauw, T. Vangeneugden, R.M. Hoetelmans, Pharmacokinetics of darunavir/ritonavir and ketoconazole following co-administration in HIV-healthy volunteers, *Br J Clin Pharmacol* (2008).
- [214] N.A. Farid, C.D. Payne, D.S. Small, K.J. Winters, C.S. Ernest, 2nd, J.T. Brandt, C. Darstein, J.A. Jakubowski, D.E. Salazar, Cytochrome P450 3A inhibition by ketoconazole affects prasugrel and clopidogrel pharmacokinetics and pharmacodynamics differently, *Clin Pharmacol Ther* 81 (2007) 735-741.
- [215] F.K. Engels, W.J. Loos, R.A. Mathot, R.H. van Schaik, J. Verweij, Influence of ketoconazole on the fecal and urinary disposition of docetaxel, *Cancer Chemother Pharmacol* 60 (2007) 569-579.
- [216] N. Gharavi, S. Sattari, A. Shayeganpour, A.O. El-Kadi, D.R. Brocks, The stereoselective metabolism of halofantrine to desbutylhalofantrine in the rat: evidence of tissue-specific enantioselectivity in microsomal metabolism, *Chirality* 19 (2007) 22-33.
- [217] L.L. von Moltke, B.W. Granda, J.M. Grassi, M.D. Perloff, D. Vishnuvardhan, D.J. Greenblatt, Interaction of triazolam and ketoconazole in P-glycoprotein-deficient mice, *Drug Metab Dispos* 32 (2004) 800-804.
- [218] D. Babovic-Vuksanovic, M.D. Donaldson, N.A. Gibson, A.M. Wallace, Hazards of ketoconazole therapy in testotoxicosis, *Acta Paediatr* 83 (1994) 994-997.

[219] N. Sonino, M. Boscaro, A. Paoletta, F. Mantero, D. Ziliotto, Ketoconazole treatment in Cushing's syndrome: experience in 34 patients, *Clin Endocrinol (Oxf)* 35 (1991) 347-352.

[220] M.F. Paine, P. Schmiedlin-Ren, P.B. Watkins, Cytochrome P-450 1A1 expression in human small bowel: interindividual variation and inhibition by ketoconazole, *Drug Metab Dispos* 27 (1999) 360-364.

[221] W.E. Lindup, M.C. Orme, Clinical pharmacology: plasma protein binding of drugs, *Br Med J (Clin Res Ed)* 282 (1981) 212-214.

[222] M.L. Howard, J.J. Hill, G.R. Galluppi, M.A. McLean, Plasma protein binding in drug discovery and development, *Comb Chem High Throughput Screen* 13 (2010) 170-187.

[223] M.P. van den Broek, M.A. Sikma, T.F. Ververs, J. Meulenbelt, Severe valproic acid intoxication: case study on the unbound fraction and the applicability of extracorporeal elimination, *Eur J Emerg Med* 16 (2009) 330-332.

[224] J. Koch-Weser, E.M. Sellers, Binding of drugs to serum albumin (first of two parts), *N Engl J Med* 294 (1976) 311-316.

[225] R.M. Procyshyn, T. Ho, K.M. Wasan, Competitive displacement of clozapine from plasma proteins in normolipidemic and hyperlipidemic plasma samples: clinical implications, *Drug Dev Ind Pharm* 31 (2005) 331-337.

[226] R. Martinez-Jorda, J.M. Rodriguez-Sasiain, E. Suarez, R. Calvo, Serum binding of ketoconazole in health and disease, *Int J Clin Pharmacol Res* 10 (1990) 271-276.

[227] Z.G. Wout, E.A. Pec, J.A. Maggiore, R.H. Williams, P. Palicharla, T.P. Johnston, Poloxamer 407-mediated changes in plasma cholesterol and triglycerides following intraperitoneal injection to rats, *J Parenter Sci Technol* 46 (1992) 192-200.

[228] T.K. Daneshmend, D.W. Warnock, Clinical pharmacokinetics of ketoconazole, *Clin Pharmacokinet* 14 (1988) 13-34.

[229] G. Lake-Bakaar, P.J. Scheuer, S. Sherlock, Hepatic reactions associated with ketoconazole in the United Kingdom, *Br Med J (Clin Res Ed)* 294 (1987) 419-422.

[230] Janssen, Product monograph: Nizoral[®], Ketoconazole (Titusville, NJ: Janssen Pharmaceuticals), in, 1995.

[231] J. Jurica, M. Dostalek, J. Konecny, Z. Glatz, E. Hadasova, J. Tomandl, HPLC determination of midazolam and its three hydroxy metabolites in perfusion medium and plasma from rats, *J Chromatogr B Analyt Technol Biomed Life Sci* 852 (2007) 571-577.

[232] J.A. Carrillo, S.I. Ramos, J.A. Agundez, C. Martinez, J. Benitez, Analysis of midazolam and metabolites in plasma by high-performance liquid chromatography: probe of CYP3A, *Ther Drug Monit* 20 (1998) 319-324.

[233] R. Kato, S. Yamashita, J. Moriguchi, M. Nakagawa, Y. Tsukura, K. Uchida, F. Amano, Y. Hirotsu, Y. Ijiri, K. Tanaka, Changes of midazolam pharmacokinetics in Wistar rats treated with lipopolysaccharide: relationship between total CYP and CYP3A2, *Innate Immun* 14 (2008) 291-297.

[234] K. Yamano, K. Yamamoto, H. Kotaki, Y. Sawada, T. Iga, Quantitative prediction of metabolic inhibition of midazolam by itraconazole and ketoconazole in rats: implication of concentrative uptake of inhibitors into liver, *Drug Metab Dispos* 27 (1999) 395-402.

[235] S. Kurosawa, S. Uchida, Y. Ito, S. Yamada, Effect of ursodeoxycholic acid on the pharmacokinetics of midazolam and CYP3A in the liver and intestine of rats, *Xenobiotica* 39 (2009) 162-170.

[236] M. Kuroha, A. Azumano, Y. Kuze, M. Shimoda, E. Kokue, Effect of multiple dosing of ketoconazole on pharmacokinetics of midazolam, a cytochrome P-450 3A substrate in beagle dogs, *Drug Metab Dispos* 30 (2002) 63-68.

- [237] R.J. Rodriguez, D. Acosta, Jr., Metabolism of ketoconazole and deacetylated ketoconazole by rat hepatic microsomes and flavin-containing monooxygenases, *Drug Metab Dispos* 25 (1997) 772-777.
- [238] M. de Diego, G. Godoy, S. Mennickent, Chemical stability of midazolam injection by high performance liquid chromatography, *J Sep Sci* 30 (2007) 1833-1838.
- [239] N. Yasui-Furukori, Y. Inoue, T. Tateishi, Sensitive determination of midazolam and 1'-hydroxymidazolam in plasma by liquid-liquid extraction and column-switching liquid chromatography with ultraviolet absorbance detection and its application for measuring CYP3A activity, *J Chromatogr B Analyt Technol Biomed Life Sci* 811 (2004) 153-157.
- [240] N.R. Badcock, Micro-determination of ketoconazole in plasma or serum by high-performance liquid chromatography, *J Chromatogr* 306 (1984) 436-440.
- [241] S.M. Tsunoda, R.L. Velez, L.L. von Moltke, D.J. Greenblatt, Differentiation of intestinal and hepatic cytochrome P450 3A activity with use of midazolam as an in vivo probe: effect of ketoconazole, *Clin Pharmacol Ther* 66 (1999) 461-471.
- [242] E.J. Portier, K. de Blok, J.J. Butter, C.J. van Boxtel, Simultaneous determination of fentanyl and midazolam using high-performance liquid chromatography with ultraviolet detection, *J Chromatogr B Biomed Sci Appl* 723 (1999) 313-318.
- [243] K. Chan, R.D. Jones, Simultaneous determination of flumazenil, midazolam and metabolites in human biological fluids by liquid chromatography, *J Chromatogr* 619 (1993) 154-160.
- [244] S.V. Mandlekar, A.V. Rose, G. Cornelius, B. Slecza, C. Caporuscio, J. Wang, P.H. Marathe, Development of an in vivo rat screen model to predict pharmacokinetic interactions of CYP3A4 substrates, *Xenobiotica* 37 (2007) 923-942.

- [245] A. Ogasawara, T. Kume, E. Kazama, Effect of oral ketoconazole on intestinal first-pass effect of midazolam and fexofenadine in cynomolgus monkeys, *Drug Metab Dispos* 35 (2007) 410-418.
- [246] V. Andersen, N. Pedersen, N.E. Larsen, J. Sonne, S. Larsen, Intestinal first pass metabolism of midazolam in liver cirrhosis -- effect of grapefruit juice, *Br J Clin Pharmacol* 54 (2002) 120-124.
- [247] T.K. Daneshmend, D.W. Warnock, A. Turner, C.J. Roberts, Pharmacokinetics of ketoconazole in normal subjects, *J Antimicrob Chemother* 8 (1981) 299-304.
- [248] P.B. Watkins, S.A. Wrighton, E.G. Schuetz, D.T. Molowa, P.S. Guzelian, Identification of glucocorticoid-inducible cytochromes P-450 in the intestinal mucosa of rats and man, *J Clin Invest* 80 (1987) 1029-1036.
- [249] I. de Waziers, P.H. Cugnenc, C.S. Yang, J.P. Leroux, P.H. Beaune, Cytochrome P 450 isoenzymes, epoxide hydrolase and glutathione transferases in rat and human hepatic and extrahepatic tissues, *J Pharmacol Exp Ther* 253 (1990) 387-394.
- [250] S. Rendic, Summary of information on human CYP enzymes: human P450 metabolism data, *Drug Metab Rev* 34 (2002) 83-448.
- [251] B. Zhu, G.L. Chen, X.P. Chen, N. He, Z.Q. Liu, C.H. Jiang, D. Wang, H.H. Zhou, Genotype of CYP3A1 associated with CYP3A activity in Chinese Han population, *Acta Pharmacol Sin* 23 (2002) 567-572.
- [252] M.R. UHING, D.W. Beno, V.A. Jiyamapa-Serna, Y. Chen, R.E. Galinsky, S.D. Hall, R.E. Kimura, The effect of anesthesia and surgery on CYP3A activity in rats, *Drug Metab Dispos* 32 (2004) 1325-1330.
- [253] X.H. Zhu, J.J. Jiao, C.L. Zhang, J.S. Lou, C.X. Liu, Limited sampling strategy in rats to predict the inhibited activities of hepatic CYP3A, *Lab Anim* 43 (2009) 284-290.

[254] C.L. Alfaro, Emerging role of drug interaction studies in drug development: the good, the bad, and the unknown, *Psychopharmacol Bull* 35 (2001) 80-93.

[255] United States Food and Drug Administration, d.a. Draft guidance for industry: drug interaction studies-study design, and implications for dosing and labeling,, <http://www.fda.gov/downloads/Drugs/GuidanceComplianceRegulatoryInformation/Guidances/UCM072101.pdf>, in, 2006. Date accessed 5 January 2010

[256] K.E. Thummel, D.D. Shen, T.D. Podoll, K.L. Kunze, W.F. Trager, C.E. Bacchi, C.L. Marsh, J.P. McVicar, D.M. Barr, J.D. Perkins, et al., Use of midazolam as a human cytochrome P450 3A probe: II. Characterization of inter- and intraindividual hepatic CYP3A variability after liver transplantation, *J Pharmacol Exp Ther* 271 (1994) 557-566.

[257] M. Takano, R. Hasegawa, T. Fukuda, R. Yumoto, J. Nagai, T. Murakami, Interaction with P-glycoprotein and transport of erythromycin, midazolam and ketoconazole in Caco-2 cells, *Eur J Pharmacol* 358 (1998) 289-294.

[258] H.M. Jones, J.B. Houston, Substrate depletion approach for determining in vitro metabolic clearance: time dependencies in hepatocyte and microsomal incubations, *Drug Metab Dispos* 32 (2004) 973-982.

[259] T. Kotegawa, B.E. Laurijssens, L.L. Von Moltke, M.M. Cotreau, M.D. Perloff, K. Venkatakrishnan, J.S. Warrington, B.W. Granda, J.S. Harmatz, D.J. Greenblatt, In vitro, pharmacokinetic, and pharmacodynamic interactions of ketoconazole and midazolam in the rat, *J Pharmacol Exp Ther* 302 (2002) 1228-1237.

[260] T. Kanazu, N. Okamura, Y. Yamaguchi, T. Baba, M. Koike, Assessment of the hepatic and intestinal first-pass metabolism of midazolam in a CYP3A drug-drug interaction model rats, *Xenobiotica* 35 (2005) 305-317.